Sustainable Energy & Fuels

ROYAL SOCIETY OF CHEMISTRY

REVIEW

View Article Online
View Journal | View Issue

Cite this: *Sustainable Energy Fuels*, 2023, **7**, 4758

A review on thermochemical based biorefinery catalyst development progress

Mortaza Gholizadeh, * Cristina Castro, Sandra Meca Fabrega* and Frederic Clarens*

Received 16th April 2023
Accepted 6th July 2023

DOI: 10.1039/d3se00496a

rsc.li/sustainable-energy

The depletion of fossil fuel resources highlighted the need for renewable energy. Among different sources of renewable energy, biorefineries, which are based on thermochemical processes, got the interest of scientists. There are several thermochemical methods, which have been investigated in recent years. However fast pyrolysis, gasification and hydrothermal liquefaction processes are the most mature ones to be industrialized. They result in different final products, which could be used in different applications. However, there is always this question "Which one to go with to get the fuel, no matter of the type, sooner, cheaper, easier and with the lowest pollution" between investors and technologists. Considering all these aspects, this article provides insights into the fundamental and applied concepts of fast pyrolysis, gasification and hydrothermal liquefaction processes. This includes the catalyst development from the past to the present. The economic and environmental aspects of these thermochemical technologies were also studied. Based on this, comparisons were carried out to highlight the Technology Readiness Level (TRL) of each technology. The possible remaining obstacles were clarified.

1. Introduction

Fossil fuels contribute significantly to air pollution by releasing greenhouse gases,[1–4] In addition, their resources are also depleting.[1–4] Therefore, renewable energy got the interest of technologists. Biomass as a cheap and the most abundant source of energy can be converted to a gas fuel or a liquid fuel, which can be used as a fuel for vehicles or an energy source for factories.[5–7] Different methods such as biological[8] and thermochemical processes have been used to convert the different types of biomass to fuel.[9–11] For the continuous operation of the biomass to fuel conversion process, thermochemical treatments are of importance as the biological process is conducted in the batch form and is mainly performed on small scales.[12]

Thermochemical processes, which are mature or near to that, include gasification, pyrolysis and hydrothermal liquefaction (HTL) and have their own advantages and disadvantages. Gasification can convert biomass into a gaseous product, which mainly consists of syngas, and it is performed at 700–1000 °C.[13–15] The pressure for the gasification process is low (below 10 bar), although some research groups used high pressure to increase the yield of syngas.[13–15] Methane and hydrogen with high concentration can be obtained by the further processing of the gaseous product through catalytic processes.[16–18] However, the selection of a suitable catalyst, which is cheap and can work for a long time, is the main challenge of this process.[19–27] In addition, gasification occurs at high temperature (>700 °C), which requires a high source of heat and also special materials for the reactor. These lead to the high cost of operation. Pyrolysis is another type of thermochemical method, which can convert biomass to a liquid fuel called bio-oil.[28,29] Pyrolysis is conducted at 400–800 °C and under atmospheric pressure.[30–33] Bio-oil cannot be used directly as an engine fuel due to its low quality.[30,31] High contents of water, oxygen, and acids, a low heating value and low stability are some of its disadvantages.[32,33] As a result, the upgrading processes such as catalytic pyrolysis and hydrotreatment were utilized to improve the quality of the bio-oil. However, the high amount of coke formed and the high cost of the process were the main obstacles to scale up these processes.[34] Biomass conversion into bio-oil was investigated by the use of hydrothermal liquefaction treatment. Compared to gasification and pyrolysis, the hydrothermal liquefaction process is carried out at lower temperature (<375 °C), but higher pressure (<22 MPa) in a water environment.[35] The aim of the liquefaction process is the increase of the rate of deoxygenation of large species and also enhance the rate of condensation of small fragments to produce a more hydrophobic phase with less water dissolved.[34] Liquefaction results in a bio-oil with more viscosity, but lower density, which cannot be used directly as an engine fuel.[34] The use of different catalysts also could not improve the properties of the bio-oil significantly due to the presence of a high amount of heavy oxygen containing species in the bio-oil. In addition,

Eurecat, Centre Tecnològic de Catalunya, Waste, Energy and Environmental Impact Unit, Plaça de la Ciència, 2, 08243 Manresa, Spain. E-mail: mortaza.gholizadeh@eurecat.org; sandra.meca@eurecat.org; frederic.clarens@eurecat.org; Fax: +34-938777373; Tel: +34-938777373

the catalysts were deactivated quickly by the formation of coke.[35–37] Therefore, still there are challenges to scale up the HTL of the biomass process.

So far, many different processes and conditions, reactor types and catalysts have been tested for the conversion of biomass to gas/liquid fuels. Each trial had its own advantages and disadvantages. There is not a clear conclusion in the literature to identify a certain pathway for the future of biomass thermochemical treatment, which can be used in large-scale applications. Many review papers have been published in the field of gasification, pyrolysis and hydrothermal treatment of biomass to summarize the progress of each process. For instance, in the gasification field, Sansaniwal *et al.*[38] reviewed the effect of different types of reactors on the efficiency of the gasification process. In addition, the effect of the catalyst and the techno-economic study of the gasification process were discussed. However, a clear pathway for the future steps was not drawn. In addition, after a few years, there is a need for updating their conclusions. In another study, Ren *et al.*[39] reviewed the development progress of different aspects in the biomass gasification process such as the effect of different reactor designs, catalysts, reaction mechanisms and mathematical models. However, the progress for the commercialization stage was not discussed in detail. Recently, Thomson *et al.*[40] summarized the effect of different parameters on the quality of the gaseous products obtained from the gasification of biomass. Many review papers were published in the field of biomass pyrolysis. For instance, Kan *et al.*[41] reviewed the influence of different parameters on the quality of bio-oil produced from the pyrolysis of biomass. Hoang *et al.*[42] summarized the results from the literature regarding the effect of different parameters on the yield of bio-oil to obtain the highest yield of the bio-oil. Hu *et al.*[43] summarized the technological development of biomass pyrolysis and the effect of different parameters on the process. Considering all these review papers, still there is a need to highlight the status of these processes in the current time. Many good review papers were also published recently on the topic of biomass hydrothermal liquefaction technology. As an example, Gollakota *et al.*[11] summarized the effect of parameters such as temperature, pressure, catalyst, *etc.*, on the yield and quality of bio-oil. Ni *et al.*[44] and Castello *et al.*[45] reviewed the technological development for the HTL of biomass. These all are good papers with significant impression on the process development and the influence of different parameters on the thermochemical conversion processes of biomass. However, there is no clear conclusion for their future development to clarify the main challenges for each process. In addition, it is not clear which technology is near to be industrialized in an optimum procedure of operation. Therefore, in this review, briefly the effect of different process parameters on the scale-up of the biomass gasification, pyrolysis and liquefaction processes is discussed. The main challenges are separately clarified for each process. The techno-economic and environmental aspects of each treatment are elaborated. Finally, suggestions are given to take the next steps to commercialize each process and also optimize the currently available large size plants.

2. Biorefinery based on the thermochemical treatment-commercial development aspect

This section provides an overview of the process development aspect, product analysis and the commercialization progress of biomass gasification, pyrolysis and hydrothermal liquefaction. In Scheme 1, the summary of the topics, which will be discussed here, is shown. It is worth mentioning that in this review, the cost to produce the biofuel through gasification, pyrolysis and hydrothermal liquefaction of biomass is shown and compared with the cost of petroleum-based fuels. The amount of possible pollution from each technology is shown. Additionally, the progress in technological development and an outlook on the commercialization stage are discussed.

2.1. Gasification

2.1.1. Products. Gas is the main product of the gasification of biomass.[46] In addition, biochar and tar are produced as by-products, which are mainly burnt to produce the required heat for the gasification process.[46] Depending on the use of air and the catalyst, ash and coke are obtained.[47] The gasification process involves different stages including a drying zone (bunker section), pyrolysis zone, partial oxidation (combustion) zone and reduction zone.[48] The presence of moisture in the biomass leads to the loss of energy and also the degradation of products obtained from the gasification process.[49] Therefore, it is required to dry the biomass prior to feeding it to the other stages. Pyrolysis reactions occur at 125–500 °C.[38] In this stage, the biomass is converted to char and volatiles, which are non-condensable (gaseous product) species and condensable (tar) species.[50] In the reduction stage, temperature is high (*e.g.* 1000 °

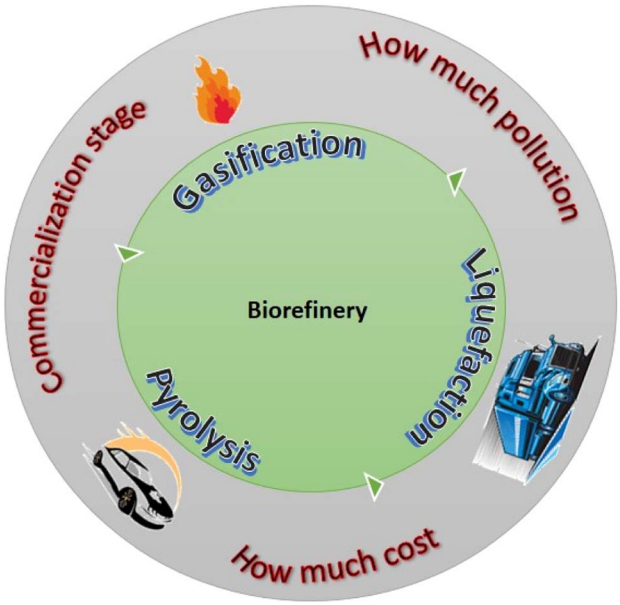

Scheme 1 Overview of thermochemical processes to convert biomass into fuel.

C) and the tar is converted to combustible gases like CO, H_2 and CH_4.[38] The main reactions in this stage are the Boudouard reaction, water gas reaction, water gas shift reaction and hydrogasification reaction. During the Boudouard reaction, C and CO_2 are reacted and CO is obtained and the reaction is endothermic (-172.6 kJ g^{-1}). In the water gas reaction, which is an endothermic reaction (-131.4 kJ g^{-1}), C and H_2O reacted together and CO and H_2 are formed. In the water gas shift reaction, which is an exothermic reaction (42.3 kJ g^{-1}), CO and H_2O are reacted together and converted to CO_2 and H_2. From the hydrogasification reaction (exothermic, 75.0 kJ g^{-1}), CH_4 is obtained by reaction of C and H_2.[38] Depending on the process conditions such as temperature, pressure, the reactor type and the use of different catalysts, the rate of these reactions can be very different. This can affect the yield and the quality of the products.

2.1.2. Reactors. Two types of reactors including fixed-bed and fluidized-bed have been utilized for the gasification of biomass, which are discussed below. It should be mentioned that fixed-bed updraft and down draft gasifiers were used on a lab scale or in small size pilot plants, whereas bubbling and circulating fluidized-bed reactors were used in both small and large sizes.

2.1.2.1. Fixed-bed reactors. Fixed-bed gasifiers are based on a batch feeding system, in which biomass is loaded into the reactor initially and gasifying agents such as air, steam, enriched air with oxygen or with both air and steam are blown into the reactor as the reaction medium and also the reactant.[51] These reactors are designed in updraft, downdraft and cross-draft forms.[52,53] In the updraft design, biomass is filled from the top of the reactor, while the gasifying agent enters the reaction media from the bottom. The advantage of this type is the high efficiency of heat transfer, low slag formation and low pressure drop. The sensitivity for the formation of tar, long start-up time and the low yield of syngas are the main disadvantages of updraft gasification reactors.[52] In the downdraft reactor, biomass enters from the top or the bottom of the reactor and moves together with the gasifying agent, which is introduced into the oxidation zone, in the same direction.[54] High quality gas with a low tar content is obtained from the outlet of the downdraft gasifier. The application on a small scale is its major disadvantage.[52] In the cross-draft design, biomass is loaded from the top or the bottom, while the gasification media enter the reactor from the side of the reactor.[55] Its high flexibility, short start-up time duration and low reactor height could be considered as its main advantages. Large and also small sizes of biomass particles cannot be used in this system due to the easy blockage of the reactor.[52]

2.1.2.2. Fluidized-bed reactors. Fluidized-bed gasifiers contain granular solids, which are used as a heat transferring bed and also mixer.[56] They can be used in both batch and continuous forms. In general, the conversion rate is higher in the fluidized-bed gasifiers compared to the fixed-bed ones. However, their controlling system in large scale applications is complicated.[57] The main sub-divisions of the fluidized-bed reactor are a bubbling fluidized-bed, circulating fluidized-bed, dual-bed indirect and entrained-bed ones.[53,58] The main difference between different types of fluidized-bed reactors is the speed of the gasification agent or the type of its contact with the biomass. For instance, in the bubbling fluidized-bed design, the speed of fluidization is in the range of 1–3 m s^{-1}.[59] All the biomass materials can be processed in this type of reactor. However, the efficiency of the gasification is low and also the yield of tar is considerably high.[59] In a circulating fluidized-bed gasifier, the speed of the gasification agent is higher compared to the bubbling fluidized-bed (3–5 times higher).[59] Therefore, the rate of mixing and consequently the gasification reaction is high. Due to the circulation of the gasification bed, the remained biomass particles are well gasified and therefore the efficiency is high and the yield of tar is low.[59] Because of these advantages, circulating fluidized-bed design is suggested for large-scale gasification plants. However, it is worth mentioning that due to its high cost and complicated controlling system, it is under development.[59] In a dual-bed indirect gasifier, there are interconnected fluidized-bed parts. The first part is a bubbling fluidized-bed reactor converting the biomass to a gaseous product.[60] The second part is a circulating fluidized-bed/fast fluidized-bed reactor, which oxides biochar to heat. These two parts are connected with a valve, but are controlled separately. The conversion efficiency of biomass to gas is high in this type of reactor. However, the formation of tar is its main concern.[60] In an entrained bed gasifier, biomass and gasification agents move co-currently. The biomass particle size is less than 1 mm.[16] The pressure and temperature inside the reactor are high (25–30 bar and 1300–1500 °C).[16] These process conditions make the gasification process fast and effective. The requirement for the small size of biomass and the removal of moisture prior to the gasification are the main obstacles, which prevent the use of this design on a commercial scale.[16]

2.1.3. Catalysts. A catalyst is used during the gasification of biomass to reduce the activation energy of the reforming reaction and tar yield and also to produce syngas in high yield.[52,61–66] The interest in the use of a catalyst in the gasification process started in the 1980s.[52] So far, several groups of catalysts have been used in catalytic gasification to reduce the amount of tar and improve the quality of the gas phase. The main groups of the catalysts, used in this field, are Ni-based catalysts, metal oxides, noble metals, metal salts, natural catalysts, zeolites, char, activated carbon and hybrid catalysts.[67] It is worth mentioning that Ni-based and noble metals are suitable catalysts for the tar removal from the gas phase and are used in an *ex situ* form, while metal salts, zeolites, dolomites, olivine, and metal oxides are used in an *in situ* form with the feedstock in the batch reactor or as a bed material in the continuous reactor or loaded on the surface of the feedstock prior to the experiment.

2.1.3.1. Ni-based catalysts. Ni-based catalysts are used for the reforming of methane to produce hydrogen-rich gas. This group of catalysts, including commercial and lab-scale produced ones, showed high activity for the reforming of methane in the absence/presence of steam.[53] It has been proved in the literature that in the presence of steam, the rate of cracking by Ni-based catalysts was high and a high yield of the gaseous product was obtained.[53] The main obstacle for Ni-based catalysts is their quick deactivation by the formation of coke. In

Table 1 The summary of the results for different types of Ni-based catalysts used in the gasification of biomass

Feedstock	Reaction temperature (°C)	Catalyst	H_2 yield (wt%)	Coke formation	Ref
Coconut shells	800	Ni/dolomite	50 wt% (H_2% in the gas)	16.5 wt% (coke amount on the catalyst)	68
Wood sawdust	800	Ni/MCM-41	51 v%	Coke yield was 0.5–4.0 wt%	69
Pine sawdust	650–850	Nickel based catalyst	46.28 v% AT 650 °C and 52.47 v% at 850 °C	—	70
Pine wood chips	830–840	Nickel based catalyst including BASF G1-50, ICI 46-1, and Topsøe R-67	Similar yields of H_2 with 28 v% for all the catalysts tested	Experiments could go on for 50 hours, and then catalysts are deactivated	71
Pig manure	650	Ni/lignite char	69 mmol g^{-1}	Carbon conversion to coke was 12 wt%	72
Pine wood, wheat straw, corn straw, peanut shells and cotton stalk	750	Fe–Ni/activated char	Peanut shells produced the highest yield of H_2 (52.31 wt%)	Significant amount of coke was formed after the experiment and the formation of coke led to the decrease of gas yield	73
Corncob	650	Ni/resin	61 mmol g^{-1}	The yield of coke was 1.9 wt%	74
Wood sawdust	850	NiO/MgO	51 v%	—	75
Palm empty fruit brunch	900	γ-NAS (the doping of Al in the Ni catalyst lattice)	20.9 v%	—	76
Rice straw	800	Ni/HZSM-5	23.63 v%	Coke yield was higher than 19.2 wt%	77
Oat hull	650	Ni/Al_2O_3 and $CeNi/Al_2O_3$	40 mol% for Ni/Al_2O_3 and 42 mol% for $CeNi/Al_2O_3$	0.05 mg g^{-1} of C on Ni/Al_2O_3 and 0.02–0.05 mg g^{-1} of C $CeNi/Al_2O_3$	78
Pine sawdust	850	NiO/olivine	56.1 v%	Coke amount was insignificant	79
Wheat stalk	450	Ni/MgO, Ni/ZnO, Ni/Al_2O_3 and Ni/ZrO_2	11 mg kg^{-1} for Ni/MgO, 10 mg kg^{-1} for Ni/ZnO, 9 mg kg^{-1} for Ni/Al_2O_3 and 8 mg kg^{-1} for Ni/ZrO_2	—	80

Table 1, the yield of hydrogen and the deactivation amount are presented for the different types of Ni-based catalysts.[68–80] As can be seen, different amounts were reported for the yields of hydrogen and coke over Ni-based catalysts. The parameters such as the concentration of Ni in the catalyst, the presence of other metals, reaction temperature, Ni to feedstock ratio, *etc.* led to the different qualities and quantities of the products. For instance, in the study by Tursun *et al.*,[79] the concentration of H_2 over NiO/olivine was 56.1 volume% (v%) and the amount of coke was negligible. Their feedstock was pine sawdust and the reaction was conducted in a decoupled triple-bed gasifier at 850 °C. The catalyst was used in a separated reactor to reform the volatiles. On the other hand, Chen *et al.*[77] observed that during the gasification of rice straw over Ni/HZSM-5 at 800 °C, the concentration of H_2 in the gas phase was 23.63 v%. In addition, the yield of coke was very high (19.2 weight% (wt%)). The reactor was fixed-bed and the catalytic bed was installed inside that following the feedstock bed. Hu *et al.*[73] investigated the effect of an Fe–Ni/activated char catalyst on the gasification of pine wood, wheat straw, corn straw, peanut shells and cotton stalk at 750 °C. The reactor type was fixed-bed and inside the reactor, the feedstock bed was followed by the catalytic bed in an *ex situ* form. Fe was used in the structure of the catalyst to control the high activity of Ni for cracking and the deactivation reaction. The results indicated that the feedstock type was very effective on the composition of the gas. Peanut shells produced the highest yield of H_2 (52.31 wt%). Additionally, the catalyst lost the activity in time-on-stream and the yield of gas reduced gradually from the initial stages of the gasification process. These contradictions indicated that still further fundamental studies were required to optimize the application of Ni catalysts during the gasification of biomass.

The formation of coke during the gasification of biomass, in a plug flow reactor at 900 °C using a Ni/Al_2O_3 catalyst, was studied by Kihlman *et al.*[81] The catalyst was used in a separate rector, which was installed after the gasification reactor. Their results indicated that the formation of coke is inevitable and after 144 h of continuous gasification of the feedstock, the deactivation of the catalyst by the formation of coke was observed (60 mg carbon in each g of catalyst). Ethylene in the gas phase was the main precursor of the coke. This phenomenon was checked by the injection of ethylene into the gas product entering the catalyst bed. With the increase of the ethylene amount from zero up to 50 000 ppm (vol-ppm in dry gas), the amount of coke increased from below 0.5 wt% up to 16 wt%. This indicated the high tendency of ethylene for polymerization during the reforming reaction of the gas products from the gasification of biomass. Pressure had a significant effect on the products and the formation of coke. The amount of carbon after 5 h of gasification at 1 bar was 0.5 mg g^{-1} of catalyst, while it enhanced to 9 mg g^{-1} of catalyst at 4 bar and then reduced to 3 mg g^{-1} of catalyst at 10 bar. The reason for this was the increase of the polymerization rate of ethylene up to 4 bar, while after that the increase of pressure could partially stabilize the free radicals and then the smaller number of these radicals were polymerized. Temperature also had a remarkable influence on the formation of coke. For instance, at 10 bar, the percentage of carbon in the feedstock converted to coke was measured to be 13 wt% at 850 °C, 5.8 wt% at 900 °C and 1.7 wt% mg g^{-1} of catalyst at 950 °C. Higher temperature could stabilize more free radicals of ethylene.

A two-stage reactor system was used by Ngo *et al.*[82] to produce hydrogen from the gasification of rice straw. The process included a fluidized-bed reactor working at 800 °C as a gasifier followed by a packed bed reactor filled with the Ni-based catalyst working at 250 °C or 400 °C to enhance the amount of H_2 in the gas product. The Ni-based catalyst increased the content of H_2 from 6.63 to 12.24 v%. Additionally, the content of tar and the amount of CH_4 in the gas phase reduced. This showed the high tendency of the Ni-based catalyst for water–gas shift and CH_4 reforming reactions. With the increase of the temperature of the catalytic bed to 400 °C, the formation of coke enhanced. The amount of coke at 250 °C was 3.92 wt%, while at 400 °C, it was 5.59 wt%. As a result, 250 °C was considered as the optimum working temperature, which led to 73 wt% removal of tar and a gas product with a heating value of 5.92 MJ kg^{-1}. There are many studies available for improving the stability of Ni based catalysts such as addition of bimetals to reduce the particle size and the formation of solid solution, which are going to be discussed in the coming sections.

2.1.3.2. Metal oxides. Metal oxides have been widely used in the gasification process to enhance the yield of hydrogen.[80] They are mainly used in a single form, a mixture of several metal oxides and supported metal oxides.[80,83] The majority of metal oxides are cheap and are highly abundant on Earth. However, the preparation of mixed metal oxides or supported metal oxides is not economically feasible or they cannot be produced on a large scale. In addition, the formation of coke deactivates the metal oxides quickly, which is another barrier for their use in commercial scale plants. The brief summary of the studies of biomass gasification in the presence of metal oxide based catalysts, which were available in the literature, is shown in Table 2. For instance, Duman *et al.*[84] studied the gasification of safflower seed cake at 600–850 °C and used CeO_2–Fe_2O_3 with different ratios to decompose tar. The system included two separate fixed-bed reactors for the gasification and reforming of volatiles. The combination of CeO_2 and Fe_2O_3 could decompose effectively the tar and enhanced the yield of H_2 remarkably. The optimum results (the yield of H_2 was 1500 cm^3 g^{-1} of biomass and tar conversion was 60 wt%) were obtained at 50 wt% combination amounts of CeO_2 and Fe_2O_3 at 700 °C. CeO_2 improved the reforming of tar and Fe_2O_3 enhanced the surface area of the catalyst. The combination of both led to a high yield of H_2 and a tiny amount of coke formation. In another study, Uddin *et al.*[85] investigated the effect of Fe_2O_3 on the gasification of cedar wood at 850 °C in a two stage process. The catalyst was loaded in the second stage, which was used to destruct the tar at 600 °C. The yield of H_2 enhanced from 90 to 290 cm^3 g^{-1} of feedstock and the yield of carbon in the gas phase enhanced from 40 to 75 wt%. However, the activity of the catalyst, especially for water gas shift reaction, declined by the loss of active sites because of the formation of coke. Moreover, the formation of coke resulted in the decrease of the catalyst specific surface area from 7.4 to below 4 m^2 g^{-1}. Iron oxide was used by

Table 2 The brief summary of the results for different types of metal oxide catalysts used in the gasification of biomass

Feedstock	Reaction temperature (°C)	Catalyst	H_2 yield (wt%)	Coke formation	Ref.
Safflower seed cake	700	CeO_2–Fe_2O_3 (50 wt% from each)	1400 cm^3 g^{-1} of biomass	—	84
Cedar wood	600	Fe_2O_3	H_2 increased from 90 to 290 cm^3 min^{-1}	Catalyst specific surface area reduced from 7.4 to below 4 m^2 g^{-1}	85
Bark-free Swedish birch	800 and 850	Iron based granules	H_2 concentration in the gas phase was 6.59 and 8.59 v% at 800 and 850 °C	No carbon deposit was seen on the catalyst	86

Nordgreen *et al.*[86] during the gasification of bark-free Swedish birch to suppress the formation of tar and increase the yield of H_2. The gasification reaction was conducted in a fluidized-bed reactor, which was followed by a fixed-bed reactor for the catalytic reaction. The highest amount of tar destruction (60 wt%) and the highest amount of H_2 (8.59 v%) were obtained at 850 °C. No carbon deposition was seen on the surface of the catalyst. These results showed the high performance of the iron oxide catalyst during the gasification of biomass. However, still a portion of tar remained and also the use of the catalyst in further cycles was required to be checked. The reason for this was to investigate the efficiency of iron oxide in the continuous operation.

The catalyst to biomass mass ratio and temperature have high influence on the production of H_2 during the gasification process.[87] Lan *et al.*[87] studied the gasification of sawdust in a fluidized-bed reactor at different temperatures and varied catalyst to biomass ratios. CaO was selected as the catalyst. To investigate the changes, they developed a model by the use of ASPEN PLUS software. The increase of temperature enhanced the amount of H_2 and CO_2 in the outlet gas, while the content of CO and CH_4 reduced. This was because of the increase of water–gas shift and CH_4 reforming reactions. The increase of the catalyst to biomass mass ratio led to the increase of H_2 and CO_2 and decrease of CO and CH_4 amounts. For instance, the change of temperature from 650 to 850 °C resulted in the increase of H_2 from 32 to 44 v%. Furthermore, by the increase of the catalyst to biomass mass ratio from 0 to 50 wt%, the content of H_2 enhanced from 40 to 68 v%.

Considering the results discussed, it is clear that metal oxides are active for the first cycle of the catalytic gasification. However, still after a few cycles of use, they lose the activity due to the formation of coke or the deformation of their structure. Therefore, further fundamental studies are required to extend the life-time of the metal oxides during the upgrading of the gasification products.

2.1.3.3. Noble metals. The use of noble metals as the catalyst in the biomass gasification process has been studied recently. They are very active to enhance the yield of H_2 and they produce low coke. They enhance the yield of H_2 through the water gas shift reaction. However, due to their high price, they are rarely selected by research groups as their application on a commercial scale is not economically feasible. Different noble metals including Rh, Pt, Pd, Ir, Ru, and Ag supported on CeO_2–Al_2O_3 were tested by Haryanto *et al.*[88] to evaluate their selectivity for the production of H_2. The reaction set-up included a two-stage in one reactor system with having the gasification reaction in the first stage at high temperature. The temperature of the second stage was lowered by the use of cold water to obtain the optimum reaction temperature for the catalyst bed. The reaction temperature was 700 °C and a steam to CO ratio of 5.2 : 1 was selected. Pt showed the highest activity to enhance the yield of H_2 (H_2 selectivity was 94.7%). Ru had the second highest activity (H_2 selectivity was 85.6%), while the lowest yield of H_2 was obtained by Ag (H_2 selectivity was 30%). By time-on-stream, coke formation declined the activity of the catalysts tested and consequently the yield of H_2 reduced. Tar obtained from the gasification of cedar wood was reformed with Rh, Pt, Pd and Ru supported on CeO_2–SiO_2 at 550–650 °C in the study by Tomishige *et al.*[89] The reactor type was fluidized-bed and the catalyst was used as the bed material. Rh showed the highest activity to produce more H_2 and less coke. At 650 °C, for Rh, the highest yield of H_2 was 3526 μmol min^{-1} and the yield of coke was 1 wt%. This indicated that still the yield of H_2 was considerably high, while the yield of coke was also high. Summarizing the results for the noble metals' application in the biomass gasification process indicates that they are more active than other catalysts in this field of the production of H_2. Furthermore, they result in the lowest amount of coke compared to the other catalysts used in the gasification process. However, the amount of coke is still high and in long term applications, they cannot be a suitable candidate for commercial biomass gasification plants. Their high price is also another obstacle, which leads to a low amount of interest in their application. Hence, noble metals are not potential catalysts for the biomass gasification technology.

Commercial automotive catalysts include platinum, palladium and rhodium, which were used in the gasification of biomass.[90] McFarlan *et al.*[90] used a commercial automotive catalyst for the reforming of tar, which was produced from woody biomass in CanmetENERGY using a fluidized-bed reactor operated at 800–820 °C with a feeding rate of 5–20 kg h^{-1}. The catalytic reforming process of tar was conducted in a fixed-bed reactor at 700 °C. A mixture of methanol, tar and water (the mass ratio was 79.5/0.5/20 for methanol/tar/water) was selected as feedstock. Methanol was added to the tar to reduce the formation of coke. The tar was completely converted to gas, which included a high content of CO, CO_2 and CH_4. The

catalyst deactivation occurred after 12 h and within 20 h, the conversion of the tar to the gas reduced by 90%. This was confirmed by the decline of CO, CO_2 and CH_4 and the appearance of methanol in the liquid phase mixed with water. The catalyst was regenerated by the burning of the coke at 700 °C for 6 h. The regenerated catalyst could destruct the tar for 20–24 h during the continuous reforming operation. However, after that, it deactivated quickly.

Bio-oil, which was obtained from the hydrothermal liquefaction of microalgae (*N. chlorella*), was gasified by Xu *et al.*[91] by a supercritical water gasification process in a batch reactor at 450 and 500 °C for 10 min. Noble metals including Pt–Pd/C, Ru/C and Pd/C were used as catalysts to improve the conversion of the bio-oil to H_2. The HTL and upgrading of the bio-oil were carried out in two separate stages in a batch reactor. Pd/C showed a slightly higher yield of H_2 followed by Pt–Pd/C and Ru/C. For instance, at 450 °C, the yield of H_2 was 0.75 mmol g^{-1} of bio-oil for the non-catalytic process, 0.68 mmol g^{-1} of bio-oil for Pd/C, 0.64 mmol g^{-1} of bio-oil for Pt–Pd/C and 0.57 mmol g^{-1} of bio-oil for Ru/C. Increasing the reaction temperature to 500 °C resulted in the formation of a higher amount of H_2. The reason for this was the higher rate of gasification reaction at 500 °C, which indicated that by the further increase of temperature, a higher amount of H_2 could be obtained. This was confirmed by the lower yield of tar and the higher yield of gas at 500 °C. Ru/C led to the formation of the highest amount of CH_4 showing its high tendency for the methanation reaction of carbon oxide and the cracking of tar.

The possibility of the decline of the tar amount during the gasification of sludge was investigated by Lin *et al.*[92] The supercritical water gasification of sludge was performed in a batch reactor for 10 min at 420 °C and 25 MPa over the Pd catalyst. Pd with a catalyst to biomass mass ratio of 10 wt% could enhance the yield of gas from 35.74 to 46.88 wt% due to the higher rate of cracking reaction in the presence of the Pd catalyst. The content of H_2 increased, while the amount of CH_4 reduced in the gas by the use of Pd. For example, the content of H_2 increased from 25 to 42 v% and the content of CH_4 reduced from 17 to 10 v%. This was because Pd enhanced the rate of steam reforming and water–gas shift reactions. CH_4 reacted with H_2O and produced H_2.

2.1.3.4. Metal salts. Alkali, alkaline earth and transition metal salts have been widely used for the gasification of biomass.[93] The majority of metal salts are cheap and active for the catalysis of gasification reactions. Their catalytic activity can be explained by redox (reduction–oxidation) reactions. In metal salts, potassium (K) and sodium (Na) salts have a higher tendency for the gasification of char and the formation of more gas.[94] Umeki *et al.*[94] studied the effect of K_2CO_3 (69.1 g K_2CO_3 in 1 L aqueous solution) impregnation on pine sawdust during the gasification process in a laminar drop-tube furnace at 900–1400 °C. The solution : biomass ratio was 16 mL g^{-1}. Their results indicated that K_2CO_3 prevented the formation of large aromatics and cracked down the tar into gaseous products and aromatics with one or two fused benzene rings. Due to the high rate of cracking reactions, the yield of char and soot reduced in the presence of K_2CO_3. As an example, at 1100 °C, the impregnation of K_2CO_3 led to the decline of the soot yield from 115 to 40 mg g^{-1} feedstock, which indicated the high tendency of K_2CO_3 for the increase of the rate of gasification reaction. The nitrate salts of alkali metals (Na and K), alkaline earth metals (Ca and Mg) and transition metal (Fe) were used during the gasification of pistachio nut shell char in a thermogravimetric analyzer (TGA) and tube furnace reactor at 800–1000 °C. The salts selected were impregnated on the surface of the feedstock (3–7 wt%) prior to the experiment. The results showed that the catalytic activity of the salts selected for the gasification of pistachio nut shell char was as follows Na > Ca > Fe > K > Mg. Nitrate sodium (loading of 3 wt%) led to the increase of feedstock reactivity 2.36 times more. The reason for the lower rate of reaction in the presence of K was the sintering tendency of biomass ash to form alkali silicates. The increase of reaction temperature enhanced the rate of cracking and therefore the yield of gas increased. The study by Koido *et al.*[95] showed that the production of H_2 was enhanced by metal salts. They selected Cs_2CO_3, CsCl, $CsNO_3$ and Cs_2SO_4 as catalysts for the gasification of timber waste in a fixed-bed downdraft-type continuous steam gasification process at 800 °C. The catalysts were doped on the surface of the feedstock in the range of 1–30 wt%. The feeding rate was 0.7 g min^{-1}. Cs_2CO_3 had the highest increase of H_2 yield (57% higher compared to the non-catalytic gasification process). The molten form of the salts was also studied.[96] The reason for this was the high heating rate in the reactor because of large heat capacity and rapid heat transfer of molten salts.[96] The molten salt enhances the breakdown of biomass and increases the formation of hydrogen and carbon monoxide.[96] Li *et al.*[96] studied the gasification of cotton stalk in a molten salt including Na_2CO_3, K_2CO_3 and Li_2CO_3 (mass ratio of 1 : 1 : 1). The reaction was carried out in a fixed-bed reactor at 750–950 °C. 150 g of the salts and 1 g of the feedstock were loaded into the reactor. The salts were melted and mixed with the feedstock at the reaction temperature. The yield of gas was 850 mL g^{-1} of feedstock. CO was obtained as the main component in the gaseous product (80 wt%) in the presence of all the catalysts used and its content increased by enhancing the reaction temperature due to the increase of the rate of Boudouard reaction. The summary of the results indicates that metal salts can be used to enhance the yield of syngas in the gas phase during the gasification of biomass. To clarify this further, experiments with longer run times should be carried out to evaluate their performance in time-on-stream. The combination of the salts can be more efficient to enhance the rate of gasification reaction.

Supercritical water gasification with $NaHCO_3$ and NaCl as catalysts (the mass ratio of catalyst to biomass was 5 wt%) was studied by Su *et al.*[97] to convert food waste to H_2. A batch reactor working at 400–450 °C was used and the reaction time was selected as 20–60 min. The reaction was conducted under 25 MPa pressure. The results showed that the increase of reaction time and temperature enhanced the efficiency of the gasification process. For instance, in the absence of the catalyst, the change of temperature from 400 to 450 °C increased the yield of H_2 from 1.5 to 1.8 mol kg^{-1} of feedstock. At higher temperatures, the rates of water gas shift and cracking reactions were

higher, which led to the formation of a higher amount of gas. The increase of reaction time from 20 to 60 min enhanced the production of H_2 up to 15%. Na^+ obtained from the catalyst promoted the water gas shift reaction and more H_2 was formed. The highest yield of gas (12 mol kg^{-1} of feedstock) at 450 °C and 60 min was obtained in the presence of $NaHCO_3$, while it was 5 mol kg^{-1} of feedstock for NaCl. Moreover, the yield of H_2 was 4.5 mol kg^{-1} of feedstock for $NaHCO_3$ and 0.5 mol kg^{-1} of feedstock for NaCl. It should be noted that NaCl reduced the yield of gas and H_2. The reason for the increase of the gas yield by $NaHCO_3$ was the enhancement of splitting of C–C bonds by Na^+ and the reason for higher H_2 was the increase of the rate of water–gas shift reaction by Na^+.

The gasification of non-edible corn stover in a batch reactor at 837, 887 and 937 °C over iron nitrate was carried out by Roncancio *et al.*[98] The reaction pressure was selected as 1.3, 4, 7, and 10 atm and the mass ratio of catalyst to biomass was 13. The catalyst led to the formation of a higher amount of gas and CO. However, the catalyst lost the activity quickly due to its reaction with CO_2, which resulted in the formation of Fe_2O_3. The rate of gasification reaction and CO production was enhanced by the increase of temperature and pressure until a certain point. CO and biochar destruction did not change by the increase of pressure above 4 atm. The limitation in diffusion was the reason for this. At pressures below 4 atm, the increase of pressure enhanced the availability of reactants, while at pressures higher than 4 atm, CO_2 filled the pores of the biochar and covered its surface, which controlled the biochar conversion and gasification reaction. The increase of temperature from 837 to 887 °C enhanced the production of CO, while the increase of the temperature from 887 to 937 °C did not change the yield of CO significantly. The reason for this was that at higher than 887 °C, the diffusion was limiting the reaction as all the surface of the biochar was covered by CO_2, which did not allow the further cracking of biochar and the formation of more CO.

2.1.3.5. Natural catalysts. Dolomite ($MgCO_3 \cdot CaCO_3$) and olivine ($2MgO \cdot SiO_2$) as the main natural and cheap catalysts have been used by some research groups to enhance the efficiency of the biomass gasification reaction.[67,80] The results indicated that due to the presence of different metals and the polar area on the surface of dolomite and olivine, they led to the increase of H_2 content and the decrease of CO content in the gas phase.[67,80] However, the content of CO_2 in the presence of olivine increased, which indicated that olivine did not enhance the selectivity of H_2.[80] The decomposition of biomass was improved by dolomite and olivine through the cracking of C–C and C–H bonds and the increase of the rate of water–gas shift reaction.[67,80]

2.1.3.5.1. Dolomite. Dolomite is a rock-forming mineral, which has a specific gravity of 2.8–2.9.[99] It is formed underground (thousands of feet below the ground) as calcium magnesium carbonate.[99] It can be colourless or black, brown, gray, green, white and pink.[99] Dolomite is used for the reforming of tar during the gasification of biomass. Depending on the ratio of Mg/Ca in dolomite, its effect on the gasification reactions can be very different.[99] A higher ratio of Mg/Ca is more favourable for water–gas shift and reforming reactions.[99] In an early study, Orio *et al.*[100] used different calcined dolomite types including Norte, Chilches, Malaga and Sevilla, which had completely different compositions, for upgrading the volatiles from the gasification of biomass in a bubbling fluidized-bed reactor. Dolomite was loaded into a fixed-bed reactor, which was used as the second stage and its working temperature was 780–920 °C. The highest content of H_2 (19.0 v%) in the gas phase was obtained in the presence of Malaga dolomite, while the highest amount of CO (17.2 v%) belonged to Sevilla dolomite. It should be noted that the content of H_2 in the absence of the dolomite bed was below 10 v% at all the temperatures tested. The content of CO_2 was measured to be 14.3–15.5 v% for the different dolomites. Fe_2O_3 in the structure of dolomite was determined as one of the main reasons to eliminate the tar. Following this study, Corella *et al.*[101] investigated the effect of dolomite on the gasification of biomass (a mixture of residue from olive oil production and pine wood chips with different mass ratios) in two different reactors including circulating fluidized-bed (working at 850–855 °C and WHSV of 0.31–1.10 h^{-1}) and bubbling fluidized-bed (working at 827–879 °C and WHSV of 0.33–0.47 h^{-1}). The highest amounts of H_2 (18.9% on dry basis for circulating fluidized-bed and 14.6% on dry basis for bubbling fluidized-bed) and CO (18.1% on dry basis for circulating fluidized-bed and 12.9% on dry basis for bubbling fluidized-bed) were obtained. This indicated the high tendency of dolomite for the production of syngas.

In situ co-gasification of coconut shells and oil palm frond blends was conducted by Inayat *et al.*[102] in a fluidized-bed reactor at 700, 800 and 900 °C. The catalyst loading (the mass ratio of the catalyst to biomass) was selected as 0, 15 and 30 wt%. The loading of more catalyst and higher temperature reduced the content of tar and enhanced the amount of H_2 and CO. For instance, by the increase of temperature from 700 to 900 °C (a mixture of 20 wt% coconut shells and 80 wt% oil palm and catalyst loading of 15 wt%), the yield of tar reduced from 14.23 to 2.12 g per Nm^3, which was due to the higher rate of cracking reaction over dolomite at 900 °C. In addition, in the gas phase, the content of H_2 increased from 7.81 to 13.68 v% and the content of CO increased from 11.48 to 17.65 v%. This was due to the increase of the rate of water–gas shift reaction and other gasification reactions such as Boudouard and water gas reactions. The presence of dolomite enhanced the content of H_2 and CO, while slightly reducing the amount of tar. This indicated the low tendency of dolomite for the cracking reaction, but its high tendency for the other gasification reactions.

Dolomite specifications change during the gasification of biomass due to several reasons, which were clarified by Hervy *et al.*[103] They selected fresh and used dolomite as bed materials from an industrial air-blow fluidized-bed biomass gasification plant. To investigate their performance, the steam reforming of benzene was conducted in a fixed bed quartz reactor in the presence of both catalysts at 800–900 °C. 0.3 g of the catalyst and 45 N per mL per min of syngas including 0.5 v% benzene were used. The results indicated that the activity of the used dolomite was 25% lower than that of fresh dolomite. The reason for this was the deposition of a Si-based layer from biomass ash

on the surface of dolomite. Additionally, coke was observed on the surface of the used dolomite. These reasons reduced the availability of active sites (CaO and MgO) for the reforming of benzene, which led to the formation of more coke on the surface of used dolomite during the reforming of benzene. This reduced the efficiency of dolomite for the reforming of benzene.

2.1.3.5.2. Olivine. Olivine, especially in the calcined form, has been widely used for the removal of tar during the gasification of biomass. It is also cheap and abundantly available in the nature.[104,105] However, its mechanical strength is low, which leads to the formation of a high amount of fine particles and consequently a high rate of environmental pollution.[104] According to the study by Rapagna,[104] the presence of iron oxides, magnesium and silica in the olivine was the main reason for its high activity during the steam gasification of almond shells at 700–850 °C. The steam/biomass mass ratio was selected as 0.5–1.0 and the reactor type was selected as fluidized-bed. Olivine was the bed material for the reaction. At 820 °C and a steam/biomass ratio of 1, the tar amount was 0.5 g per 1 normal m^3 of dry gas. The gas included 48 v% H_2, 25 v% CO, 22 v% CO_2 and 5 v% CH_4. It should be noted that under the same operating conditions (770 °C and steam/biomass mass ratio of 1), the composition of gas changed significantly by replacing olivine with sand. For instance, the content of H_2 increased from 19.4 to 35.9 moles in the gas per kg of biomass fed. In another study, Cao *et al.*[105] used olivine as the bed material during the gasification of pine sawdust in a fluidized-bed reactor at 700–850 °C. The steam/biomass ratio was 0.3–1.2 and the olivine content was 10, 30 and 50 wt%. By the increase of temperature from 700 to 850 °C, the content of H_2 and CO increased up to 15.5 and 11.0%. In addition, the increase of the steam/biomass ratio from 0.3 to 1.2 resulted in the enhancement of H_2 yield from 35.4 to 57.2 g kg^{-1}. At 800 °C, a steam/biomass ratio of 1.2 and an olivine content of 50%, the highest yield of H_2 (71.4 g kg^{-1}) and the lowest amount of tar (1.3 g per Nm^3) were obtained. Meng *et al.*[106] studied the effect of raw olivine, calcined olivine and synthesized olivine by wetness impregnation (WI) and thermal fusion (TF) methods on the products during the *in situ* gasification of pine sawdust at 750–950 °C. At higher temperatures, a lower amount of tar was observed. Compared to silica-sand, raw olivine decreased the content of tar by 40.6%. Calcined olivine further reduced the content of tar due to the immigration of Fe from inside to its surface. WI-olivine calcined at 1100 °C further reduced the content of tar (up to 81.5 wt%). The reason for this was the presence of Fe_2O_3, NiO and NiO–MgO at the surface of WI-olivine, which was calcined at 1100 °C. TF-olivine calcined at 1400 °C could reduce the content of tar up to 82.9% due to the formation of $NiFe_2O_4$ on the surface of the catalyst.

The continuous steam gasification of pine wood sawdust in a conical spouted-bed reactor at 850 °C was carried out by Cortazar *et al.*[107] Olivine was selected as the catalyst and bed material (catalyst to biomass mass ratio was 5 wt%). The yield of gas was measured to be 1.3 Nm^3 per kg and the concentration of tar in the gas phase was 21 g per Nm^3. The amount of H_2 in the gas phase was 43 v% and the amount of CO was measured to be 30 v%. The CH_4 content was detected as 8 v%. The deactivation of the catalyst occurred after few minutes, which was confirmed by the increase of the tar amount in the outlet gas and the reduction of H_2 and CO contents in the gas phase. Furthermore, the monitoring of the surface specification of the olivine showed that the BET surface of decreased by 92% and the ratio of pore volume for the fresh to the used catalyst was 0.0003, which indicated the severe formation of coke. In another study, Cortazar *et al.*[108] compared the results of non-catalytic and catalytic continuous steam gasification of pine wood sawdust in a conical spouted bed reactor at 850 °C. The process conditions were similar to those of their previous study.[107] In the non-catalytic process, sand was used as the bed material. Compared to sand, olivine reduced the content of tar from 26 to 20 g per Nm^3, which showed the low tendency of olivine for the cracking of tar. As a result, the yield of gas increased slightly from 1.25 to 1.30 Nm^3 per kg of feedstock. The H_2 yield was 4.5 wt% for sand and 5.0 wt% for olivine. The contents of other gas compounds were in a similar range. As a result, olivine could not be a potential candidate to destruct the tar into the gas with a low amount of coke.

2.1.3.6. Zeolites. Zeolites are based on microporous crystalline aluminosilicate earth metals, which have a three-dimensional network of tetrahedral $[SiO_4]^{4-}$ and $[AlO_4]^{5-}$.[67] The presence of cations on the surface of the zeolites and their mobility during the gasification process are the main reasons for their high catalytic activity.[67] Zeolites are abundantly available in the nature and they can also be synthesized. Both forms have a high tendency to enhance the rate of gasification reaction.[67] They are cheap and can be produced in a large amount. However, their quick deactivation due to the formation of coke during the gasification process is the main obstacle for their use in large-scale operations. Chin *et al.*[109] studied the effect of HZSM-5 to remove tar from the gas phase in a fixed-bed reactor at 500 °C. Almond shells were selected as feedstock for the gasification process and mixed with the catalyst in the reactor. The catalyst/biomass mass ratio was 0.2–1. HZSM-5 resulted in the decrease of phenol content up to 79 wt% (catalyst/biomass mass ratio was 0.5). By the increase of the catalyst/biomass ratio, the content of oxygen-containing compounds declined in the tar. In addition, the content of tar decreased from 11 122 to 4011 mg per Nm^3 (2.8 times) when the catalyst/biomass mass ratio was 1. The possibility of biodiesel production from the cracking of tar obtained from the gasification of virgin wood chips was investigated by Laksmono *et al.*[110] The reaction was performed over ZSM-5 in a batch reactor at 430 °C. The catalyst amount compared to the tar was 2–5 wt% and it was mixed with the tar. The yield of water and tar decreased from 7.82 to 3.63 wt%, when the catalyst amount was selected as 5 wt%. Additionally, the fuel properties of the tar were improved by the catalyst. For instance, its high heating value (HHV) increased from 37.36 to 40.55 MJ kg^{-1} in the presence of 5 wt% ZSM-5. Waluyo *et al.*[111] studied the steam gasification of palm kernel shells in a tube furnace at 750–850 °C. The steam to biomass mass ratio was between 0.0 and 2.25. A modified natural zeolite by acid leaching was selected as the catalyst. The catalyst bed was located after the feedstock in the same reactor. The results

showed that at a steam to biomass ratio of 2.25 and 750 °C, the catalyst reduced the content of tar by 98% and increased the content of H_2 up to 64%. The increase of temperature from 750 to 850 °C reduced slightly the content of H_2 and the amount of tar.

Lalsare *et al.*[112] investigated the gasification of hardwood biomass in a downdraft fixed-bed reactor in the presence of ZSM-5, which was mixed with the feedstock prior to the experiment. The catalyst to biomass mass ratio was 0.75 and the reaction temperature was 850 and 950 °C. At 850 °C, without the injection of methane, the content of H_2 in the gas phase increased from 48 to 54 v%, while the amount of CO reduced from 52 to 40 v%. This indicated the increase of the water–gas shift reaction by ZSM-5. By the increase of the temperature, the amount of H_2 reduced, while the amount of CO increased. A tiny amount of CH_4 was also formed, which was due to the reaction of CO with H_2.

The effect of temperature during the gasification of bagasse in an updraft type gasifier at 500 °C was carried out by Porawati *et al.*[113] Zeolite was selected as an *in situ* catalyst and the mass ratio of catalyst to feedstock was 0.12. At 20 mL min^{-1} water injection to the reaction environment, the outlet gas included 38.25 mol% CO, 4.01 mol% H_2 and 10.17 mol% CH_4. By the increase of the water injection amount to 40 mL min^{-1}, the amount of CO enhanced to 40.14 mol%, the amount of H_2 reduced to 1.31 mol% and the amount of CH_4 slightly decreased to 9.26 mol%. In addition, the CO_2 amount decreased by the increase of the water injection amount considerably. This showed that by the increase of temperature, CO_2 reacted with H_2 and produced more CO.

2.1.3.7. Char and activated carbon. Char is the byproduct of biomass thermochemical processing, which can be used as a catalyst during the gasification of biomass due to its unique features such as a high surface area and containing different metals.[114] It can be activated by physical and chemical processes to improve its surface specifications like the increase of polarity, functionalities and pore volume.[114] Activated carbon can have different catalytic properties compared to raw char.[114] Char is cheap and can be produced in a large amount. Additionally, the majority of activation methods are not expensive processes. However, the catalyst activity of both char and activated carbon is not very high to remain for a long duration of time and convert tar into high value components. Zhang *et al.*[115] used char, which was obtained from the pyrolysis of mallee wood, during the gasification of mallee wood, corn stalk and wheat straw to destruct tar. The temperature was 880 °C inside the gasification reactor and 800 °C in the catalyst chamber. The catalytic bed was installed after the gasification reactor. To understand the effect of minerals, char was washed with sulphuric acid (0.2 M). Both catalysts could reduce the content of tar in the gas phase to below 100 mg per Nm^3. Due to the catalytic activity of the minerals in the raw char, a higher amount of syngas (approximately 4–6% more) was produced. In another study, Wang *et al.*[116] used wood char to remove tar from the gas phase, which was produced from the gasification of sawdust in an updraft biomass gasifier system at 650–850 °C. The catalyst bed was in the second reactor. Their results indicated that the removal amount of tar was 85% in the presence of wood char. Under the same conditions, the content of H_2 enhanced from 25 to 27 v% and the concentration of CO increased from 24 to 26 v%. Char and commercial activated carbon were used by Yao *et al.*[117] to remove the tar obtained from the gasification of wheat straw at 900 °C. The char was produced from the pyrolysis of wheat straw at 500 °C. The experiments were performed in a two-stage fixed-bed reactor. The yield of H_2 was 20 mg g^{-1} for both char and activated carbon samples, while the yield of CO was slightly higher in the presence of char. Both catalysts could convert the tar to gas and consequently the yield of gas enhanced from 34.06 wt% (in the absence of the catalyst) to 66.30 wt% for the activated carbon and 45.75 wt% for the wheat straw char.

The porous structure of biochar is a key factor to control the formation of coke.[276] Buentello-Montoya *et al.*[118] carried out the reforming of tar in a fixed-bed reactor at 650–850 °C. The reaction time was considered as 3 h. A mixture of benzene (61.34 wt%), toluene (23.13 wt%) and naphthalene (15.53 wt%) was considered as the model compound of tar produced during the gasification of biomass. The tar model compound was mixed with a gas containing 25.1 v% CO, 23.7 v% CO_2, 7 v% CH_4, 16.8 v% H_2 and 27.4 v% N_2. The concentration of the tar model compound in the gas mixture was selected as 20 g per Nm^3. Steam was added to the reaction (28 v% in the gas phase). The total conversion of the tar model compound was 10% at 650 °C, while at 750 °C, the conversion enhanced to 27% and at 850 °C, the conversion amount was 88%. To enhance the conversion rate, activated biochar was used. The results showed that activated biochar increased the rate of conversion, which was due to its higher pore volume and surface area compared to biochar. Activated biochar reduced the content of CO_2, but enhanced the content of CO in the gas phase. From the initial stages of reforming, both biochar and activated biochar lost the activity similarly. For example, at 850 °C, the conversion of tar was reduced by 25% within 3 h. The reason was the formation of coke, which blocked the pores and reduced the available surface of the catalyst.

Liu *et al.*[119] used biochar, which was produced from the gasification of mallee wood at 800 °C, for the conversion of tar of mallee wood in a fixed-bed reactor at 800 °C. Tar was continuously fed into the reactor when the reactor reached the target temperature. The analysis of the gas product after 30 min indicated that the biochar led to the increase of H_2 and CO_2, while the amount of CO and CH_4 reduced. As an example, without the use of biochar as the catalyst, the content of H_2 was 4 v%, while biochar enhanced it to 22 v%. This was due to the conversion of the tar to syngas over the catalyst. In the next stage, water was mixed with the carrier gas, which was argon, with 15 v% and passed over the biochar catalyst prior to the injection of tar to activate the biochar for 0–50 min. The longer time of the activation increased the amount of H_2 more. The results showed that in the first stage of the reaction, the diffusion of tar molecules to internal catalytically active sites of the biochar occurred. In the next stage, the tar was decomposed over the active sites of the biochar, which had oxygen-containing functional groups. The conversion amount of the

tar was controlled by the catalyst surface area, pore volume and the availability of oxygen-containing functionalities, which were higher in the activated biochar. The radicals obtained further cracked to form gaseous products or recombined together to produce coke.

2.1.4. Economic analysis and potential to compete with other technologies. By the gasification of biomass, syngas and valuable chemicals such as biomethanol and dimethyl ether can be obtained.[120] In the review by Wang *et al.*,[120] the summary of the studies in the literature indicated that the cost of methanol production from biomass would be in the range of 1.66–1.95 USD per gal, while the cost of bioethanol production would be in the range of 1.62–1.77 USD per gal. It was also calculated that the lowest production cost belonged to NH_3 (0.4 $ per kg), while the highest amount (2.9 $ per kg) was related to the production of biomethanol.[120,121] To calculate the costs, Aspen Plus software was used. The methanol production cost from wood was 195–935 Euro per ton, while it was 200–935 Euro per ton of residue waste, 160–480 Euro per ton of coal and 90–290 Euro per ton of natural gas. The capacity assumption and the investment costs were 100 kton per year and 480 million USD for wood, 1000 kton per year and 420 million USD for residue waste, 1.6 kton per year and 1100 million USD for coal and 100 kton per year and 980 million USD for natural gas. Additionally, the results of calculations showed that the capital cost for the biomethanol production from wood was 5.7 times more than the capital cost for the production of biomethanol from natural gas, while the investment cost of wood based plants was 1.4 times less than that of natural gas based plants. To obtain bioethanol, the production rate was 30 to 50 million gallon per year, and the production cost and capital cost were 2.8 USD per kg and 380 million USD, respectively. To produce NH_3, the production cost was 2.9 USD per kg and the capital cost was 100 million USD. The calculations were based on 25 years of operation. AlNoussa *et al.*[122] performed the techno-economic analysis of oxygen and steam co-fed gasification of biomass by using Aspen Plus. The biomass included dates (8.67×10^2 kg h^{-1}), dried sludge (4.16×10^3 kg h^{-1}), food waste (7.99×10^2 kg h^{-1}) and manure (6.01×10^4 kg h^{-1}). The reaction temperature was selected as 850 °C. The production of methanol by steam gasification was the most economical process with a profit of $0.12 per kg of feedstock. The lowest profit (0.01 per kg of feedstock) belonged to the oxygen co-feeding gasification of biomass to produce power. The life time for the plant was 10 years and the capital cost and operating cost were 40 million USD and 6.08 million USD, respectively. You *et al.*[123] estimated the price of electricity, which was obtained from the gasification of oil palm biomass in a fixed-bed reactor, as 0.06 USD per kW h in the rural area of Indonesia. The price of electricity in Indonesia was 0.107 USD per kW h in 2022.[124] The life time of the plant was assumed 25 years and the cost of the gasification system was 1500 USD per kW. In the study by Salkuyeh *et al.*,[125] fluidized-bed and entrained-flow reactors were used for the gasification process of Canadian pine wood. The calculations showed that the thermal efficiency of the entrained-flow reactor was higher than that of the fluidized-bed reactor (11% higher). However, the amount of electricity production was slightly higher for the fluidized-bed reactor. The plant life time was 30 years, the plant capacity was 18.9 tons H_2 per year and the capital cost was 647–852 million USD for the fluidized-bed reactor and 1229–1340 million USD for the entrained flow reactor. The total annual expenses were 409–431 million USD for the fluidized-bed reactor and 338–410 million USD for the entrained flow reactor. Lo *et al.*[126] estimated the selling price of the syngas obtained from the gasification of palm-based biomass *via* Aspen Plus simulation. The process was conducted at 850 °C, a biomass feeding rate of 80 kg h^{-1} and an air inlet flow of 110 kg h^{-1}. The selling price of 1 kg syngas was 0.15 USD for empty fruit bunches, 0.097 to 0.13 USD for palm kernel shells and 0.073 to 0.097 USD for mesocarp fibre. The different prices depended on the price and availability of the feedstocks. The plant life was considered as 20 years, the capital cost was 20 million USD and the total direct and indirect costs were 18.8 million USD and 0.48 million USD, respectively. The total fixed-operating cost was 1.68 million USD.

2.1.5. Environmental analysis and potential to compete with other technologies. Life cycle assessment (LCA) of biomass gasification was studied to monitor the environmental impacts of the process. Different contaminants like greenhouse gas emission, acidic gas emission, metal contamination, *etc.* can occur during the gasification of biomass.[127] The amounts of different contaminants, which were produced from the gasification of biomass including the residue from cotton cultivation and processing, olive foot cake waste, biomass from corn and biomass from rice, were calculated by Koroneos *et al.*[127] Their results indicated that CO_2, SO_2 and PO_4 were the contaminants produced during the gasification process. In addition, CO_2 was the main pollutant, while the lowest pollution was related to PO_4 during the gasification followed by reforming. By the direct use of the gasification products for electricity production, the amount of CO_2 was the lowest and the amount of PO_4 was the highest. For instance, the amount of CO_2 from the gasification followed by reforming was 150 000 kg CO_2-eq/TJ H_2, while the CO_2 content from the use of the gas product of the gasification for the production of electricity was 20 000 kg CO_2-eq/TJ H_2. Yang *et al.*[128] measured the emission of CO_2 as 0.137 kg CO_2-eq/MJ for a biomass gasification plant in China, while it was 0.30 kg CO_2-eq/MJ for a typical combustion-based electricity production plant, which meant that 56% of CO_2-eq could be decreased by replacing the gasification plants instead of common electricity production plants. In the study by AlNoussa *et al.*,[122] the amount of CO_2 emission was estimated to be 0.68 kg of CO_2-e per biomass input for the gasification of dry pit waste to produce biomethanol. Loy *et al.*[129] estimated the amount of CO_2 from the gasification of wheat straw in the presence of a straw derived biochar catalyst. They calculated the yield of hydrogen as 25.59 g kg^{-1} of feedstock. From the production of 1 kg H_2, 50.4356 kg CO_2-eq was obtained. OpenLCA software was used by Zang *et al.*[130] to simulate the biomass gasification process and the combustion of the syngas obtained. Their results indicated that the global warming potential was lower than 240 kg CO_2-eq/MW h.

2.1.6. Commercialization status. In the past two decades, the importance of biomass gasification has been well

understood to produce fossil-based fuels and chemicals. There have been many small scale gasifiers (70 kW_e to 3 MW_e), which were successfully developed, while only some of them could pass the demonstration stage (>100 MW_e).[131] It should be noted that the commercialized gasifiers had short operational spans.[131] In Table 3,[132] the summary of the details for the majority of successfully developed gasification plants is shown. Renergi Pty Ltd's Advanced Biomass Gasification Technology developed a two-stage gasifier to convert forestry and agriculture wastes into heat and power.[132] The second stage had biochar as the catalyst to remove organic and inorganic impurities. Its process is under the development and waiting for the commercialization stage. The analysis showed that there was less than 20 mg per Nm^3 tar in the gas and its HHV was 5.1–6.9 MJ per Nm^3. Renergi Pty Ltd's gasifier was developed in Australia with a capacity of 100 kg h^{-1} biomass feeding. The Endeavour Microwave Gasification technology was developed by Endeavour Energia S.r.l. in Italy.[132] It was designed to convert the wastes like rice and wheat husks, woody biomass, sludge from anaerobic digestion and litter from animal farms to biochar, heat and electricity at 1400 °C. It was operated on a demonstration scale (100 kg h^{-1} feeding) and waiting for commercialization. The Heliostorm Gasifier by Cogent Energy Systems was based on an ultra-high temperature (3000–10000 °C) operation and was built up in USA.[132] It is under the construction of demo scale (up to 4 tons per day feeding). It was based on using hybrid plasma technology and aimed to produce electricity. The MEVA technology gasifier was developed by Meva Energy AB in Sweden to convert pellets and sawdust into biofuel.[132] Its technology was based on an entrained-flow cyclone gasifier with a capacity of 1.2 MW electricity and 2.2 MW heat production. Wildfire Energy's Moving Injection Horizontal Gasification (MIHG) technology was designed and built up in Australia to convert unprocessed biomass and waste into electricity with a production of 200 kW_{th} (pilot). The maximum feeding rate was 1 ton per day. Multifuel Conversion (MFC) technology was developed by RWE Power AG in Germany. Feedstock was phosphorus-rich substances and the type of reactor was high temperature entrained-flow. The aim was to recover carbon and phosphorus from sewage sludge or similar feedstocks and it was tested on a lab-scale (10–15 kg h^{-1}). Plasco Conversion Technology was developed by Plasco Conversion Technologies Inc. in Canada[132] on a pilot scale (electricity production of 60 kW_{th} from municipal waste). The RadGas Technology was developed by Advanced Biofuel Solutions Ltd. (ABSL) in the United Kingdom. Its feeding rate was 100 kg h^{-1} (pilot scale). SUNY Cobleskill's Rotary Gasifier was developed by SUNY Cobleskill/Caribou Biofuels in the USA.[132] It was

Table 3 The summary of gasifiers with different capacities, which were developed in the past few years[131–141]

Developer	Country	Technology	Scale	Development status
Renergi Pty Ltd.	Australia	Two-stage gasification with integrated catalytic hot gas cleaning	100 kg h^{-1}	Technical testing on a demonstration scale; pending commercialization
Endeavour Energia S. r. l	Italy	Microwave-assisted 'Imbert-type'	100 kW_e/150 kW_{th}/100 kg h^{-1} (demo unit), 100–200 kW_e (commercial unit)	Tested on a demonstration scale; awaiting first-of-a-kind commercial plant
Cogent Energy Systems	United States of America	Ionic gasification	1–5 t per day (commercial unit)	Lab-scale (unknown kg h^{-1}) tested, demo (up to 4 tons per day) under development
Wildfire Energy	Australia	Moving injection fixed bed	60 kW_{th} (pilot), 1–7 MW_{th} (off-grid module) to 5–40 MW_{th} (continuous power)	Tested on a pilot scale, integrated demo funded (2019)
MEVA Energy AB	Sweden	Entrained-flow cyclone gasification	5 MW_{th} fuel input, 1.2–2.4 MW_{el} and 2.2–2.4 MW_{th} heat product (commercial unit)	5 MW_{th} (demonstration), 2.5–5 MW_{th} (commercial offer)
RWE Power AG	Germany	Entrained-flow gasification	Lab (10–15 kg h^{-1}), pilot (130 kg h^{-1}), commercial (125 MW per gasifier unit)	Tested on a lab-scale, pilot plant under construction
Plasco Conversion Technologies	Canada	Plasma (tar) gasification	Multiple 200 t per day municipal solid waste modules in series	Parts of the configuration tested in a 60 kW_{th} pilot
Advanced Biofuel Solutions Ltd.	United Kingdom	Fluidized-bed gasification	22 t per day feed (demo), 60 MW_{th} and ~480 t per day feed (commercial)	100 kg h^{-1} feed (pilot), 6 MW_{th} (demo plant under construction)
SUNY Cobleskill/Caribou Biofuels	United States of America	Inclined rotary gasification	2 t per day (pilot unit), 0.23 t per h bone dry woody biomass full-scale demo funded	Core units tested on a pilot scale, funding for the demo/commercial unit secured
TreaTech SARL	Switzerland	Hydrothermal gasification	500–1000 kg h^{-1} feedstock (commercial unit)	Lab-scale (1 kg h^{-1}) tested; pilot (100 kg h^{-1}) in construction; demo (1–2 kg h^{-1}) planned

processing municipal solid waste, forestry residue and non-hazardous site wastes (2 t per day (pilot unit)) to produce electricity, biofuels and char. The hydrothermal gasification system was built up by TreaTech SARL in Switzerland to upgrade liquid wastes such as sewage sludge to clean water, biogas and mineral salts.[132] It was tested on a lab-scale (1 kg h^{-1}) and the pilot plant (100 kg h^{-1}) is under construction. There are other gasifiers, which are under construction; however, they have not been mentioned here due to the lack of information or data.

2.2 Fast pyrolysis

2.2.1. Products. Biochar, bio-oil and gaseous components are the main products from the pyrolysis of biomass.[137] Bio-oil as a dark brown organic liquid is considered the main product of fast pyrolysis.[142] It is an unstable liquid with full of oxygen-containing compounds such as carboxylic acids, phenolics, esters, *etc.*, and was initially supposed to replace vehicle fuels.[143–145] However, due to its low fuel properties like low heating value, high water content, high acid content, low stability, *etc.*, it cannot be used directly as an engine fuel.[146–148] Therefore, its upgrading is required. Hydrodeoxygenation is the main process to reduce the content of low value compounds inside the bio-oil.[149–151] However, the high cost of hydrogen and the quick deactivation of the catalyst by the formation of coke are the major obstacles for this process. The direct use of a catalyst in the pyrolysis process is another solution to improve the properties of the bio-oil. Many catalysts from commercial ones or other catalysts developed in the lab were used in the pyrolysis process in an *in situ* or an *ex situ* form.[152] However, still the formation of coke occurs and also the fuel properties of the bio-oil are not enhanced that much to use it directly as an engine fuel.[153] The use of different types of reactors is not also significant that much. Therefore, some of the research groups focused on biochar and considered it as the main product of pyrolysis to produce heat, fertilizers, absorbers, filters, electrodes, *etc.*[154] Some of these technologies have been recognized to be feasible such as the use of biochar as a fertilizer and others are under development. Gas compounds include H_2, CO, CO_2, CH_4 and some other hydrocarbon gases, which could be suitable for burning in a furnace to produce heat for the pyrolysis process or be utilized externally.[155] The detailed discussion on these phenomena is given in the coming sections.

2.2.2. Reactors. Different types of reactors have been developed to reduce the cost of operation, while enhancing the yield and quality of bio-oil. Below, the summary of them is presented.

2.2.2.1. Fixed-bed reactor. The fixed-bed reactor is used for lab scale operations as it is simple and does not have a complicated controlling system.[156] In a large scale operation, having homogeneous temperature, pressure and also the same reaction in all the sections of the reactor is very challenging. David *et al.*[156] studied the pyrolysis of rapeseed oil cake in a fixed bed reactor at 500 °C. They could produce bio-oil with a yield of 38.7 wt% and with a caloric value of 36.25 MJ kg^{-1}. In the study by Shah *et al.*,[157] the optimum yield and HVV of bio-oil, which was obtained from the pyrolysis of walnut shell residue at 375–750 °C, were 44.7 wt% and 27.3 MJ kg^{-1}, respectively. Cedar was pyrolyzed at 400–600 °C by Zhu *et al.*[158] in a fixed-bed reactor. The results indicated that at higher heating rates, more glucose derivatives such as acids and furans were formed. Additionally, higher temperature reduced the content of guaiacyl-contained species in the bio-oil and enhanced the rate of reactions such as demethylation and demethoxylation.

The pyrolysis of water hyacinth (*Eichhornia crassipes*) was conducted by Passos *et al.*[151] in a fixed-bed reactor at 450 °C. The higher heating value of the bio-oil was 28.35 MJ kg^{-1}, which was more than the heating value of the feedstock (63.02% more). Rahman *et al.*[159] investigated the effect of a ZSM-5 and CaO mixture on the quality of bio-oil. Pinewood sawdust was selected as feedstock and the reaction was performed at 500 °C. The catalyst to biomass mass ratio was 0.25 : 1 and the CaO to ZSM-5 mass ratio was 1 : 4. The heating value of the bio-oil was measured to be 24.27 MJ kg^{-1} and it included 21 wt% water. This indicated that the catalyst could not improve the quality of the bio-oil significantly. In addition, the bio-oil included a high content of acids, furans, phenolics, ketones and aldehydes, which indicated the low rate of deoxygenation reaction over the combination of the CaO and ZSM-5 catalyst. All the studies based on the fixed-bed reactor demonstrated that the fixed-bed reactor is not a suitable candidate for the large-scale operation of pyrolysis.

2.2.2.2. Bubbling fluidised-bed. The bubbling fluidised-bed reactor has been widely used for the pyrolysis of biomass due to the high yield of bio-oil (70–75 wt%).[43,160] Additionally, temperature is distributed homogeneously inside the bed. The well mixing of the bed materials makes the contact of biomass with hot media more efficient. The bed material could be the catalyst when the change of the bed material with fresh material is easy. The limitation for the particle size of biomass (should be less than 2–3 mm) and the risk of ash fusion are the main disadvantages of the bubbling fluidised-bed reactor.[43] The university of Waterloo in Canada was one of the initial developers of this type of reactor for the pyrolysis of biomass.[43] Later on, pilot plants based on bubbling fluidised-bed reactors were built up by Dynamotive (75 and 400 kg h^{-1} feeding rate of biomass), Wellman (250 kg h^{-1} feeding rate of biomass) and Anhui University of Science and Technology (600 kg h^{-1} feeding rate of biomass). Recently, Tran *et al.*[161] studied the pyrolysis of pitch pine biomass at 500 °C. The yield and HHV of the bio-oil were measured to be 65.5 wt% and 24 MJ kg^{-1}, respectively. The pyrolysis of poultry litter was conducted by Pandey *et al.*[162] at 500 °C. The yield of bio-oil was 27 wt% and its HHV was measured to be 32.17 MJ kg^{-1}. Gomez *et al.*[163] investigated the pyrolysis of rape straw biomass at 480 °C. The yield of bio-oil and its HHV were 39.65 wt% and 19.23 MJ kg^{-1}, respectively.

Bamboo biomass was pyrolyzed by Ly *et al.*[164] in a bubbling fluidised bed reactor at 400–550 °C with a biomass feeding rate of 100 g h^{-1}. HZSM-5 and red mud were used as the catalyst. In the presence of both catalysts, the content of phenolics, especially 4-vinylphenol, increased, which was due to the high tendency of the catalysts used for the cracking reactions. The yield of the bio-oil was in the range of 45–55 wt% and the yield of biochar was 25–30 wt% depending on the temperature and

the absence/presence of the catalyst, the particle size of the biomass, *etc.* The high heating value of the bio-oil was measured to be 25–28 MJ kg^{-1}. The use of the catalyst slightly enhanced the heating value of the bio-oil. Reaction pathways were different for HZSM-5 and red mud. Higher amounts of methoxy phenolic and aromatic compounds were formed by HZSM-5, while red mud led to the formation of more saturated phenols and furan derivatives. These all confirmed the high potential of the bubbling fluidized-bed reactor for the pyrolysis of biomass.

2.2.2.3. Circulating fluidised-bed and transported-bed. The circulating fluidised-bed reactor is used in the petroleum industry for large scale continuous processes.[43] The reason for this is the uniform temperature gradient of the bed and also the possibility to replace the bed material with fresh substances. The circulating fluidised-bed reactor has its own disadvantages such as the requirement for a pump to circulate the bed material, high pressure drop, the high rate of erosion and particle entertainment in the bio-oil.[43,165] The possibility for continuous operation and the easy change of the bed material led to the investigation of using the circulating fluidised-bed reactor in the pyrolysis of biomass. Park *et al.*[166] pyrolyzed sawdust, empty fruit bunch, and giant *Miscanthus* at 500 °C. Their results indicated that the yield of bio-oil was the highest for sawdust (60 wt%), while the calorific value was the highest (17 MJ kg^{-1}) for giant *Miscanthus*. Duanguppama *et al.*[167] could obtain bio-oil with a yield of 67 wt% and an energy value of 30 MJ kg^{-1} from the pyrolysis of sawdust at 500 °C. Ensyn built up a plant based on a circulating fluidised-bed reactor with a biomass feeding rate of 650 kg h^{-1}.[43] Metso, UPM and Fortum built up pyrolysis plants using a circulating fluidised-bed reactor with a feeding capacity of up to 400 kg h^{-1}.[43] The results from the study by Mufandi *et al.*[168] indicated that the circulating fluidised-bed reactor could be considered a suitable reactor design for the pyrolysis of biomass. They selected sugarcane trash, Napier grass, and rubber tree as feedstock. The pyrolysis was carried out at 440–520 °C. The feeding rate was 45, 60 and 75 kg h^{-1}. Under the same conditions of the operation, the yield and heating value of the bio-oil produced from sugarcane trash were higher. The reason for this was the higher content of carbon in the sugarcane trash. For instance, at 480 °C, the yield of bio-oil obtained from the sugarcane trash was 49.47 wt% compared to 47 wt% for the Napier grass and 28 wt% for the rubber tree.

2.2.2.4. Rotating cone. To enhance the efficiency of heat transferring, Twente University developed a rotating cone reactor for the pyrolysis of biomass.[43] In their design, the contact of hot inert particles with the biomass was considered the method for heat transferring. The rotating cone reactor did not require an inert gas and instead of that, the reactor was vacuumed.[169,170] Therefore, its cost of operation was considerably high. Moreover, its energy consumption was high.[43] Junsheng[171] pyrolyzed the waste of pine wood at 550 °C and under a vacuum pressure of 0.08 MPa. Bio-oil with a yield of 54.83 wt% and a HHV of 24.31 MG per kg was produced. Jun *et al.*[172] designed a rotating cone reactor for the pyrolysis of biomass at 550 °C. Bio-oil with a yield of 75.3 wt% was produced. Fu *et al.*[173] studied the pyrolysis of wheat straw at 500 °C in a dual concentric rotary cylinder reactor with ceramic balls as the recirculated heat carrier. Their results indicated that the yield of bio-oil and its HHV were 47.6 wt% and 23.8 MJ kg^{-1}, respectively.

2.2.2.5. Conical spouted-bed. The conical spouted-bed reactor is known to produce a high yield of bio-oil (above 60 wt%) for the pyrolysis of biomass.[174] The reason for the high yield of bio-oil is vigorous solid cyclic movement in the bed, which makes the heat transfer and mass transfer efficient.[174–176] The efficient movement of particles and the low cost of operation could be the other advantages of the conical spouted-bed reactor for the pyrolysis of biomass.[175] The spouted-bed reactor has been developed mainly on the pilot scale and its scale-up is still under progress. The difficulty in the controlling system is the main limit for the commercialization of spouted-bed reactors.[174] Park *et al.*[175] pyrolyzed larch sawdust at 400–550 °C. The highest yield of bio-oil (approximately 53 wt%) and the HHV of 18.5 MJ kg^{-1} were obtained at 500 °C. Fernandez-Akarregi *et al.*[177] conducted the pyrolysis of pinewood sawdust at 480 °C. The yield of bio-oil was 65.8 wt%. The bio-oil collected in the scrubber and filters had a HHV of 12.3 and 23.3 MJ kg^{-1}, respectively. Amutio *et al.*[178] performed the flash pyrolysis of pinewood sawdust at 400–600 °C. At 500 °C, the highest yield of bio-oil (75 wt%) with a LHV of 14.6 MJ kg^{-1} was obtained.

A conical spouted bed reactor was used by Fernandez *et al.*[179] for the steam pyrolysis of pinewood sawdust at 500–800 °C. The highest yield of bio-oil (75.4 wt%) was obtained at 500 °C. This showed the high efficacy of conical spouted bed design in cracking the biomass and biochar to obtain more bio-oil. The increase of the temperature reduced the yields of biochar and bio-oil, while it enhanced the amount of gas. At below 700 °C, the steam was neutral. However, by the further increase of the temperature, steam was involved in the gasification reactions. In addition, higher temperature reduced the amount of phenolics inside the bio-oil and enhanced the content of linear hydrocarbons and aromatics with no oxygen. The reason for this was the high rate of cracking, deoxygenating and saturating of double bond reactions at higher temperatures. Azizi *et al.*[180] investigated the pyrolysis of different microalgae species including Nannochloropsis (NC), Tetraselmis (TS) and Isochrysis Galbana (IG) in a conical spouted-bed reactor at 500 °C and studied the yield and quality of bio-oil to evaluate the performance of conical spouted-bed configuration during the pyrolysis process. The yield of bio-oil was relatively high (58–68 wt%) considering the type of biomass. The highest yield of bio-oil (68 wt%) belonged to IG, which was due to the high content of carbon in IG. The composition of the bio-oil was different for the different feedstocks. For instance, TS resulted in the highest amount of acids, IG produced the highest content of alcohols and NC pyrolysis led to the formation of more aldehydes.

2.2.2.6. Ablative pyrolysis. Ablative reactor design is based on the transfer of heat over a hot plate during the movement of biomass particles.[43,181] Compared to the other types of reactors, at the same rate of feeding, the size of the ablative reactor would be smaller due to its high efficiency.[43,181,182] As a result, the fixed

cost of the plant could be reduced. The absence of an inert gas is another advantage, which decreases the cost of operation.[43] Additionally, biomass with a large particle size could be fed into the reactor and also the control of the reactor is easy.[43,182] However, the cost of operation on a large scale is high and the reaction rate is limited by the heat transfer from the heating source, which needs a high cost due to the high rate of heat consumption. The pyrolysis of tobacco processing wastes was conducted by Khuenkaeo *et al.*[183] The reaction temperature was selected as 450–600 °C, which led to the formation of bio-oil with a maximum yield of 55 wt% and a HHV of 30.05 MJ kg^{-1} at 600 °C. Khuenkaeo *et al.*[184] pyrolyzed lignocellulosic biomass residues (corncobs, coconut shells, and bamboo residue) at 500 °C. The yield of bio-oil was 50 wt% for coconut shells with a HHV of 25.31 MJ kg^{-1}. The yield of bio-oil for corncobs was 72 wt% and the HHV of bio-oil was 19.98 MJ kg^{-1}. For bamboo residue, the yield and HHV were 45 wt% and 20.42 MJ kg^{-1}, respectively. Auersvald *et al.*[185] conducted the pyrolysis of different biomass materials including beech wood, poplar wood, straw and *Miscanthus* at 550 °C. The yield and HHV of the organic phase of the bio-oil were 60 wt% and 62 MJ kg^{-1} for beech wood, 60 wt% and 67 MJ kg^{-1} for poplar wood, 20 wt% and 28 MJ kg^{-1} for straw and 21 wt% and 27 MJ kg^{-1} for *Miscanthus*.

2.2.2.7. Grinding pyrolysis. Grinding pyrolysis technology was developed in Australia by Renergi Pty Ltd.[43] on a pilot scale (10 kg h^{-1} biomass feeding) and on a demonstration scale (100 kg h^{-1} biomass feeding rate). It was fundamentally based on the grinding of the outer layer of biomass particles by hot steel balls in a rotating reactor.[186,187] Hasan *et al.*[188] studied the pyrolysis of mallee wood chips with different particle sizes. Their results showed that biomass in the powder form and big particles (few cm) could be fed into the reactor. Their operating temperature was in the range of 400–500 °C. The reactor could operate for a few days on both lab and demonstration scales. However, the blocking of the feeding pipe to the reactor by biomass and also the blockage of the condensers and connection pipeline in the outlet of the reactor were the main disadvantages of the grinding pyrolyzer. The yield of bio-oil was also low (<60 wt%) with a high content of acids (up to 15 wt%) and water (up to 35 wt%) compared to the bio-oil produced from the fluidized-bed reactor.

2.2.2.8. Auger reactor. The auger reactor is made of a hot and an oxygen free cylinder, which includes an auger inside to push the biomass forward inside the reactor.[43,189] The yield of bio-oil obtained from the auger reactor is high, but lower than the yield of bio-oil, which is produced in the fluidized-bed reactor.[43,189] Due to the high efficiency of heat transfer, the auger reactor does not need a high amount of heat. It is also compact and there is no need for a carrier gas. The char with high quality is also produced by the use of the auger reactor during the pyrolysis of biomass. However, there is a risk of plugging inside the reactor and transferring pipes. On large scales, there is a limitation for uniform temperature distribution.[43] Puy *et al.*[190] conducted the pyrolysis of pine woodchips at 500–800 °C. The highest yield of bio-oil (58.7 wt%) was obtained at 500 °C. However, the content of heavy species with the boiling point of more than 350 °C was higher in the bio-oil produced at 500 °C. Papari *et al.*[191] pyrolyzed softwood sawdust at 465 °C under vacuum pressure. Bio-oil with a yield of 54 wt% and HHV of 28 MJ kg^{-1} was obtained. The pyrolysis of sawdust from the furniture industry was carried out by Ahmed *et al.*[192] at 400–600 °C. The yield of bio-oil was the highest (45.1 wt%) at 500 °C. However, the calorific value of the bio-oil was the highest (29.871 MJ kg^{-1}) at 600 °C.

Miscanthus was pyrolyzed by V. Lakshman *et al.*[193] in an auger reactor at 425–575 °C. The yield of bio-oil was low (<40 wt%) in the range of temperature, which was used. This indicated the low efficiency of the auger reactor for the production of the bio-oil. The highest yield of the bio-oil (18.8 wt% oil phase and 18.3 wt% aqueous phase) was obtained at 510 °C. The high heating value of the organic phase of the bio-oil was measured to be 15.8 MJ kg^{-1}, which was relatively low considering the bio-oil produced from the other types of reactors under the same conditions of operation and feedstock. Bio-oil included a high content of oxygen-containing species such as acids, which resulted in a low heating value. As a result, the auger reactor is not a suitable candidate for the production of bio-oil through fast pyrolysis.

2.2.3. Catalysts. Fast pyrolysis leads to the formation of bio-oil as the main product. It is aimed to replace the fossil based liquid fuels. However, the fuel properties of the bio-oil are not in the standard ranges required for the engine fuels. For instance, the heating value of the bio-oil is in the range of 16.79–19.0 MJ kg^{-1},[194,195] which is in the range of ethanol, while it is far from the heating value of the fuels such as gasoline and diesel (40–45 MJ kg^{-1}).[194] The reason for this is the high content of oxygen-containing compounds such as water, acids and phenolics in the bio-oil, which results in high acidity, aging during the storage time, corrosiveness, *etc.*[194,195] Therefore, catalytic pyrolysis was proposed to remove the oxygen from the bio-oil and crack down the large species. Many studies have been conducted on the effect of different catalysts for the improvement of bio-oil properties. However, still the high rate of polymerization reactions, which forms coke, remains the main problem in this field. In the following section, the summary of the different catalysts' performances in the pyrolysis of biomass is explained.

2.2.3.1. Zeolites. Zeolites are the most popular group of catalysts, which have been tested in the pyrolysis of biomass.[196,197] They are very active for cracking and dehydration reactions and can remove the non-desirable species such as carboxylic acids, phenolics, ethers, esters, *etc.* from bio-oil.[196,198] Their three-dimensional and porous structure enhances the possibility of the contact of bio-oil with them. This increases the cracking of large species, the deoxygenation of acids, *etc.* to improve the quality of bio-oil by the production of small linear, cyclic and aromatic compounds.[196,199] Three types of zeolites are recognized based on their pore sizes including small pore size (<0.5 nm) zeolites (ZK-5 zeolite-based catalysts), medium pore size zeolites (ZSM-5 and ZSM-11) and large pore size (0.6–0.8 nm) zeolites (Y zeolite). The main products from small and large pore size zeolites have a high tendency for the cracking reaction, which leads to the formation of small species. However,

Table 4 The summary of the results obtained by the use of zeolites during the pyrolysis of biomass. Reprinted from ref. 3 with permission from the Royal Society of Chemistry

Catalyst	Reactor	T (°C)	Feedstock	Results	Ref.
β-Zeolite and Ca–Y-zeolite	*In situ*, fluidized-bed	450	White oak	β-Zeolite and Ca–Y-zeolite were effective for deoxygenation, reducing bio-oil yield from 62 to *ca.* 30 wt%	204
Clinoptilolite	*In situ*, fixed-bed	550	Cottonseed cake	Calorific value of bio-oil was enhanced over clinoptilolite to 36.08 MJ kg^{-1} over from 17.99 MJ kg^{-1}	205
Hβ-zeolite	*In situ*, fixed-bed	400–440	Pinewood	Bio-oil yield reduced from 47.7 wt% over the catalyst to 26.0 wt% with coke yield up to 11 wt%	206
H-ZSM-5 and Hβ-zeolite	*Ex situ*, fixed-bed	400	Rapeseed cake	H-ZSM-5 was more resistant to coking than Hβ-zeolite, retaining more organics in bio-oil	207
Hβ, HZSM-5 and Ga/HZSM-5	*Ex situ*, fixed-bed	450	Particle board	Modification of HZSM-5 with Ga enhanced formation of aromatics *via* deoxygenation	208
HZSM-5, HY and Ga/HZSM-5	*Ex situ*, fluidized-bed	450–550	Radiata pine sawdust	Ga/HZSM-5 was selective for the production of aromatics, while HY catalyzed the formation of significant amounts of coke	209
ZSM-5, HY and USY	*In situ*, fixed-bed	500	Corn stalks	USY promoted the formation of aromatics but decreased he bio-oil yield. ZSM-5 was the opposite	200
HZSM-5	*In situ*, conical spouted-bed	400–500	Pinewood sawdust	High cracking rate of HZSM-5 suppressed the formation of oxygen-containing species	210
ZSM-5	*In situ*, fixed-bed	400–650	Pine wood	Coke yield on carbon basis was up to 20 wt% at 650 °C, which was suppressed by increasing temperature	211
HZSM-5 and MFI-zeolite	*Ex situ*, fixed-bed	450–550	Radiata pine sawdust	Bio-oil yield reduced from 54.2 to 46.6 wt% over HZSM-5 and to 42.9–50.6 over MFI-zeolite with a high yield of coke (13.6–21.3 wt%)	212
ZSM-5	*Ex situ*, fluidized-bed	400–600	Rice husk	High rate of cracking over the catalyst increased the yield of aromatics, but generates coke with a yield of 7.8–12.0 wt%	213
HZSM-5	*In situ*, fluidized-bed	550	Corncob	HZSM-5 enhanced the content of aromatics from 7.62 to 74.22 wt% and the HHV of bio-oil from 18.8 to 34.6 MJ kg^{-1}	214
HZSM-5	*Ex situ*, fluidized-bed	500–550	Wood mixture	High cracking activity of HZSM-5 reduced the yield of bio-oil from 40.4 to 5.5 wt%	215
HZSM-5	*In situ*, fluidized-bed	450–500	Hybrid poplar wood	The use of HZSM-5 enhanced the HHV of bio-oil from 24.48 to 30.5 MJ kg^{-1}	216
HZSM-5	*Ex situ*, fixed-bed	550	Jatropha wastes	Carbon selectivity for coke was 53.7–69.3 wt%, while the bio-oil yield reduced from 42.7 to 34.6 wt%	217
Pt-*meso*-MFI	*Ex situ*, fixed-bed	450	Rice husk	Pt enhanced the activity of *meso*-MFI for deoxygenation, decreasing the yield of oxygenates by 49%	218
ZSM-5	*In situ*, fluidized-bed	550	Rice husk	ZSM-5 showed high selectivity for naphthalene (12.1%), but the yield of coke was up to 32.2 wt%	203

Table 4 (*Contd.*)

Catalyst	Reactor	T (°C)	Feedstock	Results	Ref.
H-ZSM-5, MgO/H-ZSM-5, ZnO/H-ZSM-5, H-beta, MgO/H-beta and ZnO/H-beta	*Ex situ*, fixed-bed	500	Eucalyptus woodchips	Metal oxides reduced Brønsted acid sites, but enhanced Lewis acid sites of the zeolites	202
ZSM-5	*In situ*, micro-pyrolyzer	550	Red oak	Low yield of bio-oil (27.9 wt%) with a high content of aromatics was obtained	219
Steel slag-derived zeolite (FAU-SL)	*In situ*, fixed-bed	450–600	Oil palm mesocarp fiber	The catalyst promoted gas formation, but reduced the production of bio-oil and biochar	220
Cu/zeolite, Ni/zeolite and CuNi/zeolite	*Ex situ*, infrared image gold furnace	500	Pine wood	CuNi/zeolite showed higher deoxygenation and cracking rates, but Cu/zeolite and Ni/zeolite catalyzed the formation of more aromatics	221
Ni_2P-loaded zeolite	*Ex situ*, fixed-bed	350–500	Water hyacinth (WH) and algae bloom (AB)	The catalyst reduced oxygen content in bio-oil but enhanced the formation of aromatics	222
ZSM-5	*In situ*, fast stirred	600	Loblolly pine	Catalyst reduced the production of heavy oil and gas, but enhanced the formation of light ones and char	223
HZSM-5, Fe/ZSM-5, Ni/ZSM-5 and FeNi/ZSM-5	*In situ*, tube reactor	500	Softwood sawdust	The catalysts enhanced the formation of monoaromatics and naphthalene as well as acidity of the bio-oil, but coking was significant	224
HZSM-5	*Ex situ*, fixed-bed	491–495	Biomass	Coke formed included 9.90 wt% filamentous and 2.25 wt% graphite-like materials	225
Fe-, Co- and Cu-loaded HZSM-5	*Ex situ*, fixed-bed	500	Rape straw	Monocyclic aromatic and aliphatics yields were enhanced 2.5 time by the metal dopped catalysts, and Cu/HZSM-5 and Fe/HZSM-5 produced the least amount of coke	201
SiC@MZSM-5	*Ex situ*, fixed-bed	500	Pine sawdust	Higher yields of bio-oil (45.9 wt%) and also coke (35.1 wt% based on carbon) were obtained with internal heavy fraction recycling	226
ZSM-5(11)@SBA-15, ZSM-5(15)@SBA-15 and ZSM-5 (22)@SBA-15	*In situ*, fixed-bed	500	Corn stalk	The catalysts produced a high amount of phenolics and carbonyls in bio-oil as well as a remarkable amount of coke	227
HZSM-5	*In situ*, microfluidized-bed	500	Oak	Coke was formed initially in the pores and then on the surface, with aromatics as the main precursors of coke	228
HZSM-5	*In situ*, fluidized-bed	500	Oak	Three types of coke including coke inside micropores, formed on the outer surface of the catalyst. The coke in micropores was the main reason for catalyst deactivation	229
n-ZSM-5, h-ZSM-5 and ZrO_2/*n*-ZSM-5	*Ex situ*, fixed-bed	400	Acid-washed wheat straw	ZrO_2 reduced the rate of cracking and coke amount, but increased the conversion of oligomers into GC-MS detectable compounds	230

medium pore size zeolites are very active for aromatization reactions and they lead to the formation of approximately 35 wt% aromatics for ZSM-5 and approximately 25 wt% aromatics for ZSM-11 in bio-oil.[199] In Table 4,[200–230] the summary of the results obtained by the use of different types of zeolites in the pyrolysis of biomass is shown. Uzun *et al.*[200] studied the performance of different zeolite catalysts including ZSM-5, HY and USY for the pyrolysis of corn stalks in a tubular fixed-bed

reactor at 500 °C. The catalysts used showed a high rate of cracking and as a result the yield of bio-oil decreased in the presence of the catalysts. The highest yield of bio-oil was obtained for ZSM-5 (the yield of bio-oil was 33.30 wt% for non-catalytic pyrolysis and 27.55 wt% for ZSM-5). Furthermore, the quality of bio-oil improved, but differently for different catalysts. For instance, the HHV of the bio-oil was 29.74 MJ kg^{-1} for the non-catalytic pyrolysis, 33.30 MJ kg^{-1} for ZSM-5, 36.92 MJ kg^{-1} for HY and 33.74 MJ kg^{-1} for USY. HY had a higher tendency for deoxygenation and led to a higher HHV for the bio-oil. In addition, USY produced the highest amount of aromatics (46 wt%) in the bio-oil, while HY resulted in the highest content of aliphatics inside the bio-oil (36 wt%). The reason for the higher amount of aromatics in the bio-oil was the lower ratio of silica to alumina in USY. The higher acidity and the larger pore size of HY led to the formation of more char and coke during the pyrolysis. Li *et al.*[201] pyrolyzed rape straw over HZSM-5 in a two-stage process at 500 °C and −5 kPa. The presence of the catalyst decreased the yield of bio-oil from 44 to 37 wt%, while the HHV of bio-oil increased from 28.44 to 32.11 MJ kg^{-1}. Coke was also formed with a yield of 4 wt%. HZSM-5 was active for the deoxygenation and cracking of volatiles. As a result, the yield of the gas phase enhanced, while the yield of char stayed constant at 24 wt%. Hernando *et al.*[202] conducted the pyrolysis of eucalyptus woodchips over hierarchical ZSM-5 and beta zeolites, on which MgO and ZnO were loaded. Their results showed that the catalysts used led to the decrease of the bio-oil yield due to the high rate of cracking reaction. MgO/h-beta had the lowest rate of cracking and the bio-oil yield was 34.6 wt%, while ZnO/h-ZSM-5 showed the highest rate of cracking (the bio-oil yield was 25.4 wt%). The HHV of the bio-oil enhanced differently from 23.37 MJ kg^{-1} for non-catalytic pyrolysis to the highest (29.45 MJ kg^{-1}) for ZnO/h-ZSM-5 and the lowest (24.69 MJ kg^{-1}) for MgO/h-beta. The differences in acidity, pore size and the surface area of the catalysts led to these different results. For instance, ZnO/h-ZSM-5 had a higher Si/Al (58 on mole basis) compared to MgO/h-beta (Si/Al was 24 on mole basis).

13X zeolite showed high activity to improve the quality of the bio-oil during the pyrolysis of residual rapeseed biomass in the study by David *et al.*[231] The reaction was conducted in a two stage batch reactor at 550 °C. 13X zeolite did not change the yield of the products significantly. For instance, the yield of the bio-oil was 49 wt% in the absence of the catalyst, while it reduced to 48 wt% by loading 25 wt% (catalyst : biomass mass ratio). However, the heating value of the bio-oil enhanced from 24.95 to 32.45 MJ kg^{-1}, which was due to the increase of the rate of deoxygenation reaction by 13X zeolite. It is worth mentioning that the content of light alcohols, esters, aldehydes and ketones in the bio-oil increased by the catalyst. However, the amount of light acids, ethers and phenols reduced. The molecular shape and pore characteristic can change the properties of the bio-oil significantly.[232] Hu *et al.*[232] studied the effect of HSAPO-34, HZSM-5, HM, Hβ, HUSY, HMCM-41 and HZSM-5@ silicalite-1 catalysts on the properties of bio-oil. The pyrolysis reaction was performed in a bench scale continuous feeding two-stage fluidized-bed/fixed-bed combination reactor at 550 °C and pine sawdust was selected as feedstock. The highest BET surface area (708.1 m^2 g^{-1}) belonged to HMCM-41, while the lowest amount (355.9 m^2 g^{-1}) was related to HZSM-5. Correspondingly, the highest and lowest volumes of the pores were for HMCM-41 and HZSM-5, respectively. The results indicated that the catalyst having larger pores and higher pore volume had the pyrolysis reactions in the pores, while the lower pore volume led to the reaction to be performed on the surface of the catalyst. As a result, higher pore volume resulted in more efficient pyrolysis and the properties of the bio-oil improved more. As an example, the rate of naphthalene alkylation was lower for HZSM-5 compared to HMCM-41.

2.2.3.2. Metal-based catalysts. Metal catalysts in the forms of metals, metal oxides and metal salts have been used to upgrade the products from the pyrolysis of biomass.[233–235] Depending on the types of metals, they showed different tendencies for cracking, aromatization and deoxygenation reactions (Table 5).[203,236–243] For instance, Ni showed a high tendency for cracking and aromatization, while Cs had a high tendency for the deoxygenation reaction.[244–246] Mante *et al.*[247] studied the pyrolysis of biomass in a micro-reactor over anatase TiO_2 nanorods, CeO_x–TiO_2 mixed oxides, and pure CeO_2, ZrO_2, and MgO at 550 °C. The aim was to monitor the activity of the catalyst for the production of highly valuable ketones. The catalyst to feedstock mass ratio was selected as 8 : 1. Their results indicated that CeO_2 had a high tendency for the ketonization reaction. TiO_2 nanorods showed low activity for the ketonization reaction. However, by loading Ni on TiO_2 nanorods, the activity of the catalyst for the ketonization reaction enhanced. Commercial anatase nanopowder had a high tendency for the ketonic decarboxylation reaction. Pt/TiO_2 was very active for the deoxygenation reaction and reduced significantly the content of ketones in the bio-oil. CeO_x–TiO_2 had a lower tendency for the ketonization reaction compared to CeO_2 and TiO_2. ZrO_2 and MgO also had a lower tendency for producing ketones. Lu *et al.*[248] studied the pyrolysis of wheat straw over Fe/SiO_2, Ca/SiO_2 and Fe–Ca/SiO_2 catalysts in a fixed-bed reactor at 600–750 °C. Fe/SiO_2 was very active for decarboxylation and ketonization reactions, while Ca/SiO_2 enhanced the rate of dehydration, aromatization and waster–gas shift reactions. The yield of tar was 17 for 1Fe/16SiO_2 and 7 wt% for 1Ca/16SiO_2. Fe–Ca/SiO_2 had a high tendency for the dehydrogenation reaction and the yield of tar was 23 wt% for 1.5Ca–5Fe/16SiO_2. Li *et al.*[236] investigated the effect of $ZnCl_2$ on the pyrolysis of rape straw, corn straw, walnut shells, chestnut shells, camphor wood and pine wood in a tube furnace reactor at 500 °C. $ZnCl_2$ increased the rate of char formation reaction and consequently the yield of biochar changed from 25.45 to 36.21 wt%. The yield of bio-oil did not change. $ZnCl_2$ had a different performance during the pyrolysis of pine wood. It increased the yield of the gas phase, while decreased the yield of bio-oil. $ZnCl_2$ was very active to produce aldehydes and ketones in the bio-oil. The type of feedstock influenced the amount of different species in the bio-oil. For instance, the higher content of cellulose and hemicellulose in camphor wood and pine wood led to the formation of a higher amount of aldehydes and ketones in the bio-oil.

Metal catalysts are deactivated quickly during the pyrolysis of biomass. Different groups of metals lead to the formation of

Table 5 The summary of the results obtained by the use of metal based catalysts during the pyrolysis of biomass. Reprinted from ref. 3 with permission from the Royal Society of Chemistry

Catalyst	Process and reactor	T (°C)	Feedstock	Results	Ref.
ZrO_2–FeO_x	*Ex situ*, fixed-bed quartz	500	Cacao pod husks	Catalyst enhanced the ketonization and demethylation, forming more ketones and phenolics	237
Zn, Co, Fe, Ni, Ce and Mn salts	*In situ*, fixed-bed	500	Eucalyptus	Mn, Ni and Ce salts catalyzed the deoxygenation of bio-oil	238
$MgCl_2$	*In situ*, fluidized-bed	450–550	Yellow poplar wood	The catalyst enhanced the dehydration reaction and reduced the viscosity of bio-oil	239
TiO_2, SO_4^{2-}/TiO_2, SO_4^{2-}/TiO_2–Fe_3O_4	*In situ*, CDS pyroprobe	300	Cellulose and poplar wood	The catalysts promoted cracking reactions, especially for SO_4^{2-}/TiO_2–Fe_3O_4	240
MgO, NiO, Al_2O_3, ZrO2/TiO_2, Zr, Ti, Zr/Ti	*Ex situ*, fixed-bed	500	Beech wood	The catalysts promoted the deoxygenation and enhanced the production of aromatics, especially the Zr/Ti catalyst	241
Gamma-Al_2O_3	*In situ*, fluidized-bed	550	Rice husk	Catalyst catalyzed the formation of aromatics and C_2–C_4 olefins but the activity was low	203
Fe/SiO_2, Ca/SiO_2, Fe–Ca/SiO_2	*In situ*, fixed-bed	600–750	Wheat straw	High rates of decarboxylation and dehydration was observed for Fe/SiO_2 and Ca/SiO_2. Fe–Ca/SiO_2 enhanced the amount of H_2 and aromatics in bio-oil. Ca enhanced the rate of deoxygenation of Fe	242
$ZnCl_2$	*Ex situ*, tube furnace	500	Rape straw, *etc.*	$ZnCl_2$ increased the yield of biochar and the production of aldehydes and ketones	236
Fe_3O_4, TiO_2	*In situ*, fixed-bed	500 and 800	Sapwood	Higher rate of cracking was observed for both catalysts, enhancing the formation of aromatics	243

different amounts of coke.[249] Li *et al.*[249] studied the performance of alkali metals and alkaline earth metals during the pyrolysis of rice husk. The experiments were carried out by Py-GC/MS and Py-SVUV-PIMS at 550 °C. Prior to the experiment, Na^+ (416.67 μmol g^{-1}), K^+ (30.58 μmol g^{-1}), Ca^{2+} (16.18 μmol g^{-1}) and Mg^{2+} (10.06 μmol g^{-1}) were loaded on the feedstock. The results indicated that alkali metals had a tendency for the fragmentation and ring-fission of sugar units and their presence resulted in the formation of a higher amount of aldehydes, ketones and acids. In addition, the content of phenolics was enhanced by using alkali metals due to the higher rate of secondary decomposition reactions of lignin. Larger phenolics were further polymerized and coke with the structure of aromatics was formed. On the other hand, alkali earth metals were more active for the destruction of cellulose and hemicellulose and as a result, anhydrosugars and furfural were formed. The coke was produced mainly from the polymerization of anhydrosugars.

A Ni–Al nanosheet catalyst was used by Yang *et al.*[250] to enhance the content of H_2 during the pyrolysis of rice husk in a two-stage fixed-bed reactor at 600 °C for the first stage (pyrolysis) and 500–800 °C for the second stage (catalytic reforming). The catalyst and the increase of the temperature led to the significant increase of the H_2 content in the gas phase. In addition, the yield of the gas enhanced remarkably by the catalyst, which showed the increase of the rate of the secondary cracking and reforming reactions. For instance, the yield of H_2 in the non-catalytic and catalytic processes was 1 and 14 mmol g^{-1} of biomass, respectively.

2.2.3.3. Noble metals. Noble metals have been used for the pyrolysis of biomass in recent years.[250,251] The reason for their application was the low amount of coke and the high rate of deoxygenation reaction compared to the other groups of catalysts.[19,250,251] However, their high price and the difficulties in their regeneration prevented their uses in large scale operations. Pd/C, Pt/C and Ru/C were the common noble metal based catalysts, which have been used in the pyrolysis of biomass. The summary of the results of biomass pyrolysis in the presence of different noble metals is shown in Table 6.[252–256] For instance, in the study by Lazdovica *et al.*,[252] wheat straw was pyrolyzed in TG-FTIR over Pt/C and Pd/C at 700 °C. Pt/C showed a higher tendency for deoxygenation, while Pd/C was active for cracking and aromatization reactions. Wang *et al.*[257] investigated the effect of the Pd/C catalyst in the pyrolysis of larch sawdust in fluidized-bed and fixed-bed catalytic reactors at 550 and 450 °C, respectively. Pd/C showed relatively high activity for cracking and decarboxylation reactions. As a result, the content of phenolic compounds in the bio-oil enhanced from 19.69 to 25.03 wt%, while the amount of carboxylic acids in the bio-oil reduced from 7.83 to 4.44 wt%. The study by Lu *et al.*[253] indicated that Ru and Pd had different effects on the upgrading of

Table 6 The summary of the results obtained by the use of noble metal based catalysts during the pyrolysis of biomass. Reprinted from ref. 3 with permission from the Royal Society of Chemistry

Catalyst	Process and reactor	T (°C)	Feedstock	Results	Ref.
Pt/C, Pd/C	*In situ*, TGA-FTIR	700	Wheat straw	Both catalysts enhanced the deoxygenation, but more aromatics and olefins were formed over Pd/C, while more methane and carbon dioxide were formed over Pt/C	252
ZSM-5, Pd/C, MCM-41, Pt/C	*In situ*, TGA-FTIR	700	Wheat bran	Noble metal catalysts enhanced the formation of aromatics, while zeolites enhanced the production of aliphatics and olefins	254
TiO_2 (rutile), TiO_2 (anatase), ZrO_2 & TiO_2, *etc.*	*Ex situ*, Py-GC/MS	500	Poplar wood	Pd/$CeTiO_2$ enhanced phenolics formation, while ZrO_2 or TiO_2 reduced the production of phenols, acids and sugars, but enhanced the formation of linear ketones and cyclopentanones	253
W_2C/AC, W_2N/AC, Mo_2C/AC, Mo_2N/AC	*Ex situ*, Py-GC/MS	600	Pine wood	Tungsten-based catalysts enhanced the formation of monomeric phenolics while decreasing the production of anhydrosugars and linear aldehydes	255
Mo_2N, W_2N, MoP and WP supported on Hβ, HY and HZSM-5	*Ex situ*, Py-GC/MS	450–850	Pine wood	Modification of the zeolites enhanced the cracking and deoxygenation, producing more monoaromatics	256

volatiles during the pyrolysis of poplar wood in a pyrolysis-gas chromatography/mass spectrometry (Py-GC/MS) system at 500 °C. For this aim, Pd/$CeTiO_2$, Ru/$CeTiO_2$, Pd/$CeZrO_2$ & TiO_2 and Ru/$CeZrO_2$ & TiO_2 were selected as catalysts. Pd/$CeTiO_2$ had the highest activity to produce phenolics (phenolic content in the bio-oil during the non-catalytic pyrolysis and in the presence of Pd/$CeTiO_2$ was 25.6 and 37.2 area%, respectively). The presence of ZrO_2 in the catalyst formulation led to the further destruction of sugar and the increase of the rate of deoxygenation and ketonization reactions.

The combination of Pt and Ni over Al_2O_3 showed a high tendency for the hydrodeoxygenation reaction and reduced the formation of coke significantly in the study by Zheng *et al.*[19] Pine sawdust was selected as feedstock and the reaction was conducted in a Py-GC × GC/MS at 450 °C for pyrolysis and 500 °C for the catalytic part. The Pt to Ni mass ratio was 0 : 1, 2 : 1, 1 : 1, 1 : 2 and 1 : 0. The loading of Pt over Ni/Al_2O_3 enhanced the rate of hydrogenation. As a result, the polymerization of oxygen-containing species reduced and less coke was formed. By the increase of the Pt amount in the catalyst, the yield of coke decreased. As an example, the yield of coke was 15 wt% for Ni/Al_2O_3, while it reduced to 7 wt% for Pt–Ni/Al_2O_3 (the Pt to Ni mass ratio was 2 : 1).

2.2.3.4. Bimetallics. Bimetallics were used in the pyrolysis of biomass to reduce the amount of coke and to enhance the rate of deoxygenation, aromatization, *etc.* reactions.[258–261] The correct selection of metals can improve the fuel properties of the bio-oil. The main bimetallics used in the pyrolysis of biomass were Ni–Ca, Ni–Co and Ni–Cu. Ni was selected as the main component of bimetallics due to its high tendency for the deoxygenation reaction.[262–264] However, Ni had high activity for cracking and coking reactions, which led to the addition of the second metal to improve its performance.[262–264] The results from the literature, which are shown in Table 7,[243,262,263] indicated that the addition of Ca could reduce the rate of cracking reaction of Ni, while enhancing the rate of aromatization reaction.[262] The

Table 7 The summary of the results obtained by the use of bimetallic catalysts during the pyrolysis of biomass. Reprinted from ref. 3 with permission from the Royal Society of Chemistry

Catalyst	Process and reactor	T (°C)	Feedstock	Results	Ref.
Ni/Ca-promoted Fe	*Ex situ*, fixed-bed	600–750	Wheat straw	Iron addition enhanced the production of hydrocarbon and hydrogen, while suppressed coking	262
Ni/cordierite, Co/cordierite, Ni–Co/cordierite	*Ex situ*, fixed-bed	800	Sawdust	The catalysts showed a high tendency for the destruction of tar, especially over Ni–Co/cordierite	263
Cu/zeolite, Ni/zeolite and CuNi/zeolite	*Ex situ*	500	Pine wood	Cu/zeolite produced a higher amount of aliphatics, but Ni/zeolite produced both aliphatics and aromatics. CuNi/zeolite had a higher rate of deoxygenation	228

presence of Co increased the rate of reforming reaction, while reducing the rate of cracking reaction by Ni.[263] Cu was very active to increase the rate of dehydration, decarboxylation and decarbonylation reactions.[264] Lu *et al.*[262] studied the pyrolysis of wheat straw over a Ni/Ca-promoted Fe catalyst in a fixed-bed reactor. The reaction was conducted at 600–750 °C. Ca led to the quick formation of coke. Ni was active for cracking and gasification reactions and Fe was active for breaking C–O and C–C bonds. By the combining of Ni, Ca and Fe, the formation of coke and char slightly decreased, while the content of small aromatics such as benzene, toluene, xylene, *etc.* increased. In another study, the combination of Ni and Co was used as a catalyst by Lu *et al.*[263] to pyrolyze sawdust in a fixed-bed reactor at 800 °C in an *ex situ* process. Ni/cordierite, Co/cordierite and Ni–Co/cordierite were the catalysts. The results indicated that Ni_3–Co_1/cordierite enhanced the rate of reforming reaction and the highest amount of conversion for tar (89%) was obtained in its presence. It also increased the amount of monoaromatics such as benzene, toluene, *etc.* inside the bio-oil. Kumar *et al.*[264] investigated the effect of Cu/zeolite, Ni/zeolite and CuNi/zeolite catalysts during the pyrolysis of pine wood at 500 °C in an *ex situ* process. The CuNi/zeolite catalyst was very active for dehydration, decarboxylation, and decarbonylation reactions, while Ni/zeolite was active for cracking and Cu/zeolite led to the formation of a high amount of aliphatics in the bio-oil.

The combination of Ni and Cu reduced the formation of coke and enhanced the quality of bio-oil.[261] Zheng *et al.*[261] used Ni–Cu/HZSM-5 during the pyrolysis of pine wood in a Py-GC × GC/MS at 500 °C. The Ni–Cu loading amount over HZSM-5 was 10 wt% and the mass ratio of Ni : Cu was selected as 1 : 2, 2 : 2 and 2 : 1. The combination of Ni and Cu enhanced the rate of deoxygenation reaction and a higher content of aliphatics was produced. The higher loading ratio of Ni to Cu led to the formation of alkanes, aliphatics and aromatics due to higher rates of decarbonylation, decarboxylation and aromatization reactions. However, the higher content of Cu in the catalyst resulted in the production of more olefins and phenolics because of higher rates of dehydration and demethylation reactions. Compared to Ni/HZSM-5 and Cu/HZSM-5, the yield of coke reduced by 28.87–30.12% and the content of aliphatics in the bio-oil increased by 29.86%.

2.2.3.5. Fluid catalytic cracking (FCC) catalyst. The FCC catalyst contains a crystalline Y-zeolite, matrix, binder and filler in its structure and it is mainly used for the cracking of heavy fractions inside crude petroleum to obtain gasoline or diesel.[265–269] The use of the FCC catalyst in the pyrolysis of biomass has been investigated by several research teams (Table 8).[270–274] Bertero *et al.*[270] investigated the pyrolysis of pine sawdust at 500 °C. The reactor type was fixed-bed and the reaction was conducted in an *ex situ* process with FCC (100–120 μm) as a catalyst. The yield of hydrocarbons in the bio-oil increased up to 25% in the presence of the catalyst. Due to the high tendency of the FCC catalyst for the deoxygenation reaction, the yield of oxygen-containing compounds decreased up to 55%. A high amount of coke (yield of 11.1 wt%) was formed on the surface of the catalyst. This indicated that coke formation was the main disadvantage for the FCC catalyst. In the study by Zhang *et al.*,[203] the FCC catalyst showed high

Table 8 The summary of the results obtained by the use of the FCC catalyst during the pyrolysis of biomass. Reprinted from ref. 3 with permission from the Royal Society of Chemistry

Catalyst	Process and reactor	*T* (°C)	Feedstock	Results	Ref.
Modified FCC catalysts with alkali and acid treatment	*Ex situ*, fixed-bed	550	Pine sawdust	Alkali modified FCC showed a higher rate of deoxygenation and lower coke yield. Acid treated FCC catalyst enhanced the formation of aromatics and gasoline range compounds	272
Commercial equilibrium FCC catalyst	*Ex situ*, fixed-bed	500	Pine sawdust	Catalyst increased the yield of hydrocarbons by 25% and decreased the content of oxygen-containing compounds by 55%. Coke yield was 20 wt%	270
Spent FCC	*In situ*, fluidized-bed	550	Rice husk	Catalyst showed a high tendency to produce monoaromatics, while a high amount of coke (26.3 wt%) was also formed	203
Commercial FCC catalyst	*Ex situ*, fixed-bed	500	Spruce wood	Coke yield reached 42.08 wt% and phenolics, furans and ketones were the main compounds in the products	271
FCC-L, FCC-H and their steamed form	*Ex situ*, bubbling fluidized-bed	465	Poplar wood	Steam treatment of the FCC catalyst enhanced the activity for cracking. Higher content of zeolite in FCC-H also led to a higher rate of cracking	273
Fresh and spent FCC catalyst	*In situ*, fluidized-bed	400	Corncob	High rate of cracking and deoxygenation was seen for both catalysts. Phenolics, furan and ketones were the main compounds in the bio-oil	274

activity to produce monoaromatics. Rice husk (0.1–0.3 mm) and a fluidized-bed reactor working at 550 °C were selected to conduct the experiment. The FCC catalyst with a particle size of 0.063–0.154 mm was used. The biomass feeding rate to the reactor was 44 g h^{-1} and it continued for 30 min. The FCC catalyst led to the formation of a high amount of aromatics (carbon yield was 8 wt%) and olefins (carbon yield was 7 wt%) in the bio-oil. The yield of coke was measured to be 26.3 wt%. Adam *et al.*[271] studied the pyrolysis of spruce wood in a fixed-bed reactor at 500 °C. The process was performed in an *ex situ* form and catalyst : biomass mass ratio was selected as 0.46. A high yield of organics (19.52 wt% on feed biomass basis) was obtained in the presence of the catalyst, but the yield of coke was very high (42.08 wt% based on feed biomass).

The FCC catalyst deactivates quickly due to the formation of coke.[275] Socci *et al.*[275] investigated the effect of the FCC catalyst in the pyrolysis of beech wood in a Frontier Labs single-shot tandem micropyrolysis system at 500 °C. The catalyst enhanced slightly the yields of CO (from 3.1 to 4.1 wt%) and CO_2 (from 3.1 to 3.8 wt%) due to the increase of the rate of decarbonylation and decarboxylation reactions, respectively. The content of furans and phenolics in the bio-oil increased, while the content of anhydrosugars decreased, which indicated a higher rate of feedstock decomposition reaction in the presence of the FCC catalyst. The yield of char/coke enhanced from 19.8 to 29.5 wt%, which demonstrated the high tendency of FCC for deactivation through the formation of coke.

2.2.3.6. Red mud. Red mud contains metal oxides such as CaO, Na_2O, SiO_2, TiO_2, Fe_2O_3, Al_2O_3, *etc.*, which led to its application in the pyrolysis process.[276] However, it did not show a high tendency for pyrolysis reactions.[277–281] In Table 9,[282–286] the summary of the results obtained by the use of red mud in the pyrolysis of biomass is shown. The pyrolysis of pinyon juniper in a bubbling fluidized-bed reactor was carried out at 450 °C by Agblevor *et al.*[282] Red mud was used in the *in situ* form and the feeding rate of biomass was selected as 0.93 kg h^{-1}. Bio-oil with a yield of 43.53 wt% and a high heating value of 28 MJ kg^{-1} was produced. The pH of bio-oil was 3.3, which indicated the low rate of deoxygenation reaction. Duman *et al.*[283] studied the pyrolysis of sun flower cake. Two-stage fixed-bed reactors were used at 300–600 °C. Red mud, which was loaded in the second reactor, did not change the yield of bio-oil. However, it reduced slightly the content of pyrolytic lignin and increased the amount of extractives in the bio-oil. As a result, a higher amount of phenolics was formed in the bio-oil. At all the temperatures used, the yield of coke was below 1 wt%. Santosa *et al.*[284] pyrolyzed a mixture of pinyon juniper, pine, and forest waste at 400–400 °C. Their results showed that the yield of bio-oil was 22 wt% at 450 °C and 38 wt% at 400 °C in the presence of red mud. Red mud as a catalyst did not increase the rate of deoxygenation reaction and also the hydrogen to carbon ratio was not changed by red mud.

Mixed food waste was pyrolyzed by Ly *et al.*[281] in a bubbling fluidized-bed reactor at 400–550 °C. Red mud (100 g) with a particle size of 150–212 μm was used as the bed material. The feeding rate was 100 g h^{-1}. The yield of bio-oil slightly increased by the increase of the temperature, which was because of the slightly higher rate of the cracking reaction. By the change of the temperature from 450 to 550 °C, the oxygen content in the bio-oil reduced due to the higher rate of deoxygenation reaction, which led to the increase of the HHV of bio-oil from 31.24 to 34.07 MJ kg^{-1}. The content of H_2 and CO increased in the gas phase, which indicated a higher rate of decarbonylation and dehydrogenation reactions at 550 °C.

2.2.4. Economic analysis and potential to compete with other technologies. Different software tools such as Aspen Plus, Chamcad, Pyrol Hysys, *etc.* were used to evaluate the benefits of using pyrolysis to convert biomass to different types of fuels.[287] The main aim of the pyrolysis process is to obtain engine fuel. However, due to the difficulties and the high expenses of upgrading, the production of biochar and chemicals has also been investigated in the literature. Based on the production of engine fuel, there have been several economic studies. For instance, Khan *et al.*[288] conducted the techno-economic analysis of olive mill wastewater sludge catalytic pyrolysis including two different cooling mechanisms. The economic analysis was performed based on a plant with a 100 tonnes per day biomass feeding rate. Red mud was selected as the catalyst and the

Table 9 The summary of the results obtained by the use of the red mud catalyst during the pyrolysis of biomass. Reprinted from ref. 3 with permission from the Royal Society of Chemistry

Catalyst	Process and reactor	T (°C)	Feedstock	Results	Ref.
Sepiolite, bentonite and attapulgite, red mud	*In situ*, auger reactor	400–500	Pine wood chip	Red mud catalyzed the formation of less oxygen-containing compounds, but more aromatics and phenolics	285
Red mud	*In situ*, bubbling fluidized-bed	450	Pinyon juniper	Red mud catalyzed the formation of the bio-oil of low pH (3.3), higher heating value (28 MJ kg^{-1}) and lower viscosity (<100 cP)	282
Red mud	*In situ*, fluidized-bed	450	Pinyon juniper	The minerals such as potassium, calcium, magnesium, and phosphorus enhanced the catalytic activity of red mud	286
Red mud	*In situ*, fluidized-bed	400–450	Pinyon juniper	The red mud had low catalytic activity for deoxygenation of volatiles	284
Red mud	*Ex situ*, fixed-bed	300–600	Sun flower cake	Red mud showed reasonable activity for deoxygenation	283

reaction was conducted at 400–500 °C. The economic life time of the pyrolysis plant was considered as 20 years in the calculations. The production cost of the bio-oil was different based on the conditions used (1.78–6.19 Euros per gasoline gallon equivalent meaning 0.47–1.64 Euros per gasoline liter equivalent), which was relatively high, and by adding the transportation and other costs, it increased considerably. Therefore, the price of the bio-oil was not comparable with the price of gasoline at petrol stations. Brigagao *et al.*[289] used Aspen Hysys software to estimate the price of bio-oil produced from the pyrolysis of corncobs at 550 °C. The corncob feeding rate was 82.88 tons per h. By considering 23 years as the life time of the plant, the estimated price of bio-oil was 1.47 USD per gasoline-gallon-equivalent bio-oil. Wang *et al.*[290] studied the economy aspect for the pyrolysis of rice husk at 400–450 °C to obtain bio-oil. Their estimated selling price for the bio-oil was 0.55 USD per liter of the bio-oil. The plant life time was considered as 10 years in their calculations. Carrasco *et al.*[291] simulated the production of bio-oil from the pyrolysis of marine forest residue with a feeding rate of 2000 dry metric tons per day at 500 °C. Aspen Plus was used for this aim. By considering 30 years for the life time of the plant, the selling price of the bio-oil was calculated to be 6.25 USD per gallon. These estimations showed that depending on the parameters such as the feedstock type, process conditions, the costs in the area where the plant is going to be installed, assumptions for the prices and process parameters, the final selling price of the bio-oil could change remarkably.

2.2.5. Environmental analysis and potential to compete with other technologies. Biomass pyrolysis can emit several contaminants such as CO_2, CO, SO_2, CH_4, N_2O, particulate matters, *etc.*, into the environment.[292–294] The highest abundance of pollution belongs to CO_2, which results in greenhouse gas emission. Vienescu *et al.*[295] conducted LCA analysis of corn stover pyrolysis. The feeding rate was considered as 2000 metric tons per day and the pyrolysis was performed at 500 °C. The calculated g CO_2 per kg of pyrolysis oil was 800. In another study by Chan *et al.*,[296] the LCA analysis of Malaysian oil palm empty fruit bunch pyrolysis (at 450 °C) was performed. From their calculations, for the production of every kilogram of bio-oil, 8.27 kg of CO_2 equivalent was produced. Iribarren *et al.*[297] estimated the CO_2 emission amount to be 1.03 tons CO_2 equivalent per ton of bio-oil used, while from the combustion of an equivalent amount of fossil fuels (0.57 tons of diesel and 0.43 tons of gasoline), 3.72 tons of CO_2 equivalent was produced. Considering the calculation of Ning *et al.*,[298] by using bio-oil and biochar instead of fuel oil and coal, the decline of CO_2 emission would be 2835 kg CO_2 per m^3 of pyrolysis oil. They considered *Cryptomeria* residue as feedstock and the bio-oil production rate was assumed to be 10 000 tons. Additionally, the rate of biomass feeding was 2990 kg h^{-1}. The LCA assessment of crop straw pyrolysis at 550 °C was performed by Yang *et al.*[299] Their results indicated that CO_2 emission was 0.62 kg CO_2 equivalent per kg of crop straw.

In the study by Brassard *et al.*,[294] the pyrolysis of the 1427 kg forest residue was considered. The obtained gas was combusted to produce the energy for the pyrolyzer. Bio-oil was considered as a fuel for the boilers. Vinegar and biochar were utilized in crop cultivation and in the field, respectively. Compared to the scenario of leaving the forest residue in the field to decay, its pyrolysis led to the decrease of CO_2 production by 906.4 kg CO_2e per Mg dry biomass.

2.2.6. Commercialization status. So far, there have been many efforts to commercialize the pyrolysis of biomass. As a result, several pyrolysis plants were built up with different sizes. The summary of details for some of these plants are presented in Table 10.[43] The common issue on the pyrolysis of biomass is the possibility to extend the duration of operation and also the low quality of the bio-oil. For improving the bio-oil quality, a catalyst was used. However, the deactivation of the catalyst and the low quality of the upgraded bio-oil were the main obstacles. Therefore, hydrotreatment of bio-oil, which was designed based on the available technologies for the crude petroleum hydrotreater system, was studied. The quick deactivation of the catalyst and the high cost of the hydrotreatment process prevented this process from moving to the commercialization stage. In summary, the process development steps for the biomass pyrolysis technology are explained in the coming paragraph.

Ensyn company built up one of the initial largest biomass pyrolyzers in 1984. Joint companies of Red Arrows and Ensyn developed a fluidized-bed reactor with a large scale of feeding of biomass during 1985 to 1989. In 1996, they could build up a pyrolysis plant with a biomass feeding rate of 1667 kg h^{-1}. In 2000, Pyrovac a Canadian company developed a vacuum pyrolyzer with a feeding capacity of 3500 kg h^{-1}. Genting and BTG

Table 10 The summary of demonstration/commercial size plants for biomass pyrolysis

Year	Country	Company	Feeding rate (kg h^{-1})	Reactor type
1996	Canada	Red Arrows – Ensyn	1667	Fluidised bed/riser
2000	Canada	Pyrovac	3500	Vacuum stirred bed
2005	Malaysia	Genting	2000	Rotating cone
2013	Finland	Fortum – VALMET	10 000	Fluidised bed/riser
2014	Netherlands	BTG-BTL/EMPYRO	5000	Rotating cone
2014	USA	KiOR	21 000	Catalytic pyrolysis
2015	Netherlands	EMPYRO	36 000 tons per year	Rotating cone
2015	Finland	UPM	11 574	Circulating bed
2017	Canada	AE Cote-Nord Bioenergy/Ensyn	9000	Fluidised bed/riser
2021	Sweden	Pyrocell	40 000 tons per year dry biomass	Rotating cone

companies developed a pyrolysis plant in Malaysia in 2005 using a rotating cone reactor. In 2013, Fortum/Valmet company constructed a pyrolysis plant with a 10 000 kh per h biomass feeding rate in Finland. In 2014, BTG-BTL/EMPYRO in the Netherlands developed a rotating pyrolysis plant with a capacity of 5000 kg h^{-1} biomass feeding rate. KiOR company in USA built up a pyrolyzer with a feeding rate of 21 000 kg h^{-1} to produce bio-oil in 2014. UPM company, which is located in Finland, built up a biorefinery based on the pyrolysis with the biodiesel production rate of 11 574 kg h^{-1} in 2015. In 2017, AE Cote-Nord Bioenergy/Ensyn companies developed a biomass pyrolysis system (biomass feeding rate was 9000 kg h^{-1}). From 2015, Empyro in the Netherlands started the construction of a pyrolysis plant with 36 000 tons per year biomass feeding capacity. In 2021, Pyrocell company in Sweden developed a pyrolysis plant with a capacity of 40 000 tons per year of dry wood feeding rate. It should be mentioned that there are several other pyrolysis plants with different sizes, which are under construction in different countries, and are not included here due to the lack of information.

2.3 Hydrothermal liquefaction

2.3.1. Products. The products from the hydrothermal liquefaction of biomass are bio-oil, aqueous phase, gas phase and hydrochar.[300–302] Bio-oil from the hydrothermal liquefaction has 70–95% of the energy content of biomass.[302–305] It is full of heavy compounds containing oxygen, which require upgrading.[303] Hydrodeoxygenation is used as the main upgrading method to improve the quality of the bio-oil from the liquefaction of biomass.[302] However, still the formation of coke is one of the main obstacles for this process. Depending on the process conditions such as temperature, pressure, feedstock type, residence time, catalyst type, *etc.* different yields of bio-oil can be obtained from the liquefaction of biomass.[303–305] The gas phase with a yield of 5–10 wt%, which includes CO_2 as the main component, CO, CH_4, *etc.* is obtained from the HTL of biomass.[302] Decarboxylation and water–gas shift reactions are the main reactions to form CO_2.[302] Hydrochar is another byproduct of biomass HTL, which includes a high content of carbon, hydrogen, nitrogen and ash. Hydrochar contains a low intensity of aromatic structures, low thermal recalcitrance, low surface area and poor porosity.[302] The main applications of hydrochar are heat production, soil amendment, as an adsorbent and carbon material for fuel cells, *etc.*

2.3.2. Reactors. Different types of reactors including batch and continuous ones have been used for the HTL treatment of biomass.[306] The type of reactor can change the yields and compositions of the products.[306] Below, the summary of the performance for each reactor is given.

2.3.2.1. Batch reactors. Batch reactors are used in HTL for lab scale studies. They are cylindrical autoclaves or a straight tubing, which are mainly made from stainless steel, Hastelloy C-22 or Inconel-625 with a volume of 100–1000 mL. The feedstock, water and catalyst are loaded into the reactor prior to the experiment. The heating of the batch reactor is provided from a coil, furnace or sand bath. The operation of the batch reactor is simple, which makes it an appropriate candidate to study the fundamentals of the HTL process. However, the long duration of operation and also difficulties in loading the feedstock when the reactor is under the selected operating conditions are the main drawbacks of the batch systems. The loading of the feedstock prior to the heating up is also another issue, which increases the residence time of the solid product inside the reactor (staying inside the reactor during the heating up and cooling down). This influences the yields and also the properties of the products. Improper mixing of feedstock during the HTL process makes the temperature distribution not homogeneous at all points, which results in different process conditions inside the reactor. Different species of marine macroalgae including *Derbesia tenuissima* (Crouan), *Ulva ohnoi* (Hiraoka and Shimada), *Chaetomorpha* linum (Kutzing), *Cladophora coelothrix* (Kutzing) and two species of freshwater macroalgae (*Cladophora vagabunda* (Hoek) and *Oedogonium* sp.) were selected by Neveux *et al.*[306] as feedstock for the HTL process. The experiments were conducted in a batch reactor at 350 °C and 140–170 bar. Oedogonium had the highest yield of bio-oil (26.2 wt%) and *Chaetomorpha* showed the lowest yield of bio-oil (9.7 wt%). The HHV of bio-oil was similar for all the types of feedstock used and it was in the range of 33–34 MJ kg^{-1}. The possibility of the conversion of tobacco processing waste to bio-oil through the HTL process was studied by Saengsuriwong *et al.*[307] The reaction was performed in a batch reactor at 280–340 °C and 22 MPa. The highest yield of bio-oil (52 wt%) was obtained at 310 °C with a HHV of 31.9 MJ kg^{-1} for the heavy fraction of the bio-oil and 28.4 MJ kg^{-1} for the light fraction of the bio-oil. Hossain *et al.*[308] studied the HTL of *Scenedesmus* sp. microalgae in a batch reactor at 280–350 °C and 2 bar. The maximum yield of bio-oil (33.6 wt%) and the highest HHV of the bio-oil (29.8 MJ kg^{-1}) were obtained at 350 °C.

Stirring was used inside the batch reactor to enhance the efficiency of the HTL process. Prestigiacomo *et al.*[309] investigated the HTL processing of municipal sludge in a stirred batch reactor at 350 and 400 °C under a pressure of 0.2 MPa. The stirring rate during the HTL process was 170 rpm. The yield of bio-oil was measured to be 40 wt% at 350 °C and 32 wt% at 400 °C. The results indicated that with stirring, the yield of bio-oil was 39 wt% at 350 °C and 42 wt% at 400 °C, which meant that at high temperature, the stirring enhanced the rate of cracking, while at low temperature, it did not change the rate of cracking significantly. The HHV of the bio-oil did not change by stirring at 350 °C (it was 40.0 MJ kg^{-1} for the static and 39.9 MJ kg^{-1} for the stirring experiments). However, stirring at 400 °C slightly increased the HHV of bio-oil from 34.5 to 36.7 MJ kg^{-1}, which was due to the partial deoxygenation of heavy species. In conclusion, the batch HTL process is simple and can be used for the various types of feedstocks with variable moisture contents. However, the batch operation includes several drawbacks such as thermal transience (changing the operating conditions), difficulties in decoupling temperature and pressure (pressure of the reactor changes by the change of reactor temperature due to the presence of water, volatiles, *etc.*), difficulties in complete mixing, *etc.*

Pine wood sawdust was converted to bio-oil by Zhao *et al.*[310] through the HTL process (biomass/water mass ratio was 1 : 10) in an autoclave at 300 °C and 2 MPa. The catalyst loading amount (catalyst : biomass mass ratio) was 10 wt%. Fe_2O_3 and Fe_3O_4 were used as catalysts. Fe_2O_3 did not change the yields of the products significantly, while Fe_3O_4 reduced the yield of char and increased the yield of the gas phase, which showed a higher rate of cracking reaction. The reason was that in Fe_2O_3, Fe had the maximum oxidation state (+3) and did not participate in the HTL reactions. The performance of other catalysts including Na_2CO_3, NaOH, $FeSO_4$, MgO, Ru/C and FeS was also investigated under the same operating conditions. Na_2CO_3 resulted in the highest yield of bio-oil (38 wt%), while the lowest yield of the bio-oil (23 wt%) belonged to MgO (the yield of the bio-oil in the absence of the catalyst was 23 wt%). The highest HHV of the bio-oil was related to FeS (29.05 MJ kg^{-1}), which was due to the lower content of oxygen in the bio-oil. The bio-oil samples produced in the presence of the other catalysts had a similar HHV of almost 27 MJ kg^{-1}.

2.3.2.2. Continuous reactors. Due to the low production rate and difficulties in the control of operating conditions at a constant amount in the batch reactor, continuous operation was considered for the HTL process. Barreiro *et al.*[311] conducted the liquefaction of microalgae species including *Nannochloropsis gaditana* (*N. gaditana*, marine) and *Scenedesmus almeriensis* (*S. almeriensis*, freshwater) at 20 MPa and 350 °C in a continuous stirred-tank reactor. The yield of bio-oil was the highest (54.8 wt%) for *N. gaditana* and also it had the highest HHV (37.3 MJ kg^{-1}). The reason for this was the higher content of C (47.6 wt% for *N. gaditana versus* 38.0 wt% for *S. almeriensis*) and also the lower content of O (25.1 wt% *versus* 30.4 wt%) for *N. gaditana*. Continuous hydrothermal liquefaction of *Chlorella vulgaris* and *Nannochloropsis gaditana* was performed by Guo *et al.*[312] in a continuously stirred tank reactor at 24 MPa and 350 °C. The highest amount of bio-oil yield (36.2 wt%) belonged to *Chlorella vulgaris*, while the yield of bio-oil was 31.5 wt% for *Nannochloropsis gaditana* under the same conditions of operation. However, the HHV was slightly lower for *Chlorella vulgaris* bio-oil (35.12 MJ kg^{-1}) compared to the HHV of *Nannochloropsis gaditana* bio-oil (36.23 MJ kg^{-1}). The higher amount of oxygen in the bio-oil produced from *Chlorella vulgaris* led to the decline of the HHV in comparison with the bio-oil produced from *Nannochloropsis gaditana*. Anastasakis *et al.*[313] determined the HTL of microalgae *Spirulina* in a continuous tube reactor at 220 bar and 350 °C. Bio-oil with an average yield of 32.9 wt% and a HHV of 33.2 MJ kg^{-1} was produced. Patel *et al.*[314] measured the yield and HHV of bio-oil produced from the HTL of *Nannochloropsis* sp. *microalgae*. The reaction was carried out in a quartz lined continuous plug flow reactor at 300–380 °C. The highest yield of bio-oil (35 wt%) was obtained at 380 °C and 30 seconds (the retention time of feedstock inside the reactor). Additionally, the highest HHV (39.27 MJ kg^{-1}) was obtained at 380 °C and a retention time of 4 min. The decline of the retention time to 0.5 min at 380 °C reduced the HHV of bio-oil to 37.61 MJ kg^{-1}. The higher HHV of bio-oil at 380 °C was related to its higher carbon content compared to the bio-oil obtained at 300 °C. Different conditions (biomass loading range 1–10 wt%, temperature 250–350 °C, residence times 3–5 min and pressures 150–200 bar) were selected by Jazrawi *et al.*[315] during the continuous HTL of *Chlorella* and *Spirulina* strains. The highest yield of bio-oil (41.7 wt%) and the highest HHV (33.8 MJ kg^{-1}) of bio-oil were obtained from the processing of *Chlorella* with a solid loading of 10 wt%, 350 °C and a residence time of 3 min. Elliott *et al.*[316] studied the HTL of grape pomace in a stirred-tank reactor. The reaction was carried out at 350 °C and 20 MPa. The yield of bio-oil was measured to be 39 wt% and its HHV was 38.3 MJ kg^{-1}. The results from the continuous HTL of biomass indicated that the HTL of biomass could be performed in a continuous reactor. However, for the scale up of the reactor, the process requires further optimization, especially in pumping, filtration and oil-aqueous phase separation systems.

A plug flow reactor was used by Aierzhati *et al.*[317] for the HTL of food waste collected from a dining hall at 300 °C and 10.7 MPa. The reactor volume was 35 L and the feeding rate was 0.15 Gal per min. The yield of bio-oil was 29.5 wt% and it had a HHV of 36.5 MJ kg^{-1}, while the HHV of the feedstock was 24.5 MJ kg^{-1}. Fatty acids were the main species in the bio-oil, which stemmed from the destruction of proteins in the structure of the food waste.

2.3.3. Catalysts. Due to the low quality of the bio-oil obtained from the HTL of bio-oil and the high pressure of the HTL process, the use of a suitable catalyst can reduce the cost of operation and improve the quality of bio-oil. So far, many groups of catalysts, including alkaline earth metals, transition metals, zeolites, *etc.* have been used for upgrading the bio-oil from the HTL process.[318–321]

2.3.3.1. Alkaline earth metals. Alkaline earth metals are active for the decomposition of carbohydrates. Ca and Mg based catalysts are the most commonly studied catalysts from alkaline earth metals for the HTL of biomass.[36] The use of alkaline earth metals during the HTL of biomass enhances the yield of bio-oil, while it decreases the quality of the bio-oil because of the increase of oxygen-containing species inside the bio-oil. As a result, the HHV of bio-oil decreases. In Table 11,[322–327] the summary of the recent studies in this field is shown. Tekin *et al.*[322] studied the HTL of beech wood in an autoclave at 250 °C and 4 MPa, 300 °C and 8.5 MPa and 350 °C and 16.5 MPa in the presence of natural calcium borate mineral and colemanite, as the catalyst. The bio-oil samples produced under different conditions had two phases. The highest yield of the light phase (11.1 wt%) and the highest yield of the heavy phase (29.8 wt%) were obtained at 300 °C and 8.5 MPa. The yield of bio-oil was 22.0 wt% compared to the yield of bio-oil in the presence of the catalyst (40.9 wt%) at 300 °C and 8.5 MPa and it had two phases. The HHV of both light and heavy bio-oils did not change remarkably in the presence of colemanite. For example, the HHV of the light bio-oil was 22.86 MJ kg^{-1} in the absence of the catalyst and it was 21.21 MJ kg^{-1} in the presence of the catalyst at 300 °C. In addition, the HHV of the heavy bio-oil was 24.38 MJ kg^{-1} in the absence of the catalyst and it was 25.21 MJ kg^{-1} in the presence of the catalyst at 300 °C. This indicated that the catalyst did not change the quality of the bio-oil significantly. Tymchyshyn *et al.*[323] studied the HTL of sawdust and cornstalks

Table 11 The summary of the results obtained by the use of alkaline earth metals during the HTL of biomass

Catalyst	Process and reactor	T (°C), P (MPa)	Feedstock	Results	Ref.
CaO	Batch	395, 25	Malaysian oil palm	Catalyst was instable and did not increase the yield of bio-oil	325
Colemanite	Stirred batch	300, 2	Birchwood sawdust	Total bio-crude yield improved	326
MgO	Stirred batch	300, 2	Birchwood sawdust	Quick deactivation of the catalyst due to the formation of coke and low improvement of bio-oil quality	326
$MgMnO_2$	Autoclave	270, —	Bagasse	The yield of water soluble organic compound formation and bio-oil increased due to aldol condensation and lignin depolymerization, respectively	327
Hydrotalcite	Stirred batch	300, 2		Increase of bio-oil yield, but the quality of bio-oil did not improve due to low tendency of the catalyst for deoxygenation	326
Natural calcium borate mineral and colemanite	Autoclave	250, 4; 300, 8.5 and 350, 16.5	Beech wood	Bio-oil yield decreased and its HHV did not change	322
$Ba(OH)_2$ and Rb_2CO_3	Batch micro-reactor	250–350, 2	Sawdust and cornstalks	Rb_2CO_3 led to a lower yield of bio-oil due to a higher cracking rate. Both catalysts improved the quality of the bio-oil through deoxygenation	323
$Ca(OH)_2$	Autoclave	240–320, 5	*Micro algae*, *Scenedesmus obliquus*	Yield of bio-oil reduced due to cracking, but the heating value of bio-oil increased due to deoxygenation	324

in a batch micro-reactor at 250–350 °C and 2 MPa in the presence of $Ba(OH)_2$ and Rb_2CO_3 catalysts. The highest yield of bio-oil (32 wt% and the same for both feedstock materials) was obtained at 250 °C in the absence of the catalyst. The increase of the temperature declined the yield of bio-oil with a slightly higher rate for cornstalks. Both catalysts enhanced the yield of bio-oil depending on the feedstock type. The yield of bio-oil was higher for sawdust compared to cornstalks in the presence of both catalysts. For instance, the yield of the bio-oil was 41 wt% for the bio-oil produced from the HTL of sawdust in the presence of the Rb_2CO_3 catalyst. In addition, the lowest yield of bio-oil (33 wt%) during the catalytic process belonged to cornstalks in the presence of Rb_2CO_3 (the reaction temperature was 300 °C). Both catalysts, especially Rb_2CO_3, resulted in a lower content of phenolics in the bio-oil due to the hydrogenation or hydrocracking and converting them to cyclic or linear compounds. Arun *et al.*[324] conducted the HTL of microalgae *Scenedesmus obliquus* in an autoclave with $Ca(OH)_2$ as the catalyst. The reaction was performed at 240–320 °C and 5 MPa. The highest yield of bio-oil (39.6 wt%) with a calorific value of 35.01 MJ kg^{-1} was obtained at 300 °C. At a low loading of the catalyst (<0.6 wt%), the presence of $Ca(OH)_2$ increased the yield of bio-oil, while with the increase of the catalyst loading amount, the yield of bio-oil reduced due to more cracking, but its calorific value enhanced because of the higher deoxygenation amount of the bio-oil.

$Mg(ClO_4)_2$ was selected by Alper *et al.*[328] as a catalyst for the HTL process of teak wood in a benchtop Parr reactor at 250–350 °C and 5 MPa. The loading amount of the catalyst was 2–10 mmol/15 g wood. The presence of the catalyst reduced the yield of the bio-oil. Additionally, by the increase of the catalyst to feedstock ratio, the yield of the bio-oil declined. The reason for this was the increase of the rate of cracking reactions by $Mg(ClO_4)_2$. The catalyst resulted in a higher amount of naphtha in the bio-oil and by the increase of the catalyst to feedstock ratio, the amount of naphtha enhanced in the bio-oil. $Mg(ClO_4)_2$ enhanced the rate of deoxygenation and HHV of the bio-oil. The increase of the reaction temperature improved the quality of bio-oil. However, the yield of the bio-oil was reduced by the increase of the temperature due to the higher rate of the cracking reaction at higher temperature. For instance, in non-catalytic HTL, the yield of the bio-oil reduced from 44 to 37 wt% by the increase of the temperature from 250 to 350 °C. The HHV of the bio-oil produced in the absence of the catalyst was 14.95 MJ kg^{-1}. By the loading of 10 mmol $Mg(ClO_4)_2$, the HHV of the bio-oil increased to 29.22 MJ kg^{-1}.

2.3.3.2. Transition metals. The effect of transition metals on the HTL of biomass has been widely studied in the literature[36] due to their high performance for cracking and upgrading reactions such as deoxygenation, hydrogenation, hydrocracking, gasification, *etc.*[36] Some of these metals, which have been used during the HTL of biomass, are zinc, copper, iron, nickel, cobalt, manganese, palladium and ruthenium.[36] In Table 12,[329–342] more details of their performance are shown. Lu *et al.*[262] performed the HTL of microalgae Nannochloropsis (NAS) over M/TiO_2 (M = Fe, Co, Ni, Mo, and Mn) catalysts. The reaction was carried out in a batch reactor at 6–8 MPa and 270 °C. Ni led to the highest yield of bio-oil (42.4 wt% *versus* 30.1 wt% for the blank experiment). The lowest yield of bio-oil (29.1 at%) was obtained in the presence of Fe. The reason for this was the acceleration of the cracking reaction by Ni and the acceleration of the polymerization reaction by Fe. The HHV of bio-oil was in

Table 12 The summary of the results obtained by the use of transition metals during the HTL of biomass

Catalyst	Process and reactor	T (°C), P (MPa)	Feedstock	Results	Ref.
Ni metal	Tubular micro-reactor	280–330, —	Oak wood	Yield of bio-oil decreased. Hydrogenation rate increased and bio-oil HHV enhanced	333
RANEY® Nickel	Autoclave	340–350, 6.6 and 10.3	Poplar	Catalyst was stable for 14 h and oil quality was improved by the catalyst	334
6% Ni/HZSM-5	Autoclave	300, 0.17	Pine sawdust	Bo-oil yield and quality enhanced	330
Ni/CeO_2	Micro-autoclave	230–310, 0.5–2.5	Rice straw	Bo-oil yield and quality enhanced due to the deoxygenation reaction	335
Ni/Si–Al	Tubular	300 and 350, —	Sorghum bagasse	Increase of the hydrogenation reaction rate led to the enhancement of the bio-oil yield and quality	336
K_2O promoted Cu/γ-Al_2O_3–MgO	Batch	360, 0.5	Bagasse	Bio-oil yield and ether and alcohol contents increased	337
Co/HZSM5	Autoclave	300, 0.07	Pine sawdust	Bio-oil yield and quality increased due to the high rate of hydrotreatment reaction	338
CuZnAl	Autoclave	300, 1.2	Rice straw	The production of phenol monomers increased	339
FeS	Batch	300, 2	Pulp/paper-mill sludge and waste newspaper	Bio-oil yield increased, but the quality did not change	340
Raw iron ores	Autoclave	280–360, —	Paulownia	Bio-oil yield and quality increased due to the high rate of cracking of large phenols	341
Fe	Tubular microreactor	260–320, —	Oak wood	Bio-oil yield and quality improved	342
M/TiO_2 (M = Fe, Co, Ni, Mo, and Mn)	Batch	270, 6.8	*Microalgae Nannochloropsis*	Ni and Fe led to the highest and lowest yield of bio-oil, correspondingly. The HHV of bio-oil reduced due to the higher amount of oxygen-containing species in the bio-oil	329
Ni/HZSM-5	Autoclave	300, 11.5–13.1	Pine sawdust	The yield and HHV of bio-oil increased	330
(Co,Ni)–Fe oxide	Batch	300, 10.3	Pine wood flour	The yield and HHV of bio-oil improved	331
Ni, Co, Fe and Zn	Tubular micro-reactor	330, —	Oak wood	The yield of bio-oil increased and the highest and lowest yields belonged to Fe and Zn, correspondingly. The HHV of bio-oil slightly increased with the highest increase for Fe due to the higher deoxygenation rate	332

the range of 33–36 MJ kg^{-1} (the highest was 35.65 MJ kg^{-1} for the bio-oil from the blank experiment and the lowest was 33.24 MJ kg^{-1} for Mn). The hydrothermal liquefaction of pine sawdust was performed in an autoclave by Xu *et al.*[91] in the presence of Ni/HZSM-5 (Ni loading of 5 and 10 wt%) at 300 °C and 1680–1900 psig. The results showed that the presence of the catalyst slightly increased the yield of bio-oil and loading more Ni on the surface of the catalyst led to the increase of bio-oil yield (the yield of bio-oil was 58 wt% for the blank experiment, 61 wt% for Ni/HZSM-5 with 5 wt% Ni loading and 63 wt% for Ni/HZSM-5 with 10 wt% Ni loading). This indicated the tendency of Ni to increase the rate of cracking reaction. The HHV of the bio-oil increased in the presence of the catalyst. However, the content of Ni did not show any influence on the HHV of bio-oil. The reason for this was the release of more heavy species by the catalyst to the bio-oil. The catalyst increased the rate of deoxygenation from the bio-oil, but the Ni loading amount did not reduce the oxygen content in the bio-oil. Amar *et al.*[331] used pine wood flour as feedstock for the HTL in a batch reactor at 300 °C and 1500 psi. (Co,Ni)–Fe oxide was selected as the catalyst. The yield of bio-oil enhanced from 18 wt% in the absence of the catalyst to 26 wt% in the presence of the catalyst. The bio-oil obtained included two phases and the HHV of the light phase was 27.19 MJ kg^{-1} and the HHV of the heavy phase was 31.83 MJ kg^{-1}. Tai *et al.*[332] performed the hydrothermal liquefaction of oak wood in a tubular micro-reactor at 330 °C. Ni, Co, Fe and Zn were used as the catalysts. All the catalysts used enhanced the yield of bio-oil. For instance, the highest yield of bio-oil (44 wt%) was obtained by the use of Fe, while the lowest yield (30 wt%) belonged to Zn (the yield of bio-oil in the absence of the catalyst was 27 wt%). The HHV of the bio-oil also enhanced slightly by the use of the catalyst (the HHV of the bio-oil for the blank experiment was 28.75 MJ kg^{-1} and the highest HHV (30.61 MJ kg^{-1}) belonged to the experiment with Fe as the catalyst). This indicated the higher rate of cracking and deoxygenation of the Fe catalyst.

Brachychiton populneus biomass seeds and a mixture of seeds and shells were converted to bio-oil through the HTL process by Eladnani *et al.*[343] Ni/Al_2O_3 was selected as the catalyst and the reaction was conducted in a tubular micro-reactor at 240–330 °C and 15 MPa. The catalyst : biomass mass ratio was 1 : 10. The highest yield of bio-oil (57.18 wt% for seeds and 48.23 wt% for

the mixture of seeds and shells) was obtained at 330 °C. Additionally, the HHV of the bio-oil enhanced from 25.14 MJ kg^{-1} in the absence of the catalyst to 38.04 MJ kg^{-1} by the use of the catalyst at 330 °C. This showed that Ni/Al_2O_3 had a high tendency for the cracking and deoxygenation of large species such as fatty acids and sugars.

2.3.3.3. Zeolites. Zeolites are cheap, have a high surface area, can be modified easily and are active for cracking and deoxygenation reactions.[36,344] Therefore, they have been used in the HTL process.[36] In Table 13,[230,330,345–350] the results of the use of different zeolites during the HTL process of biomass are shown. Zhang *et al.*[345] conducted the HTL of *Euglena* sp. microalgae in a batch reactor at 280 °C. Different types of zeolites including HZSM-22, HZSM-5, H beta, MCM-22 and SAPO-11 were used. All the catalysts used enhanced the contents of carbon and hydrogen in the bio-oil, while reducing the amounts of oxygen and nitrogen. The HHV of the bio-oil was enhanced by the use of the catalyst. The HHV of the bio-oil was 33.99 MJ kg^{-1} for the experiment without the catalyst and the highest HHV of bio-oil (37.08 MJ kg^{-1}) belonged to the experiment with H beta. H beta showed the highest rate of deoxygenation and led to the highest content of carbon in the bio-oil. The HTL of microalga *Nannochloropsis* sp. was performed by Duan *et al.*[346] in a batch reactor at 350 °C and 3500 kPa. The catalyst was zeolite (aluminum silicate). The yield of bio-oil in the absence of the catalyst was 36 wt%, while the presence of the catalyst increased it to 47 wt%. Interestingly, the HHV of the bio-oil was slightly decreased by adding the catalyst to the reaction (it was 38.5 MJ kg^{-1} for the bio-oil from the non-catalytic experiment and 35.4 MJ kg^{-1} for the bio-oil from the catalytic experiment). The decline of carbon content and the increase of hydrogen content by the catalyst led to the formation of the bio-oil with a low HHV in the presence of zeolite. Cheng *et al.*[347] conducted the HTL of pine sawdust in an autoclave at 300 °C and 100 psig over HZSM-5. The yield of bio-oil increased from 58 to 68 wt% by the catalyst showing the enhancement of the cracking of feedstock by HZSM-5. The HHV of the bio-oil increased from 23.12 MJ kg^{-1} (non-catalytic experiment) to 27.51 MJ kg^{-1} (catalytic experiment) because of the increase of the carbon content in the bio-oil, which showed the higher rate of deoxygenation reaction over HZSM-5 compared to the experiment without the catalyst. The content of the species such as furans, phenols, acids, ketones, and alcohols in the bio-oil reduced, while the amount of hydrocarbons was enhanced by the catalyst. Ma *et al.*[348] performed the hydrothermal liquefaction of Ulva prolifera macroalgae in an autoclave at 260–300 °C and 70 bar. ZSM-5, Y-zeolite and mordenite were selected as catalysts. The results indicated that the catalyst loading amount influenced the yield of the bio-oil. The catalyst to feedstock mass ratio percentage was selected as 10, 15 and 20 wt%. As an example, for ZSM-5, the yield of the bio-oil was 29 wt% at 15 wt% loading of the catalyst (reaction temperature was kept at 280 °C), while under the same conditions of the operation, the yield of bio-oil was 24 wt% for Y-zeolite and it was 32 wt% for mordenite at a catalyst loading of 15 wt%. It should be noted that the yield of bio-oil for the non-catalytic experiment was 17 wt% showing the increase of the cracking of the feedstock by the catalyst used. ZSM-5 increased the HHV of the bio-oil more than the other catalysts. The HHV of the bio-oil from the non-catalytic process was 21.2 MJ kg^{-1} and the HHV of the bio-oil produced in the presence of ZSM-5 was 34.8 MJ kg^{-1}. This indicated that ZSM-5 had a higher tendency for deoxygenation and the production of more hydrocarbons. The HTL of *Chlorella pyrenoidosa* was carried out by Xu *et al.*[349] in an autoclave at 300 °C over HZSM-5. The catalyst led to a slight increase of the yield of bio-oil (from 32 wt% for non-catalytic to 34 wt% in the presence of HZSM-5) showing the low increase of the rate for the

Table 13 The summary of the results obtained by the use of zeolites during the HTL of biomass

Catalyst	Process and reactor	T (°C), P (MPa)	Feedstock	Results	Ref.
HZSM-5	Autoclave	300, 0.17	Pine sawdust	Improvement of bio-oil quality due to dehydration, cracking and oligomerization reactions	330
ZSM-5	Autoclave	285, —	Sugarcane bagasse	Improvement of bio-oil quality due to esterification and decarburization reactions	350
HZSM-22, HZSM-5, H beta, MCM-22 and SAPO-11	Batch	280, —	*Euglena* sp. microalgae	Increase of the HHV of bio-oil and the highest increase belonged to H-beta	345
Zeolite (aluminum silicate)	Batch	350, 3.5	*Microalga Nannochloropsis* sp.	Increase of the bio-oil yield and slight decrease of the bio-oil HHV	346
HZSM-5	Autoclave	300, 0.7	Pine sawdust	Increase of the bio-oil yield and HHV due to a high rate of cracking and deoxygenation	347
ZSM-5, Y-zeolite and mordenite	Autoclave	270–300, 7	Ulva prolifera macroalgae	Mordenite resulted in the highest yield of bio-oil due to its high cracking tendency and ZSM-5 led to the highest HHV because of high deoxygenation rate	348
HZSM-5	Autoclave	300, —	Chlorella pyrenoidosa	Slight increase of the bio-oil yield and HHV	349

cracking reaction. HZSM-5 resulted in the increase of the HHV of the bio-oil from 19.79 to 22.82 MJ kg^{-1}.

2.3.4. Economic analysis and potential to compete with other technologies. The hydrothermal liquefaction of biomass has advantages over other thermochemical treatments of biomass such as high energy density of the bio-oil, short reaction duration time, ability to use different feedstock materials, *etc.*[351–354] Therefore, so far many researchers have studied the possibility of the commercialization of the HTL process of biomass. Zhu *et al.*[355] considered the production of biofuel through the HTL of woody biomass followed by the upgrading of the bio-oil through hydrotreatment. The capacity of the plant was considered as 2000 metric tons of dry biomass feeding per day. The temperature and pressure for the HTL process were 336 °C and 16.6 MPa. The hydrotreatment conditions were 376 °C and 10.5 MPa. The life time of the plant was 20 years. Their results indicated that the production rate of biofuel would be 69.9 million gallon gasoline-equivalent with a minimum selling price of fuel of $2.52 per gallon gasoline-equivalent, which was comparable with the price of gasoline. The economic study of wastewater-based algal biofuel production through HTL and hydroprocessing technology was carried out by Ranganathan *et al.*[356] The minimum selling price of the hydrocarbon fuel was estimated to be $4.3 per gallon gasoline-equivalent. The algae slurry flow rate was assumed to be 3175.3 tons per day. HTL was performed at 350 °C and 20 MPa and the hydroprocessing temperature and pressure were 400 °C and 10 MPa. The plant lifespan was considered as 20 years. Pedersen *et al.*[357] used an Aspen Plus process model to estimate the final price of biofuel produced from the HTL of wood followed by hydrotreatment. The plant capacity was 1000 tonnes organic matter per day. HTL process conditions were selected as 400 °C and 300 bar and the hydroprocessing conditions were 360 °C and 77.5 bar. The life time of the plant was considered as 20 years. The minimum selling price of the biofuel was calculated to be $0.82 per liter of gasoline equivalent. A process model was developed using Aspen Plus by Chen *et al.*[358] to estimate the price of the biofuel obtained from the HTL of microalgae at 350 °C and 20 MPa. The plant life time was considered 30 years. The selling price of the bio-oil obtained was $0.45 per liter gasoline equivalent. Kumar *et al.*[359] estimated that by considering the production of H_2 in the plant, the price of the biofuel could be reduced to $0.68 per liter gasoline equivalent. They considered whole tree chips as the feedstock and the process conditions for the HTL were selected as 355 °C and 20.3 MPa. The process parameters for upgrading by the hydrotreatment process were 400 °C and 14 MPa. The plant capacity was considered 4000 dry tons per day and its life time was 20 years. It should be noted that the price of the biofuel could increase to $0.82 per liter gasoline equivalent without the production of hydrogen in the plant.

Masoumi *et al.*[360] studied the economic aspect of microalgae HTL in methanol and water. To simulate the process, Aspen Plus and SimaPro software tools were utilized. The feeding rate was selected as 200 dry metric tonnes per day. A solvent to biomass mass ratio of 1 : 5 and a methanol to water ratio of 1 : 3 led to the highest yield of the bio-oil (57.8 wt%). The bio-oil included 14.5 wt% oxygen and had a HHV of 33.4 MJ kg^{-1}. The calculation showed that the minimum selling price of the fuel obtained would be 2.2 USD per liter. Li *et al.*[361] calculated the selling price of the fuel produced from the HTL of wet waste containing lipids, proteins, and carbohydrates with a feeding capacity of 110 dry-tons per day. Aspen Plus and the economic model in Microsoft Excel were used for the simulation and calculations. The temperature and pressure were considered as 350 °C and 20 MPa. The average fuel selling price was estimated to be 1.01 USD per liter.

2.3.5. Environmental analysis and potential to compete with other technologies. CO_2 is the main greenhouse gas, which is produced from the decarboxylation and decarbonylation reactions during the hydrothermal liquefaction of biomass.[9,10,362–365] It was estimated that the global warming effect from the HTL process of biomass would be lower (almost 50%) than its amount from biomass pyrolysis. Chan *et al.*[366] studied the life cycle assessment (LCA) of HTL for Malaysian oil palm empty fruit bunch. The plant operated at 390 °C and 25 MPa. They calculated the CO_2 amount to be 2.29 kg CO_2 equal per kg of the bio-oil produced. Connelly *et al.*[367] estimated that in comparison with the petroleum jet fuel, the biofuel obtained from the HTL of algae followed by hydrotreatment contributed 25% less in global warming potential. Fortier *et al.*[368] calculated the amount of CO_2 produced from the HTL of microalgae and compared it with CO_2 produced from the fossil fuel based jet fuel. They concluded that the HTL of microalgae followed by hydrotreatment had 76% less CO_2 compared to the production of conventional jet fuel. Zhang *et al.*[369] calculated that the amount of CO_2 production could be 1.31 kg per 1 kg of bio-oil produced ignoring syngas, while by considering the syngas production it could increase to 13.03 kg CO_2 per production of 1 kg of bio-oil. Zoppi *et al.*[362] estimated that by the use of electricity obtained from the HTL of corn stover (residue) and lignin-rich stream (waste), the global warming pollution will reduce by 72%. The CO_2 production amount was 56.1 and 58.4 g CO_2 eq per $MJ_{biofuel}$ for corn stover (residue) and lignin-rich stream (waste), respectively. In addition, the use of fuel produced from the HTL process will produce 37% lower emission compared to diesel.

2.3.6. Commercialization status. There have been a large number of research studies on the HTL of biomass and so far, several HTL plants have been built up on the scale of demonstration.[28] The summary is shown in Table 14. The scale-up of this technology has been conducted by a few companies/research centers. However, the high cost of the process and also the low quality of the bio-oil prevent their continuous operation. In addition, mainly, hydrotreatment has been used to improve the quality of the bio-oil. However, the quick deactivation of the catalysts and high cost of hydrogen hampered the further progress of this process.

In the 1970s, the Pittsburgh Energy Research Center in the USA constructed a plant with a capacity of 230–270 kg h^{-1}. The Lawrence Berkeley Laboratory (USA) developed a pilot plant with 0.25 kg h^{-1}. In 1982, the Shell Research Institute (NL) built up a plant with 25 000 tons dry biomass per year processing capacity. In the 1980s, a German company called HAW developed a HTL process with a capacity of 5 kg h^{-1}. The EPA's Water

Table 14 The summary of demonstration/commercial size plants for biomass hydrothermal liquefaction

Year	Country	Company	Feed type	Plant size	Process condition (°C, MPa)
1970s	USA	Pittsburgh Energy Research Center	Wood chips	230–270 kg h^{-1}	330–370, 20
1970s	USA	Lawrence Berkeley Laboratory	Wood chips	0.25 kg h^{-1}	330–360, 10–24
1982	The Netherlands	Shell Research Institute	All types of biomass, domestic, agricultural and industrial residues, wood	25 000 tons dry biomass per year	300–350, 12–18
1980s	Germany	HAW	Lignocellulosic biomass (*e.g.* wood, straw)	5 kg h^{-1}	350–500, 8
Not available	USA	EPA's Water Engineering Research Laboratory	Sewage sludge	30 L h^{-1}	300, not known
1990s	Japan	Organo Corp.	Sewage sludge	5 tons of dewatered sludge per day	300, 10
1998	USA	Changing World Technologies Inc.	Turkey offal and fats	250 tons per day	200–300, 4
2003	Denmark	SCF Technologies A/S	Dried distiller grains with solubles	20 L h^{-1}	280–350, 22.5–25
2006	USA	University of Illinois	Swine manure	0.9–2.0 kg h^{-1}	305, 103
2011–2015	Germany	Karlsruhe Institute of Technology (KIT)	Waste biomass; yeast, pomace; algae	0.29–0.63; 0.06–0.61; 0.76	330–350, 250; 330–450, 200–250; 350, 200
2012	Denmark	CatLiq® process SCF Technologies	Wet digested grains with solubles	30 kg h^{-1}	350, 250
2015	UK	University of Leeds	Chlorella	0.6–2.4	350, 185
2015	UK	Imperial College London	Algae	0.03–0.24 kg h^{-1}	300–380, 180
2013–2016	Australia	University of Sydney	Algae	24–40 kg h^{-1}	350, 200–250
2016	USA	Iowa State University	Fungi	3.0–7.5 kg h^{-1}	300–400, 270
2016–2017	Denmark	Aalborg University	Wood, glycerol wood	20	390–420, 300–350
2017	UK	Bath University	Wastewater algae	0.18–0.42	302–344, 160
2017	Denmark-Canada	Hydrofaction™ process Steeper Energy	Wood	20 kg h^{-1}	390–420, 300–350
2013–2018	USA	Pacific Northwest National Laboratories (PNNL)	Algae, macroalgae, grape pomace, wastewater solids	1.5 kg h^{-1}	350, 200
2014–2018	Sweden	Chalmers University of Technology	Kraft-lignin	1–2 kg h^{-1}	350, 250
2015–2018	Denmark	Aarhus University	Dried digested grains with soluble wood; sewage sludge, spirulina	0.36–1.44 kg h^{-1}; 60 kg h^{-1}	250–350, 250; 350, 220
2015–2018	Turkey	CatLiq® process Altaca Enerji	Different wastes and residues	15 000 kg h^{-1} (announced number)	350, 250
2018	The Netherlands	University of Twente	*Scenedesmus* sp.	0.06–0.33	250–350, 150–300
2018	Australia	Cat-HTR™ process Licella	Pulp/paper, plastics	10 000 ton per year (announce number)	Not available, not available
2018	Australia	Green2black™ process Muradel	Tires, algae	168 kg h^{-1}	360, 200
2018	USA	HTP process Genifuel	Sewage sludge	Not available	350, 200
2018	Italy	W2F process ENI S.p.A.	Organic fraction of municipal solid waste	1–5 kg h^{-1}	250–310, 100
2018	USA	TDP process Changing World Technologies	Turkey waste	8500 kg h^{-1}	200–300, not available

Engineering Research Laboratory developed a HTL plant with 30 L h^{-1} capacity of sewage sludge feeding. In the 1990s, Organo Corp. in Japan built up a plant with a processing capacity of 5 tons of dewatered sludge per day. Changing World Technologies Inc. had a plant in the USA in 1998 with 250 tons per day processing capacity of turkey offal and fats. In 2003, SCF Technologies A/S in Denmark developed a plant with a capacity of 20 L h^{-1} dried distiller grains with solubles. In recent years, many other companies such as Licella/Ignite Energy Resources (Australia) and Arbios Biotech (Australia) have built up plants with commercial sizes.

3. Technology status of the biorefineries based on thermochemical conversion

Due to the immaturity and confidentially of data, many data have not been published by companies, research institutes and universities. Therefore, the assessment of the status for gasification, pyrolysis and hydrothermal liquefaction processes has been performed based on the available data. The summary of the data indicates that based on the biomass type, the developments in biorefinery processes are in different stages. The biorefineries based on starch (corn, wheat and cassava), sugar crops (sugarcane and sugar beet) and wood are in the last stage of development.[370–376] They are at a Technology Readiness Level of 9 (TRL-9) showing that the biorefinery technology based on these feedstock materials has been proven in an operational environment. On the other hand, biorefineries based on marine feedstock including microalgae and macroalgae had the lowest TRL (TRL-5–6) meaning that they are in the technology validation and demonstration stages. The biorefineries based on other biomass materials have the technology development status between these two categories of biomass. The reason for the lower TRL of biorefineries based on the other types of biomass could be their low abundance, high price, complexity of the chemical structure, being more economic in other uses such as the use of vegetable oil as food, *etc.*[370–376]

Gasification is a mature technology, but its use for biomass is still under optimization. Based on the available data, the gasification plant based on biomass made by GoBiGas is at TRL-8 (the system is complete and qualified) and its main product is biomethane. Biomass pyrolysis technology is not as mature as biomass gasification technology. It has been commercialized for tyre feedstock by Alphaco and Reoil Sp. with TRL-9. For the biomass feedstock, the pyrolysis technology is mainly at the TRL-7 level (system prototype demonstration is in an operational environment). The HTL of biomass is not a complete mature technology. The Pittsburgh Energy Research Centre of U.S. Bureau of Mines developed one of the initial HTL plants with a large size with TRL-9. There are also other HTL plants under construction on the commercial scale in Australia, the UK, *etc.*, which are at TRL-6–8.[370–376]

4. Commercial aspects of the biorefineries based on thermochemical conversion

There are many commercial barriers such as the cost of biomass production, difficulties in harvesting and storing, transportation cost and the high cost of operation, especially the cost of catalyst, *etc.*, which are still the main economic barriers to produce biofuel with a competitive price of fossil fuels. Some governments consider subsidies for the use of biofuel. However, it should be noted that subsidies could be affordable for the low quantity of biofuel production.

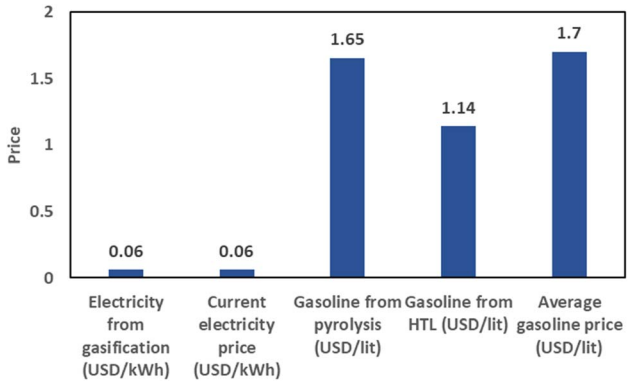

Fig. 1 Economic analysis of electricity and gasoline equivalent fuel from different thermochemical processes.[120–125,288–291,355–361] (Note) Based on the studied papers, the highest possible selling price is considered for the products from gasification, pyrolysis and HTL of biomass. According to the parameters such as the type of feedstock, process conditions, the use of different catalysts, *etc.* the costs presented can change. (Note) For the gasification part, the data are the summary of Section 2.1.4 and the biomass types were considered in this section are woody biomass, dates, dried sludge, food waste, manure, oil palm biomass, and Canadian pine wood. The gasification temperature was selected as 850 °C and the reactor type was fluidized-bed operating at atmospheric pressure. (Note) For the pyrolysis part, the data in the figure are extracted from part 3.2.4, which studied the use of olive mill wastewater sludge, corncobs, rice husk and marine forest residue in continuous feeding reactors (working at atmospheric pressure), working at 400–550 °C. (Note) For the HTL part, the data are taken from Section 4.3.4 and woody biomass, algae sludge, whole tree chips, microalgae and wet waste containing lipid, protein and carbohydrate were selected as feedstock. The reaction was conducted in continuous reactors working at 336–355 °C and 7.75–20 MPa. (Note) The range of prices is selected based on the lowest and the highest prices, which were available in ref. 120–125, 288–291 and 355–361.

The summary of the price ranges for the production of electricity and fuel through gasification, pyrolysis and HTL processes is shown in Fig. 1.[120–125,288–291,355–361] The data indicate that the highest price of electricity from the combustion of fuel gas produced from the gasification of biomass could be approximately 0.06 USD per kW h, which is the same as the average current price of the electricity in Europe. The average price of gasoline in many European countries is close to 1.7 USD per liter, while the highest selling price of gasoline equivalent fuel from the pyrolysis and HTL of biomass could be 1.65 and 1.14 USD per liter, respectively. This indicates that by the further optimization of the thermochemical processing of biomass, the price of electricity and fuel from these technologies could be lower than that of fossil based ones.

5. Environmental aspects of the biorefineries based on thermochemical conversion

Different types of contaminants can be produced from fossil fuel refineries such as CO_2, NO_x, SO_2, *etc.* CO_2 as the most important contaminant can lead to global warming. The use of biorefineries based on thermochemical conversion can reduce

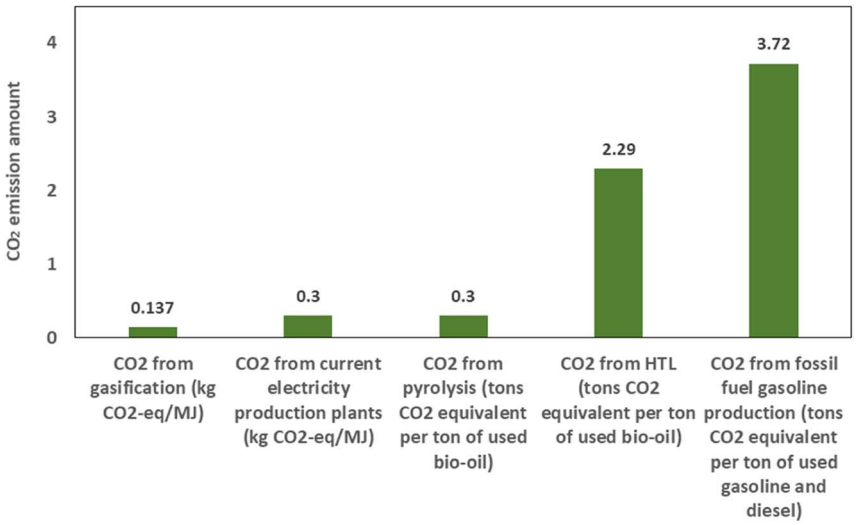

Fig. 2 CO_2 production amount for different processes.[122,127–130,295–298,362,366–369] (Note) The highest possible CO_2 production amount is considered for the products from gasification, pyrolysis and HTL of biomass. (Note) The data in the graph are extracted from the papers, which were used in this review. (Note) For the gasification part, woody biomass, residue from cotton cultivation and processing, olive foot cake waste, biomass from corn and biomass from rice, dry pit and wheat straw were the feedstock. The reaction was mainly conduced in a fluidized-bed reactor at 850 °C and atmospheric pressure. The data in this graph are taken from Section 2.1.5. (Note) For the pyrolysis part, the data were extracted from 3.2.5. The feedstock was corn stover, Malaysian oil palm empty fruit bunch, crop straw and forest residue. The reactor was continuous and working at 450–550 °C and atmospheric pressure. (Note) For the HTL part, the data were taken from Section 4.3.5. The feedstock was Malaysian oil palm empty fruit bunch, algae, microalgae, wood and corn stover. The reactors were continuously working at 350–390 °C and 20–25 MPa. (Note) The range of CO_2 emission is selected based on the lowest and the highest CO_2 amounts, which were available in ref. 122, 127–130, 295–298, 362 and 366–369.

the content of NO_x and SO_2 due to the low amount of N and S in biomass. It can also decrease the amount of CO_2 compared to the use of fossil fuels. In Fig. 2,[122,127–130,295–298,362,366–369] the comparison of the CO_2 production amount from different processes is shown. The data indicated that the CO_2 amount for the production of electricity from biomass gasification is two times less than that of conventional fossil fuel based electricity producers. Pyrolysis showed lower CO_2 amount production compared to HTL (7.6 times less). Additionally, the amount of CO_2 produced from the combustion of the same amount of gasoline and diesel is higher than the CO_2 amount from the combustion of bio-oil (12.4 times less for the bio-oil from pyrolysis and 1.6 times less for the bio-oil from HTL).

6. Summary and outlooks

The available data and comparisons demonstrated that biorefineries based on thermochemical conversion methods can replace the conventional refineries. The price of biofuel could be competitive with the price of fossil fuels. Additionally, the amount of green gas could be depleted by the construction of biorefineries. However, there are some key points, which require to be addressed prior to the advancement of biorefineries to the next stages.

(1) Gasification

The technology for the gasification of biomass is well developed. The reactor design and process stages are clarified. The yield of gas and its composition are well-known. However, one major concern, which still remains, is the formation of tar. Tar can result in coke formation and consequently the plugging of the transferring tube lines and instruments can occur. Catalytic reforming of the tar is considered to convert the tar into gaseous products. However, the quick deactivation of the catalyst prevents the use of this process on a large scale. Another issue for the gasification of biomass is that the high amount of carbon in the biomass is converted to CO_2. This affects the economic and environmental aspects of the process. Therefore, the currently available gasification plants or the plants under construction are required to use a high resistance catalyst before the coke formation and also decrease the amount of CO_2 by converting CO_2 to other compounds. This can make the process techno-economically more feasible. In the available techno-economic studies, there is a need for considering other parameters such as the catalyst regeneration and its replacement cost after the several times of regeneration. Therefore, the price of the electricity and chemicals produced from the gasification of biomass can increase slightly. As a result, further optimization of the process is needed.

(2) Fast pyrolysis

Pyrolysis technology is not as mature as gasification. There are a few large scale pyrolysis plants. However, the upgrading of the quality of the bio-oil is the main issue. Hydrotreatment as the main process for the conversion of the bio-oil to the engine fuel suffers from the deactivation of the catalyst and also the high cost of the process, especially hydrogen. Therefore, the conversion of biomass to biofuel through pyrolysis and

hydrotreatment is not still techno-economically optimized well. The development of a cheap catalyst, which produce low amount of coke, could be considered as the main obstacle for this process. It should be mentioned that pyrolysis leads to the formation of the lowest amount of CO_2 compared to the gasification and HTL processes. However, the production of water with a high content of acids and poisonous compounds could be another issue, which requires further consideration to prevent the contamination of the environment.

(3) Hydrothermal liquefaction

Biomass hydrothermal liquefaction is a mature technology, which has been developed on a commercial scale during recent years. One of the concerns is the catalyst, which can upgrade the bio-oil into engine fuels. The main issue for the further progress of the HTL process is the pumping of a viscous biomass slurry into the reactor. Another issue is the high amount of CO_2 production in comparison with pyrolysis. The cost of the process is also high due to the use of high pressure. The use of solvents to reduce the severity of the process conditions is needed to be considered. Detailed optimization of the process conditions (temperature and pressure) is necessary to obtain the optimum conditions. Therefore, even the current large size plants require further optimization of the process to reduce the cost and CO_2 production.

(4) Overall

Biorefineries are going to play a key role in the world in near future. At the current time, there are plants based on gasification, pyrolysis and HTL processes on a large scale. Their processes are well developed. The standard methods for the analysis of the products are well known. However, further modifications are required to optimize the processes. All three technologies need active catalysts, which results in low amount of coke. The cost of processes is still high for obtaining the products that can compete economically and technically with the current fossil based fuels/chemicals. Environmental issues such as the decline of CO_2 production and the treatment of water obtained from these processes should be considered. The water produced includes a high amount of acids and other compounds, which can contaminate easily soil and water resources. Therefore, further fundamental studies and technical optimization are necessary to make the technology of biorefineries, based on thermochemical methods, more feasible. It is worth mentioning that it is important to judiciously manage the available biomass resources with respect to their use in other applications such as food for animals. This can entail the risk of socio-economic, ecological and environmental impacts such as the lack of trees for taking CO_2 from the atmosphere. As a result, there should be the consideration of the growth of specific types of biomass with the aim of use for energy production.

Conflicts of interest

There are no conflicts to declare.

Acknowledgements

Mortaza Gholizadeh received funding from the European Union's Horizon 2020 research and innovation programme under the Marie Skłodowska-Curie grant agreement No. 712949 (TECNIOspring PLUS) and from the Agency for Business Competitiveness of the Government of Catalonia. This work was financially supported by the Catalan Government through the funding grant ACCIÓ-Eurecat (Project TRAÇA GREEN-H2, 2022–2024).

References

1 E. R. Sadik-Zada and A. Gatto, The puzzle of greenhouse gas footprints of oil abundance, *Socio-Econ. Plan. Sci.*, 2021, **75**, 1–12.
2 M. D. Staples, R. Malina and S. R. H. Barrett, The limits of bioenergy for mitigating global life-cycle greenhouse gas emissions from fossil fuels, *Nat. Energy*, 2017, **2**, 1–8.
3 M. Gholizadeh and X. Hu, Progress in understanding the coking behavior of typical catalysts in the catalytic pyrolysis of biomass, *Sustainable Energy Fuels*, 2022, **6**, 2113–2148.
4 I. Capellan-Perez, I. Arto, J. M. Polanco-Martinez, M. Gonzalez-Eguino and M. B. Neumann, Likelihood of climate change pathways under uncertainty on fossil fuel resource availability, *Energy Environ. Sci.*, 2016, **9**, 2482–2492.
5 P. D. Parakh, S. Nanda and J. A. Kozinski, Eco-friendly transformation of waste biomass to biofuels, *Curr. Biochem. Eng.*, 2020, **6**, 120–134.
6 Q. Li, A. Faramarzi, S. Zhang, Y. Wang, X. Hu and M. Gholizadeh, Progress in catalytic pyrolysis of municipal solid waste, *Energy Convers. Manage.*, 2020, **226**, 1–30.
7 M. Gholizadeh, X. Hu and Q. Liu, A mini review of the specialties of the bio-oils produced from pyrolysis of 20 different biomasses, *Renewable Sustainable Energy Rev.*, 2019, **114**, 1–28.
8 H. K. Sharma, C. Xu and W. Qin, Biological pretreatment of lignocellulosic biomass for biofuels and bioproducts: an overview, *Waste Biomass Valorization*, 2019, **10**, 235–251.
9 V. Esmaeili, J. Ajalli, A. Faramarzi, M. Abdi and M. Gholizadeh, Gasification of wastes: the impact of the feedstock type and co-gasification on the formation of volatiles and char, *Int. J. Energy Res.*, 2020, **44**, 3587–3606.
10 X. Hu, H. Guo, M. Gholizadeh, B. Sattari and Q. Liu, Pyrolysis of different wood species: impacts of C/H ratio in feedstock on distribution of pyrolysis products, *Biomass Bioenergy*, 2019, **120**, 28–39.
11 A. R. K. Gollakota, N. Kishore and S. Gu, A review on hydrothermal liquefaction of biomass, *Renewable Sustainable Energy Rev.*, 2018, **81**, 1378–1392.
12 H. P. Vu, L. N. Nguyen, M. T. Vu, M. A. H. Johir, R. McLaughlan and L. D. Nghiem, A comprehensive review on the framework to valorise lignocellulosic

biomass as biorefinery feedstocks, *Sci. Total Environ.*, 2020, **743**, 1–54.

13 S. Salavati, C. T. Zhang, S. Zhang, Q. Liu, M. Gholizadeh and X. Hu, Cross-interaction during Co-gasification of wood, weed, plastic, tire and carton, *J. Environ. Manage.*, 2019, **250**, 1–15.

14 A. A. Ahmad, N. A. Zawawi, F. H. Kasim, A. Inayat and A. Khasri, Assessing the gasification performance of biomass: a review on biomass gasification process conditions, optimization and economic evaluation, *Renewable Sustainable Energy Rev.*, 2016, **53**, 1333–1347.

15 M. Asadullah, Barriers of commercial power generation using biomass gasification gas: a review, *Renewable Sustainable Energy Rev.*, 2014, **29**, 201–215.

16 J. Ren, J.-P. Cao, X.-Y. Zhao, F.-L. Yang and X.-Y. Wei, Recent advances in syngas production from biomass catalytic gasification: a critical review on reactors, catalysts, catalytic mechanisms and mathematical models, *Renewable Sustainable Energy Rev.*, 2019, **116**, 1–25.

17 J. Ren, Y.-L. Liu, X.-Y. Zhao and J.-P. Cao, Biomass thermochemical conversion: a review on tar elimination from biomass catalytic gasification, *J. Energy Inst.*, 2020, **93**, 1083–1098.

18 A. A. Arpia, T.-B. Nguyen, W.-H. Chen, C.-D. Dong and Y. S. Ok, Microwave-assisted gasification of biomass for sustainable and energy-efficient biohydrogen and biosyngas production: a state-of-the-art review, *Chemosphere*, 2022, **288**, 1–13.

19 Y. Zheng, J. Wang, D. Li, C. Liu, Y. Lu, X. Lin and Z. Zheng, Highly efficient catalytic pyrolysis of biomass vapors upgraded into jet fuel range hydrocarbon-rich bio-oil over a bimetallic Pt-Ni/γ-Al_2O_3 catalyst, *Int. J. Hydrogen Energy*, 2021, **46**, 27922–27940.

20 M. W. Seo, S. H. Lee, H. Nam, D. Lee, D. Tokmurzin, S. Wang and Y.-K. Park, Recent advances of thermochemical conversion processes for biorefinery, *Bioresour. Technol.*, 2022, **343**, 1–15.

21 J. Y. Seo, D. Tokmurzin, D. Lee, S. H. Lee, M. W. Seo and Y.-K. Park, Production of biochar from crop residues and its application for biofuel production processes – an overview, *Bioresour. Technol.*, 2022, **361**, 1–15.

22 J. Lee, W.-H. Chen and Y.-K. Park, Recent achievements in platform chemical production from food waste, *Bioresour. Technol.*, 2022, **366**, 1–15.

23 H. W. Ryu, D. H. Kim, J. Jae, S. S. Lam, E. D. Park and Y.-K. Park, Recent advances in catalytic co-pyrolysis of biomass and plastic waste for the production of petroleum-like hydrocarbons, *Bioresour. Technol.*, 2020, **310**, 1–8.

24 O. A. Qamar, F. Jamil, M. Hussain, A. H. Al-Muhtaseb, A. Inayat, A. Waris, P. Akhter and Y.-K. Park, Feasibility-to-applications of value-added products from biomass: current trends, challenges, and prospects, *Chem. Eng. J.*, 2023, **454**, 1–15.

25 J. Y. Kim, J.-M. Jung, S. Jung, Y.-K. Park, Y. F. Tsang, K.-Y. A. Lin, Y.-E. Choi and E. E. Kwon, Biodiesel from microalgae: recent progress and key challenges, *Prog. Energy Combust. Sci.*, 2022, **93**, 1–15.

26 S. Nawaz, F. Jamil, P. Akhter, M. Hussain, H. Jang and Y.-K. Park, Valorization of lignocellulosic rice husk producing biosilica and biofuels – a review, *J. Phys.: Energy*, 2023, **5**, 1–21.

27 F. Jamill, M. Saleem, O. A. Qamar, M. S. Khurram, A. H. Al-Muhtaseb, A. Inayat, P. Akhter, M. Hussain, S. Rafiq, H. Yim and Y.-K. Park, State-of-the-art catalysts for clean fuel (methyl esters) production-a comprehensive review, *J. Phys.: Energy*, 2023, **5**, 1–30.

28 Y. Sun, C. Li, S. Zhang, D. Dong, M. Gholizadeh, S. Wang and X. Hu, Pyrolysis behaviors of rapeseed meal: products distribution and properties, *Biomass Convers. Biorefin.*, 2021, **1**, 1–16.

29 Y. Sun, C. Li, S. Zhang, Q. Li, M. Gholizadeh, Y. Wang, S. Hu, J. Xiang and X. Hu, Pyrolysis of soybean residue: understanding characteristics of the products, *Renewable Energy*, 2021, **174**, 487–500.

30 M. Gholizadeh, R. Gunawan, X. Hu, F. M. Mercader, R. Westerhof, W. Chaitwat, M. M. Hasan, D. Mourant and C.-Z. Li, Effects of temperature on the hydrotreatment behaviour of pyrolysis bio-oil and coke formation in a continuous hydrotreatment reactor, *Fuel Process. Technol.*, 2016, **148**, 175–183.

31 Y. Han, M. Gholizadeh, C.-C. Tran, S. Kaliaguine, C.-Z. Li, M. Olarte and M. Garcia-Perez, Hydrotreatment of pyrolysis bio-oil: a review, *Fuel Process. Technol.*, 2019, **195**, 106–140.

32 X. Li, R. Gunawan, Y. Wang, W. Chaiwat, X. Hu, M. Gholizadeh, D. Mourant, J. Bromly and C.-Z. Li, Upgrading of bio-oil into advanced biofuels and chemicals. Part III. Changes in aromatic structure and coke forming propensity during the catalytic hydrotreatment of a fast pyrolysis bio-oil with Pd/C catalyst, *Fuel*, 2014, **116**, 642–649.

33 A. Dimitriadis, G. Meletidis, U. Pfisterer, M. Auersvald, D. Kubicka and S. Bezergianni, Integration of stabilized bio-oil in light cycle oil hydrotreatment unit targeting hybrid fuels, *Fuel Process. Technol.*, 2022, **230**, 1–11.

34 X. Hu, Z. Zhang, M. Gholizadeh, S. Zhang, C. H. Lam, Z. Xiong and Y. Wang, Coke formation during thermal treatment of bio-oil, *Energy Fuels*, 2020, **34**, 7863–7914.

35 D. C. Elliott, P. Biller, A. B. Ross, A. J. Schmidt and S. B. Jones, Hydrothermal liquefaction of biomass: developments from batch to continuous process, *Bioresour. Technol.*, 2015, **178**, 147–156.

36 M. Scarsella, B. Caprariis, M. Damizia and P. D. Filippis, Heterogeneous catalysts for hydrothermal liquefaction of lignocellulosic biomass: a review, *Biomass Bioenergy*, 2020, **140**, 1–15.

37 S. Nagappan, R. R. Bhosale, D. D. Nguyen, N. T. L. Chi, V. K. Ponnusamy, C. S. Woong and G. Kumar, Heterogeneous catalysts for hydrothermal liquefaction of lignocellulosic biomass: a review, *Fuel*, 2020, **140**, 1–11.

38 S. K. Sansaniwal, K. Pala, M. A. Rosen and S. K. Tyagi, Recent advances in the development of biomass

gasification technology: a comprehensive review, *Renewable Sustainable Energy Rev.*, 2017, **72**, 363–384.

39 J. Ren, J.-P. Cao, X.-Y. Zhao, F.-L. Yang and X.-Y. Wei, Recent advances in syngas production from biomass catalytic gasification: a critical review on reactors, catalysts, catalytic mechanisms and mathematical models, *Renewable Sustainable Energy Rev.*, 2019, **116**, 1–25.

40 R. Thomson, P. Kwong, E. Ahmad and K. D. P. Nigam, Clean syngas from small commercial biomass gasifiers; a review of gasifier development, recent advances and performance evaluation, *Int. J. Hydrogen Energy*, 2020, **45**, 21087–21111.

41 T. Kan, V. Strezov and T. J. Evans, Lignocellulosic biomass pyrolysis: a review of product properties and effects of pyrolysis parameters, *Renewable Sustainable Energy Rev.*, 2016, **57**, 1126–1140.

42 A. T. Hoang, H. C. Ong, I. M. R. Fattah, C. T. Chong, C. K. Cheng, R. Sakthivel and Y. S. Ok, Progress on the lignocellulosic biomass pyrolysis for biofuel production toward environmental sustainability, *Fuel Process. Technol.*, 2021, **223**, 1–27.

43 X. Hu and M. Gholizadeh, Biomass pyrolysis: a review of the process development and challenges from initial researches up to the commercialisation stage, *J. Energy Chem.*, 2019, **39**, 109–143.

44 J. Ni, L. Qian, Y. Wang, B. Zhang, H. Gu, Y. Hu and Q. Wang, A review on fast hydrothermal liquefaction of biomass, *Fuel*, 2022, **327**, 1–15.

45 D. Castello, T. H. Pedersen and L. A. Rosendahl, Continuous hydrothermal liquefaction of biomass: a critical review, *Energies*, 2018, **11**, 1–35.

46 Q. He, Q. Guo, K. Umeki, L. Ding, F. Wang and G. Yu, Soot formation during biomass gasification: a critical review, *Renewable Sustainable Energy Rev.*, 2021, **139**, 1–21.

47 J. Li, J. Tao, B. Yan, L. Jiao, G. Chen and J. Hu, Review of microwave-based treatments of biomass gasification tar, *Renewable Sustainable Energy Rev.*, 2021, **150**, 1–20.

48 A. A. P. Susastriawan and H. Saptoadi, Purnomo, Small-scale downdraft gasifiers for biomass gasification: a review, *Renewable Sustainable Energy Rev.*, 2017, **76**, 989–1003.

49 I. L. Motta, N. T. Miranda, R. M. Filho and M. R. W. Maciel, Biomass gasification in fluidized beds: a review of biomass moisture content and operating pressure effects, *Renewable Sustainable Energy Rev.*, 2018, **94**, 998–1023.

50 A. Molino, V. Larocca, S. Chianese and D. Musmarra, Biofuels production by biomass gasification: a review, *Energies*, 2018, **11**, 1–31.

51 S. Zhang, S. He, N. Gao, J. Wang, Y. Duan, C. Quan, B. Shen and C. Wu, Hydrogen production from autothermal CO_2 gasification of cellulose in a fixed-bed reactor: influence of thermal compensation from CaO carbonation, *Int. J. Hydrogen Energy*, 2022, **47**, 1–15.

52 J. Ren, Y.-L. Liu, X.-Y. Zhao and J.-P. Cao, Methanation of syngas from biomass gasification: an overview, *Int. J. Hydrogen Energy*, 2020, **45**, 4223–4243.

53 S. S. Siwal, Q. Zhang, C. Sun, S. Thakur, V. K. Gupta and V. K. Thakur, Energy production from steam gasification processes and parameters that contemplate in biomass gasifier – a review, *Bioresour. Technol.*, 2020, **297**, 1–51.

54 M. Costa, M. L. Villetta, D. Piazzullo and D. Cirillo, A phenomenological model of a downdraft biomass gasifier flexible to the feedstock composition and the reactor design, *Energies*, 2021, **14**, 1–29.

55 J. Cespiva, L. Niedzwiecki, J. Veres, J. Skrinsky, M. Wnukowski, K. Borovec and T. Ochodek, Evaluation of the performance of the cross/updraft type gasification technology with the sliding bed over a circular grate, *Biomass Bioenergy*, 2022, **167**, 1–15.

56 G. Gopan, L. Hauchhum, P. Kalita and S. Pattanayak, Biomass gasification in a double-tapered bubbling fluidized bed reactor using preheated air, *Int. J. Energy Environ. Eng.*, 2022, **13**, 643–656.

57 C. Wang, L. Zhu, M. Zhang, Z. Han, X. Jia, D. Bai, W. Duo, X. Bi, A. Abudula, G. Guan and G. Xu, A two-stage circulated fluidized bed process to minimize tar generation of biomass gasification for fuel gas production, *Applied Energy*, 2022, **323**, 1–15.

58 Z. Lian, Y. Wang, X. Zhang, A. Yusuf, L. Famiyeh, D. Murindababisha, H. Jin, Y. Liu, J. He, Y. Wang, G. Yang and Y. Sun, Hydrogen production by fluidized bed reactors: a quantitative perspective using the supervised machine learning approach, *J: Multidiscip. Sci. J.*, 2021, **4**, 266–287.

59 Y. A. Situmorang, Z. Zhao, A. Yoshida, A. Abudula and G. Guan, Small-scale biomass gasification systems for power generation (<200 kW class): a review, *Renewable Sustainable Energy Rev.*, 2020, **117**, 1–14.

60 N. Hanchate, S. Ramani, C. S. Mathpati and V. H. Dalvi, Biomass gasification using dual fluidized bed gasification systems: a review, *J. Cleaner Prod.*, 2021, **280**, 1–133.

61 A. Farooq, G. H. Rhee, I.-H. Lee, M. A. Khan, S. H. Lee, S.-C. Jung, B.-H. Jeon, W.-H. Chen and Y.-K. Park, Waste furniture gasification using rice husk based char catalysts for enhanced hydrogen generation, *Bioresour. Technol.*, 2021, **341**, 1–6.

62 S. Valizadeh, H. Hakimian, A. Farooq, B.-H. Jeon, W.-H. Chen, S. H. Lee, S.-C. Jung, M. W. Seo and Y.-K. Park, Valorization of biomass through gasification for green hydrogen generation: a comprehensive review, *Bioresour. Technol.*, 2022, **365**, 1–15.

63 S. Moogi, S. S. Lam, W.-H. Chen, C. H. Ko, S.-C. Jung and Y.-K. Park, Household food waste conversion to biohydrogen via steam gasification over copper and nickel-loaded SBA-15 catalysts, *Bioresour. Technol.*, 2022, **366**, 1–15.

64 C. B. Felix, W.-H. Chen, A. T. Ubando, Y.-. Park, K. A. Lin, A. Pugazhendhi, T.-B. Nguyen and C.-D. Dong, A comprehensive review of thermogravimetric analysis in lignocellulosic and algal biomass gasification, *Chem. Eng. J.*, 2022, **445**, 1–15.

65 Y. Fang, M. C. Paul, S. Varjani, X. Li, Y.-K. Park and S. You, Concentrated solar thermochemical gasification of biomass: principles, applications, and development, *Renewable Sustainable Energy Rev.*, 2021, **150**, 1–15.

66 S. Valizadeh, S.-H. Jang, G. H. Rhee, J. Lee, P. L. Show, M. A. Khan, B.-H. Jeon, K.-Y. A. Lin, C. H. Ko, W.-H. Chen and Y.-K. Park, Biohydrogen production from furniture waste via catalytic gasification in air over Ni-loaded Ultra-stable Y-type zeolite, *Chem. Eng. J.*, 2022, **433**, 1–15.

67 M. L. V. Rios, A. M. Gonzalez, E. E. S. Lora and O. A. A. Olmoc, Reduction of tar generated during biomass gasification: a review, *Biomass Bioenergy*, 2018, **108**, 345–370.

68 P. Chaiprasert and T. Vitidsant, Effects of promoters on biomass gasification using nickel/dolomite catalyst, *Korean J. Chem. Eng.*, 2009, **26**, 1545–1549.

69 C. Wu, L. Wang, P. T. Williams, J. Shi and J. Huang, Hydrogen production from biomass gasification with Ni/MCM-41 catalysts: influence of Ni content, *Appl. Catal., B*, 2011, **108–109**, 6–13.

70 P. Lv, Z. Yuan, C. Wu, L. Ma, Y. Chen and N. Tsubaki, Bio-syngas production from biomass catalytic gasification, *Energy Convers. Manage.*, 2007, **48**, 1132–1139.

71 M. A. Caballero, J. Corella, M.-P. Aznar and J. Gil, Biomass gasification with air in fluidized bed. Hot gas cleanup with selected commercial and full-size nickel-based catalysts, *Ind. Eng. Chem. Res.*, 2000, **39**, 1143–1154.

72 W. Li, J. Ren, X. Y. Zhao and T. Takarada, H_2 and syngas production from catalytic cracking of pig manure and compost, *Pol. J. Chem. Technol.*, 2018, **20**, 8–14.

73 J. Hu, Z. Jia, S. Zhao, W. Wang, Q. Zhang, R. Liu and Z. Huang, Activated char supported Fe–Ni catalyst for syngas production from catalytic gasification of pine wood, *Bioresour. Technol.*, 2021, **340**, 1–8.

74 J. P. Cao, T. L. Liu, J. Ren, X. Y. Zhao, Y. Wu, J. X. Wang, X. Y. Ren and X. Y. Wei, Preparation and characterization of nickel loaded on resin char as tar reforming catalyst for biomass gasification, *J. Anal. Appl. Pyrolysis*, 2017, **127**, 82–90.

75 Z. Ma, S. P. Zhang, D. Y. Xie and Y. J. Yan, A novel integrated process for hydrogen production from biomass, *Int. J. Hydrogen Energy*, 2014, **39**, 1274–1279.

76 S. H. Teo, D. K. Y. Yap, N. Mansir, A. Islam and Y. H. Taufiq-Yap, Facile recoverable and reusable macroscopic alumina supported Ni-based catalyst for efficient hydrogen production, *Sci. Rep.*, 2019, **9**, 1–14.

77 G. Chen, J. Li, C. Liu, B. Yan, Z. Cheng, W. Ma, J. Yao and H. Zhang, Low-temperature catalytic cracking of biomass gasification tar over Ni/HZSM-5, *Waste Biomass Valorization*, 2019, **10**, 1013–1020.

78 A. Abedi and A. K. Dalai, Steam gasification of oat hull pellets over Ni-based catalysts: syngas yield and tar reduction, *Fuel*, 2019, **254**, 1–9.

79 Y. Tursun, S. Xu, A. Abulikemu and T. Dilinuer, Biomass gasification for hydrogen rich gas in a decoupled triple bed gasifier with olivine and NiO/olivine, *Bioresour. Technol.*, 2019, **272**, 241–248.

80 L. Cao, I. K. M. Yu, X. Xiong, D. C. W. Tsang, S. Zhang, J. H. Clark, C. Hu, Y. H. Ng, J. Shang and Y. S. Ok, Biorenewable hydrogen production through biomass gasification: a review and future prospects, *Environ. Res.*, 2020, **186**, 1–13.

81 J. Kihlman and P. Simell, Carbon formation in the reforming of simulated biomass gasification gas on nickel and rhodium catalysts, *Catalysts*, 2022, **12**, 1–21.

82 T. N. L. T. Ngo, K.-Y. Chiang, C.-F. Liu, Y.-H. Chang and H.-P. Wan, Hydrogen production enhancement using hot gas cleaning system combined with prepared Ni-based catalyst in biomass gasification, *Int. J. Hydrogen Energy*, 2021, **46**, 11269–11283.

83 S. Abdpour and R. M. Santos, Recent advances in heterogeneous catalysis for supercritical water oxidation/gasification processes: insight into catalyst development, recent advances in heterogeneous catalysis for supercritical water oxidation/gasification processes: insight into catalyst development, *Process Saf. Environ. Prot.*, 2021, **149**, 169–184.

84 G. Duman, T. Watanabe, M. A. Uddin and J. Yanik, Steam gasification of safflower seed cake and catalytic tar decomposition over ceria modified iron oxide catalysts, *Fuel Process. Technol.*, 2014, **126**, 276–283.

85 M. A. Uddin, H. Tsuda, S. Wu and E. Sasaoka, Catalytic decomposition of biomass tars with iron oxide catalysts, *Fuel*, 2008, **87**, 451–459.

86 T. Nordgreen, V. Nemanova, K. Engvall and K. Sjostrom, Iron-based materials as tar depletion catalysts in biomass gasification: dependency on oxygen potential, *Fuel*, 2012, **95**, 71–78.

87 W. Lan, H. Ding, X. Jin, D. Yin, Y. Wang and J. Ji, Catalytic biomass gasification of sawdust: integrated experiment investigation with process modelling and analysis, *Int. J. Low-Carbon Technol.*, 2022, **17**, 482–487.

88 A. Haryanto, S. Fernando and S. Adhikari, Ultrahigh temperature water gas shift catalysts to increase hydrogen yield from biomass gasification, *Catal. Today*, 2007, **129**, 269–274.

89 K. Tomishige, T. Miyazawa, M. Asadullah, S. Ito and K. Kunimori, Catalyst performance in reforming of tar derived from biomass over noble metal catalysts, *Green Chem.*, 2003, **5**, 399–403.

90 A. McFarlan and N. Maffei, Assessing tar removal in biomass gasification by steam reforming over a commercial automotive catalyst, *Fuel*, 2018, **233**, 291–298.

91 D. Xu, L. Liu, N. Wei, Y. Guo, S. Wang, Z. Wu and P. Duan, Catalytic supercritical water gasification of aqueous phase directly derived from microalgae hydrothermal liquefaction, *Int. J. Hydrogen Energy*, 2019, **44**, 26181–26192.

92 J. Lin, S. Sun, C. Cui, R. Ma, L. Fang, P. Zhang, Z. Quan, X. Song, J. Yan and J. Luo, Hydrogen-rich bio-gas generation and optimization in relation to heavy metals immobilization during Pd-catalyzed supercritical water gasification of sludge, *Energy*, 2019, **189**, 1–9.

93 P. Lahijani, Z. A. Zainal, A. R. Mohamed and M. Mohammadi, CO_2 gasification reactivity of biomass char: catalytic influence of alkali, alkaline earth and transition metal salts, *Bioresour. Technol.*, 2013, **144**, 288–295.

94 K. Umeki, G. Haggstrom, A. Bach-Oller, K. Kirtania and E. Furusjo, Reduction of tar and soot formation from entrained-flow gasification of woody biomass by alkali impregnation, *Energy Fuels*, 2017, **31**, 5104–5110.
95 K. Koido, T. Iwasaki, K. Kurosawa, R. Takaku, H. Ohashi and M. Sato, Cesium-catalyzed hydrogen production by the gasification of woody biomass for forest decontamination, *ACS Omega*, 2021, **6**, 5233–5243.
96 J. Li, Y. Xie, K. Zeng, G. Flamant, H. Yang, X. Yang, D. Zhong, Z. Du and H. Chen, Biomass gasification in molten salt for syngas production, *Energy*, 2020, **210**, 1–10.
97 W. Su, C. Cai, P. Liu, W. Lin, B. Liang, H. Zhang, Z. Ma, H. Ma, Y. Xing and W. Liu, Supercritical water gasification of food waste: effect of parameters on hydrogen production, *Int. J. Hydrogen Energy*, 2020, **45**, 14744–14755.
98 R. Roncancio, M. S. Ulcay, J. E. Arango and J. P. Gore, Experimental study of CO_2 corn stover char gasification using iron nitrate as a catalyst under a high-pressure environment, *Fuel*, 2020, **267**, 1–8.
99 M. W. Islam, A review of dolomite catalyst for biomass gasification tar removal, *Fuel*, 2020, **267**, 1–17.
100 A. Orio, J. Corella and I. Narvaez, Performance of different dolomites on hot raw gas cleaning from biomass gasification with air, *Ind. Eng. Chem. Res.*, 1997, **36**, 3800–3808.
101 J. Corella, J. M. Toledo and R. Padilla, Olivine or dolomite as in-bed additive in biomass gasification with air in a fluidized bed: which is better?, *Energy Fuels*, 2004, **18**, 713–720.
102 M. Inayat, S. A. Sulaiman and J. C. Kurnia, Catalytic co-gasification of coconut shells and oil palm fronds blends in the presence of cement, dolomite, and limestone: parametric optimization via Box Behnken Design, *J. Energy Inst.*, 2019, **92**, 871–882.
103 M. Hervy, R. Olcese, M. M. Bettahar, M. Mallet, A. Renard, L. Maldonado, D. Remy, G. Mauviel and A. Dufour, Evolution of dolomite composition and reactivity during biomass gasification, *Appl. Catal., A*, 2019, **572**, 97–106.
104 S. Rapagna, N. Jand, A. Kiennemann and P. U. Foscolo, Steam-gasification of biomass in a fluidised-bed of olivine particles, *Biomass Bioenergy*, 2000, **19**, 187–197.
105 Y. Cao, Y. Bai and J. Du, Study on gasification characteristics of pine sawdust using olivine as in-bed material for combustible gas production, *J. Energy Inst.*, 2021, **96**, 168–172.
106 J. Meng, X. Wang, Z. Zhao, A. Zheng, Z. Huang, G. Wei, K. Lv and H. Li, Highly abrasion resistant thermally fused olivine as in situ catalysts for tar reduction in a circulating fluidized bed biomass gasifier, *Bioresour. Technol.*, 2018, **268**, 212–220.
107 M. Cortazar, L. Santamaria, G. Lopez, J. Alvarez, M. Amutio, J. Bilbao and M. Olazar, Fe/olivine as primary catalyst in the biomass steam gasification in a fountain confined spouted bed reactor, *J. Ind. Eng. Chem.*, 2021, **99**, 364–379.
108 M. Cortazar, G. Lopez, J. Alvarez, M. Amutio, J. Bilbao and M. Olazar, Behaviour of primary catalysts in the biomass steam gasification in a fountain confined spouted bed, *Fuel*, 2019, **253**, 1446–1456.
109 B. L. F. Chin, A. Gorin, H. B. Chua and F. Twaiq, Experimental investigation on tar produced from palm shells derived syngas using zeolite HZSM-5 catalyst, *J. Energy Inst.*, 2015, **89**, 1–12.
110 N. Laksmono, M. Paraschiv, K. Loubar and M. Tazerout, Biodiesel production from biomass gasification tar via thermal/catalytic cracking, *Fuel Process. Technol.*, 2013, **106**, 776–783.
111 J. Waluyo, P. M. Ruya, D. Hantoko, J. Rizkiana, I. G. B. N. Makertihartha, M. Yan and H. Susanto, Utilization of modified zeolite as catalyst for steam gasification of palm kernel shell, *Bull. Chem. React. Eng. Catal.*, 2021, **16**, 623–631.
112 A. Lalsare, Y. Wang, Q. Li, A. Sivri, R. J. Vukmanovich, C. E. Dumitrescu and J. Hu, Hydrogen-rich syngas production through synergistic methane-activated catalytic biomass gasification, *ACS Sustain. Chem. Eng.*, 2019, **7**, 16060–16071.
113 H. Porawati, A. Kurniawan and E. Yuliwati, Effect of temperature on gasification of biomass using zeolite, *J. Phys.: Conf. Ser.*, 2021, **1845**, 1–11.
114 M. Gholizadeh, X. Hu and Q. Liu, Progress of using biochar as a catalyst in thermal conversion of biomass, *Rev. Chem. Eng.*, 2019, **35**, 1–30.
115 S. Zhang, Y. Song, Y. C. Song, Q. Yi, L. Dong, T. T. Li, L. Zhang, J. Feng, W. Y. Li b and C.-Z. Li, An advanced biomass gasification technology with integrated catalytic hot gas cleaning. part III: effects of inorganic species in char on the reforming of tars from wood and agricultural wastes, *Fuel*, 2016, **183**, 177–184.
116 D. Wang, W. Yuan and W. Ji, Char and char-supported nickel catalysts for secondary syngas cleanup and conditioning, *Applied Energy*, 2011, **88**, 1656–1663.
117 D. Yao, Q. Hu, D. Wang, H. Yang, C. Wu, X. Wang and H. Chen, Hydrogen production from biomass gasification using biochar as a catalyst/support, *Bioresour. Technol.*, 2016, **216**, 159–164.
118 D. Buentello-Montoya, X. Zhang, J. Li, V. Ranade, S. Marques and M. Geron, Performance of biochar as a catalyst for tar steam reforming: effect of the porous structure, *Applied Energy*, 2020, **259**, 1–12.
119 Y. Liu, M. Paskevicius, H. Wang, G. Parkinson, J. Wei, M. A. Akhtar and C.-Z. Li, Insights into the mechanism of tar reforming using biochar as a catalyst, *Fuel*, 2021, **296**, 1–7.
120 S.-W. Wang, D.-X. Li, W.-B. Ruan, C.-L. Jin and M. R. Farahani, A techno-economic review of biomass gasification for production of chemicals, *Energy Sources, Part B*, 2018, **13**, 351–356.
121 S. Sarkar and A. Kumar, *Potential of Syngas based biofuels and biochemicals for Drayton valley, Alberta technical and economic state-of-the-art and development*, Final report by University of Alberta, Edmonton, Canada, 2010.
122 A. AlNoussa, G. McKaya and T. Al-Ansari, A comparison of steam and oxygen fed biomass gasification through

a techno-economic-environmental study, *Energy Convers. Manage.*, 2020, **208**, 1–15.
123 S. You, H. Tong, J. Armin-Hoiland, Y. W. Tong and C.-H. Wang, Techno-economic and greenhouse gas savings assessment of decentralized biomass gasification for electrifying the rural areas of Indonesia, *Applied Energy*, 2017, **208**, 495–510.
124 L. M. Putranto, T. Widodo, H. Indrawan, M. A. Imron and S. A. Rosyadi, Grid parity analysis: the present state of PV rooftop in Indonesia, *Renew. Energy Focus*, 2022, **40**, 23–38.
125 Y. K. Salkuyeh, B. A. Saville and H. L. MacLean, Techno-economic analysis and life cycle assessment of hydrogen production from different biomass gasification processes, *Int. J. Hydrogen Energy*, 2018, **43**, 9514–9528.
126 S. L. Y. Lo, B. S. How, S. Y. Teng, H. L. Lam, C. H. Lim, M. A. Rhamdhani and J. Sunarso, Stochastic techno-economic evaluation model for biomass supply chain: a biomass gasification case study with supply chain uncertainties, *Renewable Sustainable Energy Rev.*, 2021, **152**, 1–23.
127 C. Koroneos, A. Dompros and G. Roumbas, Hydrogen production via biomass gasification – a life cycle assessment approach, *Chem. Eng. Process.*, 2008, **47**, 1261–1268.
128 Q. Yang, H. Zhou, X. Zhang, C. P. Nielsen, J. Li, X. Lu, H. Yang and H. Chen, Hybrid life-cycle assessment for energy consumption and greenhouse gas emissions of a typical biomass gasification power plant in China, *J. Cleaner Prod.*, 2018, **205**, 661–671.
129 A. C. M. Loy, H. Alhazmi, S. S. M. Lock, C. L. Yiin, K. W. Cheah, B. L. F. Chin, B. S. How and S. Yusup, Life-cycle assessment of hydrogen production via catalytic gasification of wheat straw in the presence of straw derived biochar catalyst, *Bioresour. Technol.*, 2021, **341**, 1–9.
130 G. Zang, J. Zhang, J. Jia, E. S. Lora and A. Ratner, Life cycle assessment of power-generation systems based on biomass integrated gasification combined cycles, *Renewable Energy*, 2020, **149**, 336–346.
131 R. Thomson, P. Kwong, E. Ahmad and K. D. P. Nigam, Clean syngas from small commercial biomass gasifiers; a review of gasifier development, recent advances and performance evaluation, *Int. J. Hydrogen Energy*, 2020, **45**, 21087–21111.
132 Y. Jafri, L. Waldheim and J. Lundgren, *Emerging gasification technologies for waste & biomass*, IEA Bioenergy, 2020, pp. 1–83.
133 T. Y. A. Fahmy, Y. Fahmy, F. Mobarak, M. El-Sakhawy and R. E. Abou-Zeid, Biomass pyrolysis: past, present, and future, *Environ. Dev. Sustain.*, 2020, **22**, 17–32.
134 H. Mohammed, K. Garba, S. I. Ahmed and L. G. Abubakar, Recent advances on strategies for upgrading biomass pyrolysis vapour to value-added bio-oils for bioenergy and chemicals, *Sustain. Energy Technol. Assess.*, 2023, **55**, 1–20.
135 Z. Zhang, Y. Li, L. Luo, D. Yellezuome, M. M. Rahman, J. Zou, H. Hu and J. Cai, Insight into kinetic and Thermodynamic Analysis methods for lignocellulosic biomass pyrolysis, *Renewable Energy*, 2023, **202**, 154–171.
136 D. Radlein and A. Quignard, A short historical review of fast pyrolysis of biomass, *OGST J.*, 2013, **68**, 621–783.
137 A. Eschenbacher, P. Fennell and A. D. Jensen, A review of recent research on catalytic biomass pyrolysis and low-pressure hydropyrolysis, *Energy Fuels*, 2021, **35**, 18333–18369.
138 M. Sajdak, R. Muzyka, G. Gałko, E. Ksepko, M. Zajemska, S. Sobek and D. Tercki, Actual trends in the usability of biochar as a high-value product of biomass obtained through pyrolysis, *Energies*, 2023, **16**, 1–30.
139 B. Li, J. Tang, X. Xie, J. Wei, D. Xu, L. Shi, K. Ding, S. Zhang, X. Hu, S. Zhang and D. Liu, Char structure evolution during molten salt pyrolysis of biomass: effect of temperature, *Fuel*, 2023, **331**, 1–8.
140 S. Zhou, S. Tang, G. Li, S. Xin, F. Huang, X. Liu, T. Mi, K. Huang and L. Zeng, Catalytic fast pyrolysis of herbal medicine wastes over zeolite catalyst for aromatic hydrocarbons production, *Fuel*, 2023, **333**, 1–15.
141 W. Shen, B. Cao, M. Mu, C. Yuan, C. Li, X. Hu, S. Wang and A. Abomohra, Monophenols recovery by catalytic pyrolysis of waste sawdust over activated biochar from the brown macroalgae Hizikia fusiformis: mechanism and life-cycle assessment, *J. Anal. Appl. Pyrolysis*, 2023, **169**, 1–10.
142 Y. Sun, C. Li, S. Zhang, D. Dong, M. Gholizadeh, S. Wang and X. Hu, Pyrolysis behaviors of rapeseed meal: products distribution and properties, *Biomass Convers. Biorefin.*, 2021, **1**, 1–16.
143 P. Brassard, S. Godbout and V. Raghavan, Pyrolysis in auger reactors for biochar and bio-oil production: a review, *Biosyst. Eng.*, 2017, **161**, 80–92.
144 S. R. Naqvi, A. H. Khoja, I. Ali, M. Naqvi, T. Noor, A. Ahmad, R. Luque and N. A. S. Amin, Recent progress in catalytic deoxygenation of biomass pyrolysis oil using microporous zeolites for green fuels production, *Fuel*, 2023, **333**, 1–15.
145 K. Cen, X. Zhuang, Z. Gan, H. Zhang and D. Chen, Biomass pyrolysis polygeneration with bio-oil recycling: Co-pyrolysis of heavy bio-oil and pine wood leached with light bio-oil for product upgradation, *Fuel*, 2023, **335**, 1–15.
146 Y. Zhang, P. Chen, S. Liu, P. Peng, M. Min, Y. Cheng, E. Anderson, N. Zhou, L. Fan, C. Liu, G. Chen, Y. Liu, H. Lei, B. Li and R. Ruan, Effects of feedstock characteristics on microwave-assisted pyrolysis – a review, *Bioresour. Technol.*, 2017, **230**, 143–151.
147 A. Farooq, S. Valizadeh, G. H. Rhee, J. Lee, J. Jae, S.-C. Jung, W.-H. Chen and Y.-K. Park, Valorization of furniture industry-processed residue via catalytic pyrolysis with methane, *Energy Convers. Manage.*, 2022, **261**, 1–15.
148 S. Moogi, S. Pyo, A. Farooq, S. Valizadeh, Y. J. Choi, G. H. Rhee, J. Lee, J. Jae, M. Hussain, M. A. Khan, B.-H. Jeon, K.-Y. A. Lin, W.-H. Chen and Y.-K. Park, Enhancement of bioaromatics production from food waste through catalytic pyrolysis over Zn and Mo-loaded HZSM-5 under an environment of decomposed methane, *Chem. Eng. J.*, 2022, **446**, 1–15.
149 M. Gholizadeh, R. Gunawan, X. Hu, S. Kadarwati, R. Westerhof, W. Chaiwat, M. M. Hasan and C.-Z. Li, Importance of hydrogen and bio-oil inlet temperature

during the hydrotreatment of bio-oil, *Fuel Process. Technol.*, 2016, **150**, 132–140.

150 A. Dimitriadis, N. Bergvall, A.-C. Johansson, L. Sandstrom, S. Bezergianni, N. Tourlakidis, L. Meca, P. Kukula and L. Raymakers, Biomass conversion via ablative fast pyrolysis and hydroprocessing towards refinery integration: Industrially relevant scale validation, *Fuel*, 2023, **332**, 1–15.

151 J. S. Passos, P. Straka, M. Auersvald and P. Biller, Upgrading of hydrothermal liquefaction biocrudes from mono- and co-liquefaction of cow manure and wheat straw through hydrotreating and distillation, *Chem. Eng. J.*, 2023, **452**, 1–15.

152 N. Dewayanto and M. R. Nordin, Catalytic pyrolysis of biomass to synthesize bio-oil and chemicals: a review, *Chemica*, 2015, **2**, 29–37.

153 Y. Sun, C. Li, S. Zhang, Q. Li, M. Gholizadeh, Y. Wang, S. Hu, J. Xiang and X. Hu, Pyrolysis of soybean residue: Understanding characteristics of the products, *Renewable Energy*, 2021, **174**, 487–500.

154 J. Wang and S. Wang, Preparation, modification and environmental application of biochar: a review, *J. Cleaner Prod.*, 2019, **227**, 1002–1022.

155 H. Sun, D. Feng, S. Sun, Y. Zhao, L. Zhang, G. Chang, Q. Guo, J. Wu and Y. Qin, Thermal evolution of gas-liquid-solid products and migration regulation of C/H/O elements during biomass pyrolysis, *J. Anal. Appl. Pyrolysis*, 2021, **156**, 1–10.

156 E. David and J. Kopac, Pyrolysis of rapeseed oil cake in a fixed bed reactor to produce bio-oil, *J. Anal. Appl. Pyrolysis*, 2018, **134**, 495–502.

157 M. A. Shah, N. S. Khan, V. Kumar and A. Qurashi, Pyrolysis of walnut shell residues in a fixed bed reactor: effects of process parameters, chemical and functional properties of bio-oil, *J. Environ. Chem. Eng.*, 2021, **9**, 1–15.

158 J. Zhu, L. Jin, J. Li, Z. Bao, Y. Li and H. Hu, Fast pyrolysis behaviors of cedar in an infrared-heated fixed-bed reactor, *Bioresour. Technol.*, 2019, **290**, 1–6.

159 M. M. Rahman, Nishu, M. Sarker, M. Chai, C. Li, R. Liu and J. Cai, Potentiality of combined catalyst for high quality bio-oil production from catalytic pyrolysis of pinewood using an analytical Py-GC/MS and fixed bed reactor, *J. Energy Inst.*, 2020, **93**, 1737–1746.

160 A. Soria-Verdugo, E. Cano-Pleite, A. Passalacqua and R. O. Fox, Effect of particle shape on biomass pyrolysis in a bubbling fluidized bed, *Fuel*, 2023, **339**, 1–15.

161 Q. K. Tran, M. L. Le, H. V. Ly, H. C. Woo, J. Kim and S.-S. Kim, Fast pyrolysis of pitch pine biomass in a bubbling fluidized-bed reactor for bio-oil production, *J. Ind. Eng. Chem.*, 2021, **98**, 168–179.

162 D. S. Pandey, G. Katsaros, C. Lindfors, J. J. Leahy and S. A. Tassou, Fast pyrolysis of poultry litter in a bubbling fluidised bed reactor: Energy and nutrient recovery, *Sustainability*, 2019, **11**, 1–17.

163 N. Gomez, S. W. Banks, D. J. Nowakowski, J. G. Rosas, J. Cara, M. E. Sanchez and A. V. Bridgwater, Effect of temperature on product performance of a high ash biomass during fast pyrolysis and its bio-oil storage evaluation, *Fuel Process. Technol.*, 2018, **172**, 97–105.

164 H. V. Ly, J. W. Park, S.-S. Kim, H. T. Hwang, J. Kim and H. C. Woo, Catalytic pyrolysis of bamboo in a bubbling fluidized-bed reactor with two different catalysts: HZSM-5 and red mud for upgrading bio-oil, *Renewable Energy*, 2020, **149**, 1434–1445.

165 P. Peltola, L. Ruottu, M. Larkimo, A. Laasonen and K. Myohanen, A novel dual circulating fluidized bed technology for thermal treatment of municipal sewage sludge with recovery of nutrients and energy, *Waste Manage.*, 2023, **155**, 329–337.

166 J. Y. Park, J.-K. Kim, C.-H. Oh, J.-W. Park and E. E. Kwon, Production of bio-oil from fast pyrolysis of biomass using a pilot-scale circulating fluidized bed reactor and its characterization, *J. Environ. Manage.*, 2019, **234**, 138–144.

167 K. Duanguppama, N. Suwapaet and A. Pattiya, Fast pyrolysis of contaminated sawdust in a circulating fluidised bed reactor, *J. Anal. Appl. Pyrolysis*, 2016, **118**, 63–74.

168 I. Mufandi, W. Treede, P. Singbua and R. Suntivarakorn, The comparison of bio-oil production from sugarcane trash, napier grass, and rubber tree in the circulating fluidized bed reactor, *Test Eng. Manag.*, 2020, **82**, 4557–4563.

169 W. Cai, Z. Luo, J. Zhou and Q. Wang, A review on the selection of raw materials and reactors for biomass fast pyrolysis in China, *Fuel Process. Technol.*, 2021, **221**, 1–14.

170 A. Al-Rumaihi, M. Shahbaz, G. Mckay, H. Mackey and T. Al-Ansari, A review of pyrolysis technologies and feedstock: a blending approach for plastic and biomass towards optimum biochar yield, *Renewable Sustainable Energy Rev.*, 2022, **167**, 1–15.

171 L. Junsheng, The optimal of pyrolysis process in the rotating cone reactor and pyrolysis product analysis, in *International Conference on Challenges in Environmental Science and Computer Engineering*, 2010, vol. 1, pp. 1–4.

172 Z. Jun, W. S. Yang, Q. G. Chao, C. Y. Wei and Z. S. Yu, Development of rotating cone biomass pyrolysis mechanical system, *Trans. Chin. Soc. Agric. Eng.*, 2007, **23**, 198–200.

173 P. Fu, X. Bai, W. Yi, Z. Li and Y. Li, Fast pyrolysis of wheat straw in a dual concentric rotary cylinder reactor with ceramic balls as recirculated heat carrier, *Energy Convers. Manage.*, 2018, **171**, 855–862.

174 R. E. Guedes, A. S. Luna and A. R. Torres, Operating parameters for bio-oil production in biomass pyrolysis: a review, *J. Anal. Appl. Pyrolysis*, 2018, **129**, 134–149.

175 H. C. Park, B.-K. Lee, H. S. Yoo and H. S. Choi, Influence of operating conditions for fast pyrolysis and pyrolysis oil production in a conical spouted-bed reactor, *Chem. Eng. Technol.*, 2019, **42**, 1–13.

176 J. Grams, Upgrading of lignocellulosic biomass to hydrogen-rich gas, *Energies*, 2023, **16**, 1–5.

177 A. R. Fernandez-Akarregi, J. Makibar, G. Lopez, M. Amutio and M. Olazar, Design and operation of a conical spouted

bed reactor pilot plant (25 kg/h) for biomass fast pyrolysis, *Fuel Process. Technol.*, 2013, **112**, 48–56.

178 M. Amutio, G. Lopez, M. Artetxe, G. Elordi, M. Olazar and J. Bilbao, Influence of temperature on biomass pyrolysis in a conical spouted bed reactor, *Resour., Conserv. Recycl.*, 2012, **59**, 23–31.

179 E. Fernandez, L. Santamaria, M. Amutio, M. Artetxe, A. Arregi, G. Lopez, J. Bilbao and M. Olazar, Role of temperature in the biomass steam pyrolysis in a conical spouted bed reactor, *Energy*, 2022, **238**, 1–12.

180 K. Azizi, M. K. Moravejia, A. Arregi, M. Amutio, G. Lopez and M. Olazar, On the pyrolysis of different microalgae species in a conical spouted bed reactor: bio-fuel yields and characterization, *Bioresour. Technol.*, 2020, **311**, 1–8.

181 A. Pawar and N. L. Panwar, Influence of pyrolysis technologies on biofuel production and its physicochemical properties: a review, in *Smart Technologies for Energy, Environment and Sustainable Development*, 2022, vol. 1, pp. 1–15.

182 R. Kaur and S. P. Singh, Commercial or pilot-scale pyrolysis units for conversion of biomass to bio-oils: state of the art, *Environ. Prog. Sustain. Energy*, 2022, **1**, 1–15.

183 N. Khuenkaeo, S. Phromphithak, T. Onsree, S. R. Naqvi and N. Tippayawong, Production and characterization of bio-oils from fast pyrolysis of tobacco processing wastes in an ablative reactor under vacuum, *PLoS One*, 2021, **16**, 1–13.

184 N. Khuenkaeo and N. Tippayawong, Production and characterization of bio-oil and biochar from ablative pyrolysis of lignocellulosic biomass residues, *Chem. Eng. Commun.*, 2020, **207**, 1–9.

185 M. Auersvald, T. Macek, T. Schulzke, M. Stas and P. Simacek, Influence of biomass type on the composition of bio-oils from ablative fast pyrolysis, *J. Anal. Appl. Pyrolysis*, 2020, **150**, 1–10.

186 C.-Z. Li, X. S. Wang and H. Wu, *Method of and system for grinding pyrolysis of particulate carbonaceous feedstock*, PCT/AU2011/000741, 2010.

187 S. Xu, X. Chen, Q. Tang, A. Li, X. Lu, X. Liu and F. Yu, Pyrolysis of dealkaline lignin to phenols by loading grinding beads in a rotary kiln reactor, *J. Anal. Appl. Pyrolysis*, 2023, **169**, 1–15.

188 M. D. M. Hasan, X. S. Wang, D. Mourant, R. Gunawan, C. Yu, X. Hu, S. Kadarwati, M. Gholizadeh, H. Wu, B. Li, L. Zhang and C.-Z. Li, Grinding pyrolysis of Mallee wood: effects of pyrolysis conditions on the yields of bio-oil and biochar, *Fuel Process. Technol.*, 2017, **167**, 215–220.

189 M. M. Hasan, M. G. Rasul, M. I. Jahirul and M. M. K. Khan, Fast pyrolysis of Macadamia nutshell in an auger reactor: process optimization using response surface methodology (RSM) and oil characterization, *Fuel*, 2023, **333**, 1–15.

190 N. Puy, R. Murillo, M. V. Navarro, J. M. Lopez, J. Rieradevall, G. Fowler, I. Aranguren, T. Garcia, J. Bartroli and A. M. Mastral, Valorisation of forestry waste by pyrolysis in an auger reactor, *Waste Manage.*, 2011, **31**, 1339–1349.

191 S. Papari, K. Hawboldt and P. Fransham, Study of selective condensation for woody biomass pyrolysis oil vapours, *Fuel*, 2019, **245**, 233–239.

192 A. Ahmed, M. S. A. Bakar, R. S. Sukri, M. Hussain, A. Farooq, S. Moogi and Y.-K. Park, Sawdust pyrolysis from the furniture industry in an auger pyrolysis reactor system for biochar and bio-oil production, *Energy Convers. Manage.*, 2020, **226**, 1–10.

193 V. Lakshman, P. Brassard, L. Hamelin, V. Raghavan and S. Godbout, Pyrolysis of Miscanthus: developing the mass balance of a biorefinery through experimental tests in an auger reactor, *Bioresour. Technol. Rep.*, 2021, **14**, 1–6.

194 G. Kabir and B. H. Hameed, Recent progress on catalytic pyrolysis of lignocellulosic biomass to high-grade bio-oil and bio-chemicals, *Renewable Sustainable Energy Rev.*, 2017, **70**, 945–967.

195 J. A. Oyebanji, O. S. I. Fayomi, O. I. Oyeniyi, P. G. Akor and S. T. Ajayi, Physico-chemical analysis of pyrolyzed bio-oil from lophira alata (ironwood) wood, *J. Environ. Manage.*, 2022, **4**, 1–9.

196 P. R. Bhoi, A. S. Ouedraogo, V. Soloiu and R. Quirino, Recent advances on catalysts for improving hydrocarbon compounds in bio-oil of biomass catalytic pyrolysis, *Renewable Sustainable Energy Rev.*, 2020, **121**, 1–13.

197 M. C. Rangel, F. M. Mayer, M. S. Carvalho, G. Saboia and A. M. Andrade, Selecting catalysts for pyrolysis of lignocellulosic biomass, *Biomass*, 2023, **3**, 31–63.

198 P. Yan, E. M. Kennedy, H. Zhang and M. Stockenhuber, Catalytic hydropyrolysis of lignocellulosic biomass to BTX and biofuels over zeolite beta based catalysts, *Fuel*, 2023, **332**, 1–15.

199 j. Jae, G. A. Tompsett, A. J. Foster, K. D. Hammond, S. M. Auerbach, R. F. Lobo and G. W. Hubber, Investigation into the shape selectivity of zeolite catalysts for biomass conversion, *J. Catal.*, 2011, **279**, 257–268.

200 B. B. Uzun and N. Sarioglu, Rapid and catalytic pyrolysis of corn stalks, *Fuel Process. Technol.*, 2009, **90**, 705–716.

201 X. Li, W. Dong, J. Zhang, S. Shao and Y. Cai, Preparation of bio-oil derived from catalytic upgrading of biomass vacuum pyrolysis vapor over metal-loaded HZSM-5 zeolites, *J. Energy Inst.*, 2020, **93**, 605–613.

202 H. Hernando, I. Moreno, J. Fermoso, C. Ochoa-Hernandez, P. Pizarro, J. M. Coronado, J. Cejka and D. P. Serrano, Biomass catalytic fast pyrolysis over hierarchical ZSM-5 and Beta zeolites modified with Mg and Zn oxides, *Biomass Convers. Biorefin.*, 2017, **7**, 289–304.

203 H. Zhang, R. Xiao, B. Jin, D. Shen, R. Chen and G. Xiao, Catalytic fast pyrolysis of straw biomass in an internally interconnected fluidized bed to produce aromatics and olefins: effect of different catalysts, *Bioresour. Technol.*, 2013, **137**, 82–87.

204 C. A. Mullen, A. A. Boateng, D. J. Mihalcik and N. M. Goldberg, Catalytic fast pyrolysis of white oak wood in a bubbling fluidized bed, *Energy Fuels*, 2011, **25**, 5444–5451.

205 E. Putun, B. B. Uzun and A. E. Putun, Fixed-bed catalytic pyrolysis of cotton-seed cake: effects of pyrolysis temperature, natural zeolite content and sweeping gas flow rate, *Bioresour. Technol.*, 2006, **97**, 701–710.

206 A. Aho, A. Tokarev, P. Backman, N. Kumar, K. Eranen, M. Hupa, B. Holmbom, T. Salmi and D. Y. Murzin, Catalytic pyrolysis of pine biomass over H-Beta zeolite in a dual-fluidized bed reactor: effect of space velocity on the yield and composition of pyrolysis products, *Top. Catal.*, 2011, **54**, 941–948.

207 K. Giannakopoulou, M. Lukas, A. Vasiliev, C. Brunner and H. Schnitzer, Conversion of rapeseed cake into bio-fuel in a batch reactor: effect of catalytic vapor upgrading, *Microporous Mesoporous Mater.*, 2010, **128**, 126–135.

208 S. J. Choi, S. H. Park, J. K. Jeon, I. G. Lee, C. Ryu, D. J. Suh and D. Y. Murzin, Catalytic conversion of particle board over microporous catalysts, *Renewable Energy*, 2013, **54**, 105–110.

209 H. J. Park, J. I. Dong, J. K. Jeon, K. S. Yoo, J. H. Yim and J. M. Sohn, Conversion of the pyrolytic vapor of radiata pine over zeolites, *J. Ind. Eng. Chem.*, 2007, **13**, 182–189.

210 M. Olazar, R. Aguado, J. Bilbao and A. Barona, Pyrolysis of sawdust in a conical spouted-bed reactor with a HZSM-5 catalyst, *AIChE J.*, 2000, **46**, 1025–1033.

211 H. Zhang, T. R. Carlson, R. Xiao and G. W. Huber, Catalytic fast pyrolysis of wood and alcohol mixtures in a fluidized bed reactor, *Green Chem.*, 2012, **14**, 98–110.

212 H. J. Park, H. S. Heo, J. K. Jeon, J. Kim, R. Ryoo, K. E. Jeong and Y. K. Park, Highly valuable chemicals production from catalytic upgrading of radiata pine sawdust- derived pyrolytic vapors over mesoporous MFI zeolites, *Appl. Catal., B*, 2010, **95**, 365–373.

213 P. T. Williams and N. Nugranad, Comparison of products from the pyrolysis and catalytic pyrolysis of rice husks, *Energy*, 2000, **25**, 493–513.

214 H. Zhang, R. Xiao, H. Huang and G. Xiao, Comparison of non-catalytic and catalytic fast pyrolysis of corncob in a fluidized bed reactor, *Bioresour. Technol.*, 2009, **100**, 1428–1434.

215 P. T. Williams and P. A. Horne, The influence of catalyst regeneration on the composition of zeolite-upgraded biomass pyrolysis oils, *Fuel*, 1995, **74**, 1839–1851.

216 F. A. Agblevor, S. Beis, O. Mante and N. Abdoulmoumine, Fractional catalytic pyrolysis of hybrid poplar wood, *Ind. Eng. Chem. Res.*, 2010, **49**, 3533–3538.

217 K. Murata, Y. Liu, M. Inaba and I. Takahara, Catalytic fast pyrolysis of jatropha wastes, *J. Anal. Appl. Pyrolysis*, 2012, **94**, 75–82.

218 M. J. Jeon, S. S. Kim, J. K. Jeon, S. H. Park, J. M. Kim, J. M. Sohn, S. H. Lee and Y. K. Park, Catalytic pyrolysis of waste rice husk over mesoporous materials, *Nanoscale Res. Lett.*, 2012, **7**, 1–5.

219 T. C. Hoffa, D. W. Gardnera, R. Thilakaratneb, J. Proano-Avilesb, R. C. Brownb and J.-P. Tessonniera, Elucidating the effect of desilication on aluminum-rich ZSM-5 zeoliteand its consequences on biomass catalytic fast pyrolysis, *Appl. Catal., A*, 2017, **529**, 68–78.

220 G. Kabir, A. T. Mohd Din and B. H. Hameed, Pyrolysis of oil palm mesocarp fiber catalyzed with steel slag-derived zeolite for bio-oil production, *Bioresour. Technol.*, 2018, **249**, 42–48.

221 R. Kumar, V. Strezov, E. Lovell, T. Kan, H. Weldekidan, J. He, B. Dastjerdi and J. Scott, Bio-oil upgrading with catalytic pyrolysis of biomass using Copper/zeolite-Nickel/zeolite and Copper-Nickel/zeolite catalysts, *Bioresour. Technol.*, 2019, **279**, 404–409.

222 F. Li, X. He, C. A. Shoemaker and C.-H. Wang, Experimental and numerical study of biomass catalytic pyrolysis using Ni_2P-loaded zeolite: Product distribution, characterization and overall benefit, *Energy Convers. Manage.*, 2020, **208**, 1–17.

223 A. K. Mondal, C. Qin, A. J. Ragauskas, Y. Ni and F. Huang, Conversion of Loblolly pine biomass residues to bio-oil in a two-step process: fast pyrolysis in the presence of zeolite and catalytic hydrogenation, *Ind. Crops Prod.*, 2020, **148**, 1–8.

224 H. Persson, I. Duman, S. Wang, L. J. Pettersson and W. Yang, Catalytic pyrolysis over transition metal-modified zeolites: a comparative study between catalyst activity and deactivation, *J. Anal. Appl. Pyrolysis*, 2019, **138**, 54–61.

225 Y. Fan, Y. Cai, X. Li, H. Yin and J. Xia, Coking characteristics and deactivation mechanism of the HZSM-5 zeolite employed in the upgrading of biomass-derived vapors, *J. Ind. Eng. Chem.*, 2017, **46**, 139–149.

226 Y. Hu, M. Li, Y. Fang and T. Tan, Resolving challenges in biomass catalytic pyrolysis by co-optimization of process and catalyst: removal of heavy fraction in pyrolysis vapours and application of novel zeolite catalyst with high thermal conductivity, *Renewable Energy*, 2020, **156**, 951–963.

227 X. Xue, L. Wu, X. Wei, J. Liang and Y. Sun, Product modification in catalytic fast pyrolysis of corn stalk: The decoupled effect of acidity and porosity within a core-shell micro-/mesoporous zeolite, *ACS Sustain. Chem. Eng.*, 2020, **8**, 7445–7453.

228 J. Hertzog, V. Carre, L. Jia, C. L. Mackay, L. Pinard, A. Dufour, O. Masek and F. Aubriet, Catalytic fast pyrolysis of biomass over microporous and hierarchical zeolites: characterization of heavy products, *ACS Sustain. Chem. Eng.*, 2018, **6**, 4717–4728.

229 L. Y. Jia, M. Raad, S. Hamieh, J. Toufaily, T. Hamieh, M. Bettahar, G. Mauviel, M. Tarrighi, L. Pinard and A. Dufour, Catalytic fast pyrolysis of biomass: superior selectivity of hierarchical zeolite to aromatics, *Green Chem.*, 2017, **19**, 5442–5459.

230 H. Hernando, A. M. Hernandez-Gimenez, C. Ochoa-Hernandez, P. C. A. Bruijnincx, K. Houben, M. Baldus, P. Pizarro, J. M. Coronado, J. Fermoso, J. Cejka, B. M. Weckhuysen and D. P. Serrano, Engineering the acidity and accessibility of the zeolite ZSM-5 for efficient bio-oil upgrading in catalytic pyrolysis of lignocellulose, *Green Chem.*, 2018, **20**, 3499–3511.

231 E. David and J. Kopac, Assessment of the catalytic performances of nanocomposites materials based on 13X zeolite, calcium oxide and metal zinc particles in the residual biomass pyrolysis process, *Nanomaterials*, 2022, **12**, 1–25.

232 C. Hu, H. Zhang, S. Wu and R. Xiao, Molecular shape selectivity of HZSM-5 in catalytic conversion of biomass pyrolysis vapors: the effective pore size, *Energy Convers. Manage.*, 2020, **210**, 1–10.

233 Q. Lu, S. Yuan, J. Li, X. Chen, K. Li, X. Xie, X. Fu and Z. He, Influence of Mg and Co addition on Fe based catalyst for in situ biomass pyrolysis, *J. Anal. Appl. Pyrolysis*, 2023, **169**, 1–15.

234 D. Rammohan, N. Kishore and R. V. S. Uppaluri, Thermogravimetric analysis of pyrolysis of Delonix regia biomass in the presence of zeolite, mixed metal oxides and carbon supported noble metal catalysts, *Results Eng.*, 2023, **17**, 1–14.

235 L. Li, D. Cai, L. Zhang, Y. Zhang, Z. Zhao, Z. Zhang, J. Sun, Y. Tan and G. Zou, Synergistic effects during pyrolysis of binary mixtures of biomass components using microwave-assisted heating coupled with iron base tip-metal, *Renewable Energy*, 2023, **203**, 312–322.

236 B.-Z. Li, D.-M. Bi, Q. Dong, Y.-J. Li, Y. Y. Liu and F. P. Huang, Effect of $ZnCl_2$ on the distribution of aldehydes and ketones in bio-oils from catalytic pyrolysis of different biomass, *Bioresources*, 2020, **15**, 5666–5678.

237 D. Mansur, T. Tago, T. Masuda and H. Abimanyu, Conversion of cacao pod husks by pyrolysis and catalytic reaction to produce useful chemicals, *Biomass Bioenergy*, 2014, **66**, 275–285.

238 S. Eibner, F. Broust, J. Blin and A. Julbe, Catalytic effect of metal nitrate salts during pyrolysis of impregnated biomass, *J. Anal. Appl. Pyrolysis*, 2015, **113**, 143–152.

239 H. Hwang, S. Oh, I.-G. Choi and J. W. Choi, Catalytic effects of magnesium on the characteristics of fast pyrolysis products-bio-oil, bio-char, and non-condensed pyrolytic gas fractions, *J. Anal. Appl. Pyrolysis*, 2015, **113**, 27–34.

240 Q. Lu, X. Ye, Z. Zhang, C. Dong and Y. Zhang, Catalytic fast pyrolysis of cellulose and biomass to produce levoglucosenone using magnetic SO_4^{2-}/TiO_2-Fe_3O_4, *Bioresour. Technol.*, 2014, **171**, 10–15.

241 S. D. Stefanidis, K. G. Kalogiannis, E. F. Iliopoulou, A. A. Lappas and P. A. Pilavachi, In situ upgrading of biomass pyrolysis vapors: catalyst screening on a fixed bed reactor, *Bioresour. Technol.*, 2011, **102**, 8261–8267.

242 Q. Lu, S. Yuan, C. Liu, T. Zhang, X. Xie, X. Deng and R. He, A Fe-Ca/SiO_2 catalyst for efficient production of light aromatics from catalytic pyrolysis of biomass, *Fuel*, 2020, **279**, 1–11.

243 S. Honma, T. Hata and T. Watanabe, Effect of catalytic pyrolysis conditions using pulse current heating method on pyrolysis products of wood biomass, *Sci. World J.*, 2014, 1–10.

244 Y. Wang, L. Huang, T. Zhang and Q. Wang, Hydrogen-rich syngas production from biomass pyrolysis and catalytic reforming using biochar-based catalysts, *Fuel*, 2022, **313**, 1–15.

245 J. Grams, M. Niewiadomski, A. M. Ruppert and W. Kwapinski, Catalytic performance of Ni catalyst supported on CeO_2, ZrO_2 and CeO_2-ZrO_2 in the upgrading of cellulose fast pyrolysis vapors, *C. R. Chim.*, 2015, **18**, 1223–1228.

246 M. Zabeti, K. B. S. S. Gupta, G. Raman, L. Lefferts, S. Schallmoser, J. A. Lercher and K. Seshan, Aliphatic hydrocarbons from lignocellulose by pyrolysis over cesium-modified amorphous silica alumina catalysts, *ChemCatChem*, 2015, **7**, 3386–3396.

247 O. D. Mante, J. A. Rodriguez, S. D. Senanayake and S. P. Babua, Catalytic conversion of biomass pyrolysis vapors into hydrocarbon fuel precursors, *Green Chem.*, 2015, **17**, 2362–2368.

248 Q. Lu, S. Yuan, C. Liu, T. Zhang, X. Xie, X. Deng and R. He, A Fe-Ca/SiO_2 catalyst for efficient production of light aromatics from catalytic pyrolysis of biomass, *Fuel*, 2020, **279**, 1–11.

249 S. Li, C. Wang, Z. Lou and X. Zhu, Investigation on the catalytic behavior of alkali metals and alkaline earth metals on the biomass pyrolysis assisted with real-time monitoring, *Energy Fuels*, 2020, **34**, 12654–12664.

250 S. Yang, L. Chen, L. Sun, X. Xie, B. Zhao, H. Si, X. Zhang and D. Hua, Novel NieAl nanosheet catalyst with homogeneously embedded nickel nanoparticles for hydrogen-rich syngas production from biomass pyrolysis, *Int. J. Hydrogen Energy*, 2021, **46**, 1762–1776.

251 Y. He, R. Liu, D. Yellezuome, W. Peng and M. Tabatabaei, Upgrading of biomass-derived bio-oil via catalytic hydrogenation with Rh and Pd catalysts, *Renewable Energy*, 2022, **184**, 487–497.

252 K. Lazdovica, L. Liepina and V. Kampars, Comparative wheat straw catalytic pyrolysis in the presence of zeolites, Pt/C, and Pd/C by using TGA-FTIR method, *Fuel Process. Technol.*, 2015, **138**, 645–653.

253 Q. Lu, Y. Zhang, Z. Tang, W. Li and X. Zhu, Catalytic upgrading of biomass fast pyrolysis vapors with titania and zirconia/titania based catalysts, *Fuel*, 2010, **89**, 2096–2103.

254 K. Lazdovica, L. Liepina and V. Kampars, Catalytic pyrolysis of wheat bran for hydrocarbons production in the presence of zeolites and noble-metals by using TGA-FTIR method, *Bioresour. Technol.*, 2016, **207**, 126–133.

255 Q. Lu, M. Zhou, W. Li, X. Wang, M. Cui and Y. Yang, Catalytic fast pyrolysis of biomass with noble metal-like catalysts to produce high-grade bio-oil: analytical Py-GC/MS study, *Catal. Today*, 2018, **302**, 169–179.

256 Q. Lu, H. Guo, M. Zhou, M. Cui, C. Dong and Y. Yang, Selective preparation of monocyclic aromatic hydrocarbons from catalytic cracking of biomass fast pyrolysis vapors over Mo2N/HZSM-5 catalyst, *Fuel Process. Technol.*, 2018, **173**, 134–142.

257 W. Wang, X. Li, D. Ye, L. Cai and S. Q. Shi, Catalytic pyrolysis of larch sawdust for phenol-rich bio-oil using different catalysts, *Renewable Energy*, 2018, **121**, 146–152.

258 G. Zhang, L. Ma, Y. Dong, Y. Fang and X. Kong, Fabrication of hierarchical flower-like NiMo bimetallic catalyst for valorization of biomass platforms, *Fuel*, 2023, **333**, 1–15.

259 H. Dong, W. Luo, X. Yan, B. Li, J. Hu, S. Huang, M. Xia, M. Zhong, Q. Tang, Z. Zhou and N. Zhou, Production of

catalytic-upgraded pyrolysis products from oiltea camellia shell and polypropylene using NiCe-X/Al_2O_3 and ZrO_2 catalyst (X = Fe, Co), *Fuel*, 2022, **325**, 1–15.

260 S. Xia, H. Yang, W. Lu, N. Cai, H. Xiao, X. Chen, Y. Chen, X. Wang, S. Wang, P. Wu and H. Chen, Fe–Co based synergistic catalytic graphitization of biomass: Influence of the catalyst type and the pyrolytic temperature, *Energy*, 2022, **239**, 1–15.

261 Y. Zheng, J. Wang, D. Li, C. Liu, Y. Lu, X. Lin and Z. Zheng, Activity and selectivity of Ni-Cu bimetallic zeolites catalysts on biomass conversion for bio-aromatic and bio-phenols, *J. Energy Inst.*, 2021, **97**, 58–72.

262 Q. Lu, W. Li, X. Zhang, Z. Liu, Q. Cao, X. Xie and S. Yuan, Experimental study on catalytic pyrolysis of biomass over a Ni/Ca-promoted Fe catalyst, *Fuel*, 2020, **263**, 1–12.

263 M. Lu, P. Lv, Z. Yuan and H. Li, The study of bimetallic NieCo/cordierite catalyst for cracking of tar from biomass pyrolysis, *Renewable Energy*, 2013, **60**, 522–528.

264 R. Kumar, V. Strezov, T. Kan, H. Weldekidan, J. He and S. Jahan, Investigating the effect of mono and bimetallic/zeolite catalysts on hydrocarbon production during bio-oil upgrading from *ex situ* pyrolysis of biomass, *Energy Fuels*, 2020, **34**, 389–400.

265 A. Ibarra, I. Hita, J. M. Arandes and J. Bilbao, A hybrid FCC/HZSM-5 catalyst for the catalytic cracking of a VGO/bio-oil blend in FCC conditions, *Catalysts*, 2020, **10**, 1–15.

266 D. Stratiev, I. Shishkova, M. Ivanov, R. Dinkov, B. Georgiev, G. Argirov, V. Atanassova, P. Vassilev, K. Atanassov, D. Yordanov, A. Popov, A. Padovani, U. Hartmann, S. Brandt, S. Nenov, S. Sotirov and E. Sotirova, Role of catalyst in optimizing fluid catalytic cracking performance during cracking of H-oil-derived gas oils, *ACS Omega*, 2021, **6**, 7626–7637.

267 E. Fernandez, L. Santamaria, M. Artetxe, M. Amutio, A. Arregi, G. Lopez, J. Bilbao and M. Olazar, Conditioning the volatile stream from biomass fast pyrolysis for the attenuation of steam reforming catalyst deactivation, *Fuel*, 2022, **312**, 1–15.

268 K. Magrini, J. Olstad, B. Peterson, R. Jackson, Y. Parent, C. Mukarakate, K. Iisa, E. Christensen and R. Seiser, Feedstock and catalyst impact on bio-oil production and FCC Co-processing to fuels, *Biomass Bioenergy*, 2022, **163**, 1–15.

269 Y. Zhang, J. Guan, P. Qiao, G. Li, J. Li, W. Zhang and M. Liu, Study on the pyrolysis characteristics of sawdust catalyzed by spent FCC catalyst and blast furnace ash, *J. Fuel Chem. Technol.*, 2022, **50**, 1524–1534.

270 M. Bertero and U. Sedran, Conversion of pine sawdust bio-oil (raw and thermally processed) over equilibrium FCC catalysts, *Bioresour. Technol.*, 2013, **135**, 644–651.

271 J. Adam, E. Antonakou, A. Lappas, M. Stocker, M. H. Nilsen, A. Bouzga, J. E. Hustad and G. Oye, In situ catalytic upgrading of biomass derived fast pyrolysis vapours in a fixed bed reactor using mesoporous materials, *Microporous Mesoporous Mater.*, 2006, **96**, 93–101.

272 M. Bertero, J. R. Garcia, M. Falco and U. Sedran, Equilibrium FCC catalysts to improve liquid products from biomass pyrolysis, *Renewable Energy*, 2019, **132**, 11–18.

273 O. D. Mante, F. A. Agblevor and R. McClung, Fluid catalytic cracking of biomass pyrolysis vapors, *Biomass Convers. Biorefin.*, 2011, **1**, 189–201.

274 H. Zhang, R. Xiao, D. Wang, Z. Zhong, M. Song, Q. Pan and G. He, Catalytic fast pyrolysis of biomass in a fluidized bed with fresh and spent fluidized catalytic cracking (FCC) catalysts, *Energy Fuels*, 2009, **23**, 6199–6206.

275 J. Socci, A. Saraeian, S. D. Stefanidis, S. W. Banks, B. H. Shanks and T. Bridgwater, The role of catalyst acidity and shape selectivity on products from the catalytic fast pyrolysis of beech wood, *J. Anal. Appl. Pyrolysis*, 2022, **162**, 1–11.

276 E. Karimi, C. Briens, F. Berruti, S. Moloodi, T. Tzanetakis, M. J. Thomson and M. Schlaf, Red mud as a catalyst for the upgrading of hemp-Seed pyrolysis bio-oil, *Energy Fuels*, 2010, **24**, 6586–6600.

277 S. Shao, P. Zhang, X. Xiang, X. Li and H. Zhang, Promoted ketonization of bagasse pyrolysis gas over red mud-based oxides, *Renewable Energy*, 2022, **190**, 11–18.

278 X. Li, J. Sun, H. Zhang, S. Shao and Y. Cai, Enhanced production of monocyclic aromatic hydrocarbons by catalytic pyrolysis of rape straw in a cascade dual-catalyst system of modified red mud and HZSM-5, *Fuel Process. Technol.*, 2022, **236**, 1–15.

279 L. Wang, B. Si, X. Han, W. Yi, Z. Li and A. Zhang, Study on the effect of red mud and its component oxides on the composition of bio-oil derived from corn stover catalytic pyrolysis, *Ind. Crops Prod.*, 2022, **184**, 1–15.

280 X. Zhou, L. Zhang, Q. Chen, X. Xiao, T. Wang, S. Cheng and J. Li, Study on the mechanism and reaction characteristics of red-mud-catalyzed pyrolysis of corn stover, *Fuel*, 2023, **338**, 1–15.

281 H. V. Ly, Q. K. Tran, S.-S. Kim, J. Kim, S. S. Choi and C. Oh, Catalytic upgrade for pyrolysis of food waste in a bubbling fluidized-bed reactor, *Environ. Pollut.*, 2021, **275**, 1–15.

282 F. A. Agblevor, D. C. Elliott, D. M. Santosa, M. V. Olarte, S. D. Burton, M. Swita, S. H. Beis, K. Christian and B. Sargent, Red mud catalytic pyrolysis of Pinyon Juniper and single-stage hydrotreatment of oils, *Energy Fuels*, 2016, **30**, 7947–7958.

283 G. Duman, M. Pala, S. Ucar and J. Yanik, Two-step pyrolysis of safflower oil cake, *J. Anal. Appl. Pyrolysis*, 2013, **103**, 352–361.

284 D. M. Santosa, C. Zhu, F. A. Agblevor, B. Maddi, B. Q. Roberts, I. V. Kutnyakov, S.-J. Lee and H. Wang, In situ catalytic fast pyrolysis using red mud catalyst: Impact of catalytic fast pyrolysis temperature and biomass feedstocks, *ACS Sustain. Chem. Eng.*, 2020, **8**, 5156–5164.

285 A. Veses, M. Aznar, J. M. Lopez, M. S. Callen, R. Murillo and T. Garcia, Production of upgraded bio-oils by biomass catalytic pyrolysis in an auger reactor using low cost materials, *Fuel*, 2015, **141**, 17–22.

286 F. A. Agblevor, H. Wang, S. Beis, K. Christian, A. Slade, O. Hietsoi and D. M. Santosa, Reformulated red mud:

a robust catalyst for in situ catalytic pyrolysis of biomass, *Energy Fuels*, 2020, **34**, 3272–3283.

287 A. Inayat, A. Ahmed, R. Tariq, A. Waris, F. Jamil, S. F. Ahmed, C. Ghenai and Y.-K. Park, Techno-economical evaluation of bio-oil production via biomass fast pyrolysis process: a review, *Front. Energy Res.*, 2022, **9**, 1–9.

288 M. S. A. Khan, N. Grioui, K. Halouani and R. Benelmir, Techno-economic analysis of production of bio-oil from catalytic pyrolysis of olive mill wastewater sludge with two different cooling mechanisms, *Energy Convers. Manage.: X*, 2022, **13**, 1–19.

289 G. V. Brigagao, O. Q. F. Araujo, J. L. Medeiros, H. Mikulcic and N. Duic, A techno- economic analysis of thermochemical pathways for corncob-toenergy: fast pyrolysis to bio-oil, gasification to methanol and combustion to electricity, *Fuel Process. Technol.*, 2019, **193**, 102–113.

290 W.-C. Wang and J.-J. Jan, From laboratory to pilot: design concept and techno-economic analyses of the fluidized bed fast pyrolysis of biomass, *Energy*, 2018, **155**, 139–151.

291 J. L. Carrasco, S. Gunukula, A. A. Boateng, C. A. Mullen, W. J. DeSisto and M. C. Wheeler, Pyrolysis of forest residues: an approach to techno-economics for bio-fuel production, *Fuel*, 2017, **193**, 477–484.

292 S. Gupta, P. Patel and P. Mondal, Life cycle analysis and operating cost assessment of a carbon negative catalytic pyrolysis technique using a spent aluminum hydroxide nanoparticle adsorbent-derived catalyst: insights into coproduct utilization and sustainability, *Energy Fuels*, 2023, **37**, 2960–2971.

293 Z. Yu, H. Ma, X. Liu, M. Wang and J. Wang, Review in life cycle assessment of biomass conversion through pyrolysis-issues and recommendations, *Green Chem. Eng.*, 2022, **3**, 304–312.

294 P. Brassard, S. Godbout and L. Hamelin, Framework for consequential life cycle assessment of pyrolysis biorefineries: a case study for the conversion of primary forestry residues, *Renewable Sustainable Energy Rev.*, 2021, **138**, 1–15.

295 D. N. Vienescu, J. Wang, A. Le-Gresley and J. D. Nixon, A life cycle assessment of options for producing synthetic fuel via pyrolysis, *Bioresour. Technol.*, 2018, **249**, 626–634.

296 Y. H. Chan, R. R. Tan, S. Yusup, H. L. Lam and A. T. Quitain, Comparative life cycle assessment (LCA) of bio-oil production from fast pyrolysis and hydrothermal liquefaction of oil palm empty fruit bunch (EFB), *Clean Technol. Environ. Policy*, 2016, **18**, 1759–1768.

297 D. Iribarren, J. F. Peters and J. Dufour, Life cycle assessment of transportation fuels from biomass pyrolysis, *Fuel*, 2012, **97**, 812–821.

298 S.-K. Ning, M.-C. Hung, Y.-H. Chang, H.-P. Wan, H.-T. Lee and R.-F. Shih, Benefit assessment of cost, energy, and environment for biomass pyrolysis oil, *J. Cleaner Prod.*, 2013, **59**, 141–149.

299 X. Yang, D. Han, Y. Zhao, R. Li and Y. Wu, Environmental evaluation of a distributed-centralized biomass pyrolysis system: a case study in Shandong, China, *Sci. Total Environ.*, 2020, **716**, 1–11.

300 H. R. Appell, Y. C. Fu, E. G. Illig, F. W. Steffgen and R. D. Miller, *Conversion of cellulosic wastes to oil*, U.S. Bureau of Mines, Washington, DC, USA, Report No. 8013, 1975.

301 H. R. Appell, Y. C. Fu, S. Friedman, P. M. Yavorsky and I. Wender, *Converting organic wastes to oil: a replenishable energy source*, U.S. Bureau of Mines, Washington, DC, USA, Report No. 7560, 1971.

302 L. Cao, C. Zhang, H. Chen, D. C. W. Tsang, G. Luo, S. Zhang and J. Chen, Hydrothermal liquefaction of agricultural and forestry wastes: state-of-the-art review and future prospects, *Bioresour. Technol.*, 2017, **245**, 1184–1193.

303 Q. Fan, P. Fu, C. Song and Y. Fan, Valorization of waste biomass through hydrothermal liquefaction: a review with focus on linking hydrothermal factors to products characteristics, *Ind. Crops Prod.*, 2023, **191**, 1–15.

304 S. Mukundan, J. Xuan, S. E. Dann and J. L. Wagner, Highly active and magnetically recoverable heterogeneous catalyst for hydrothermal liquefaction of biomass into high quality bio-oil, *Bioresour. Technol.*, 2023, **369**, 1–15.

305 V. Rajput, V. Kumar, M. S. Vlaskin, M. Nanda and M. Verma, Hydrothermal liquefaction of waste agricultural biomass for biofuel and biochar, in *Agriculture Waste Management and Bioresource: The Circular Economy Perspective*, 2022, vol. 1, pp. 1–15.

306 N. Neveux, A. K. L. Yuen, C. Jazrawi, M. Magnusson, B. S. Haynes, A. F. Masters, A. Montoya, N. A. Paul, T. Maschmeyer and R. de Nys, Biocrude yield and productivity from the hydrothermal liquefaction of marine and freshwater green macroalgae, *Bioresour. Technol.*, 2014, **155**, 334–341.

307 R. Saengsuriwong, T. Onsree, S. Phromphithak and N. Tippayawong, Conversion of tobacco processing waste to biocrude oil via hydrothermal liquefaction in a multiple batch reactor, *Clean Technol. Environ. Policy*, 2021, **1**, 1–11.

308 F. M. Hossain, J. Kosinkova, R. J. Brown, Z. Ristovski, B. Hankamer, E. Stephens and T. J. Rainey, Experimental investigations of physical and chemical properties for microalgae HTL bio-crude using a large batch reactor, *Energies*, 2017, **10**, 1–16.

309 C. Prestigiacomo, V. A. Laudicina, A. Siragusa, O. Scialdone and A. Galia, Hydrothermal liquefaction of waste biomass in stirred reactors: one step forward to the integral valorization of municipal sludge, *Energy*, 2020, **201**, 1–9.

310 B. Zhao, H. Li, H. Wang, Y. Hu, J. Gao, G. Zhao, M. B. Ray and C. C. Xu, Synergistic effects of metallic Fe and other homogeneous/heterogeneous catalysts in hydrothermal liquefaction of woody biomass, *Renewable Energy*, 2021, **176**, 543–554.

311 D. L. Barreiro, B. R. Gomez, U. Hornung, A. Kruse and W. Prins, Hydrothermal liquefaction of microalgae in a continuous stirred-tank reactor, *Energy Fuels*, 2015, **29**, 6422–6432.

312 B. Guo, V. Walter, U. Hornung and N. Dahmen, Hydrothermal liquefaction of Chlorella vulgaris and Nannochloropsis gaditana in a continuous stirred tank reactor and hydrotreating of biocrude by nickel catalysts, *Fuel Process. Technol.*, 2019, **191**, 168–180.

313 K. Anastasakis, P. Biller, R. B. Madsen, M. Glasius and I. Johannsen, Continuous hydrothermal liquefaction of biomass in a novel pilot plant with heat recovery and hydraulic oscillation, *Energies*, 2018, **11**, 1–23.

314 B. Patel and K. Hellgardt, Hydrothermal upgrading of algae paste in a continuous flow reactor, *Bioresour. Technol.*, 2015, **191**, 460–468.

315 C. Jazrawi, P. Biller, A. B. Ross, A. Montoya, T. Maschmeyer and B. S. Haynes, Pilot plant testing of continuous hydrothermal liquefaction of microalgae, *Algal Res.*, 2013, **2**, 268–277.

316 D. C. Elliott, A. J. Schmidt, T. R. Hart and J. M. Billing, Conversion of a wet waste feedstock to biocrude by hydrothermal processing in a continuous-flow reactor: grape pomace, *Biomass Convers. Biorefin.*, 2017, **7**, 455–465.

317 A. Aierzhati, J. Watson, B. Si, M. Stablein, T. Wang and Y. Zhang, Development of a mobile, pilot scale hydrothermal liquefaction reactor: food waste conversion product analysis and techno-economic assessment, *Energy Convers. Manage.: X*, 2021, **10**, 1–10.

318 I. A. Basar, H. Liu, H. Carrere, E. Trably and C. Eskicioglu, A review on key design and operational parameters to optimize and develop hydrothermal liquefaction of biomass for biorefinery applications, *Green Chem.*, 2021, **23**, 1404–1446.

319 L. Leng, J. Zhou, T. Li, M. Vlaskin, H. Zhan, H. Peng, H. Huang and H. Li, Nitrogen heterocycles in bio-oil produced from hydrothermal liquefaction of biomass: a review, *Fuel*, 2023, **335**, 1–15.

320 Y. Wei, S. Fakudze, S. Yang, Y. Zhang, T. Xue, J. Han and J. Chen, Synergistic citric acid-surfactant catalyzed hydrothermal liquefaction of pomelo peel for production of hydrocarbon-rich bio-oil, *Sci. Total Environ.*, 2023, **857**, 1–15.

321 Y. Liu, H. Du, Y. Meng, S. Lu, J. Zhang and H. Wang, Catalytic hydrothermal liquefaction of microalgae over reduced graphene oxide support Ni catalyst, *Fuel Process. Technol.*, 2023, **242**, 1–15.

322 K. Tekin, S. Karagoz and S. Bektas, Hydrothermal liquefaction of beech wood using a natural calcium borate mineral, *J. Supercrit. Fluids*, 2012, **72**, 134–139.

323 M. Tymchyshyn and C. Xu, Liquefaction of bio-mass in hot-compressed water for the production of phenolic compounds, *Bioresour. Technol.*, 2010, **101**, 2483–2490.

324 J. Arun, K. P. Gopinath, P. Rajan, R. Malolan, S. Adithya, R. S. Jayaraman and P. S. Ajay, Hydrothermal liquefaction of Scenedesmus obliquus using a novel catalyst derived from clam shells: solid residue as catalyst for hydrogen production, *Bioresour. Technol.*, 2020, **310**, 1–7.

325 S. C. Yim, A. T. Quitain, S. Yusup, M. Sasaki, Y. Uemura and T. Kida, Metal oxide-catalyzed hydrothermal liquefaction of Malaysian oil palm biomass to bio-oil under supercritical condition, *J. Supercrit. Fluids*, 2017, **120**, 384–394.

326 L. Nazari, Z. Yuan, S. Souzanchi, M. B. Ray and C. C. Xu, Hydrothermal liquefaction of woody biomass in hot-compressed water : catalyst screening and comprehensive characterization of bio-crude oils, *Fuel*, 2015, **162**, 74–83.

327 J. Long, Y. Li, X. Zhang, L. Tang, C. Song and F. Wang, Comparative investigation on hydrothermal and alkali catalytic liquefaction of bagasse: process efficiency and product properties, *Fuel*, 2016, **186**, 685–693.

328 K. Alper, Y.-Y. Wang, X. Meng, K. Tekin, S. Karagoz and A. J. Ragauskas, Use of a Lewis acid, a Brønsted acid, and their binary mixtures for the hydrothermal liquefaction of lignocellulose, *Fuel*, 2021, **304**, 1–15.

329 W. Wang, Y. Xu, X. Wang, B. Zhang, W. Tian and J. Zhang, Hydrothermal liquefaction of microalgae over transition metal supported TiO_2 catalyst, *Bioresour. Technol.*, 2018, **250**, 474–480.

330 S. Cheng, L. Wei, M. Alsowij, F. Corbin, E. Boakye, Z. Gu and D. Raynie, Catalytic hydrothermal liquefaction (HTL) of biomass for bio-crude production using Ni/HZSM-5 catalysts, *Environ. Sci.*, 2017, **4**, 417–430.

331 V. S. Amar, A. Shende and R. V. Shende, *BTMO catalyzed hydrothermal liquefaction of lignocellulosic biomass*, TechConnect Briefs, 2019, vol. 1, pp. 195–198.

332 L. Tai, B. Caprariis, M. Scarsella, P. Filipps and F. Marra, Improved quality bio-crude from hydrothermal liquefaction of oak wood assisted by zero-valent metals, *Energy Fuels*, 2021, **35**, 10023–10034.

333 B. Caprariis, M. P. Bracciale, I. Bavasso, G. Chen, M. Damizia, V. Genova, F. Marra, L. Paglia, G. Pulci, M. Scarsella, L. Tai and P. De Filippis, Unsupported Ni metal catalyst in hydrothermal liquefaction of oak wood : effect of catalyst surface modification, *Sci. Total Environ.*, 2020, **709**, 1–9.

334 D. G. B. Boocock, D. Mackay, H. Franc and P. Lee, The production of synthetic organic liquids from wood using a modified nickel catalyst, *Can. J. Chem. Eng.*, 1980, **58**, 466–469.

335 D. Chen, Q. Ma, L. Wei, N. Li, Q. Shen and W. Tian, Hydroliquefaction of rice straw for bio-oil production using Ni/CeO_2 catalysts, *J. Anal. Appl. Pyrolysis*, 2018, **130**, 169–180.

336 Z. Bi, J. Zhang, E. Peterson, Z. Zhu, C. Xia, Y. Liang and T. Wiltowski, Biocrude from pretreated sorghum bagasse through catalytic hydrothermal liquefaction, *Fuel*, 2017, **188**, 112–120.

337 A. Tavasoli, M. Barati and A. Karimi, Conversion of sugarcane bagasse to gaseous and liquid fuels in near-critical water media using K_2O promoted Cu/g-Al_2O_3-MgO nanocatalysts, *Biomass Bioenergy*, 2015, **80**, 63–72.

338 S. Cheng, L. Wei and M. Rabnawaz, Catalytic liquefaction of pine sawdust and in-situ hydrogenation of bio-crude over bifunctional Co-Zn/HZSM-5 catalysts, *Fuel*, 2018, **223**, 252–260.

339 C. Zhou, X. Zhu, F. Qian, W. Shen, H. Xu, S. Zhang and J. Chen, Catalytic hydrothermal liquefaction of rice straw

in water/ethanol mixtures for high yields of monomeric phenols using reductive CuZnAl catalyst, *Fuel Process. Technol.*, 2016, **154**, 1–6.

340 L. Zhang, P. Champagne and C. Charles, Bio-crude production from secondary pulp/paper-mill sludge and waste newspaper via co-liquefaction in hot-compressed water, *Energy*, 2011, **36**, 2142–2150.

341 P. Sun, M. Heng, S. Sun and J. Chen, Direct liquefaction of paulownia in hot compressed water : influence of catalysts, *Energy*, 2010, **35**, 5421–5429.

342 B. De Caprariis, I. Bavasso, M. P. Bracciale, M. Damizia, P. De Filippis and M. Scarsella, Enhanced bio-crude yield and quality by reductive hydrothermal liquefaction of oak wood biomass : effect of iron addition, *J. Anal. Appl. Pyrolysis*, 2019, **139**, 123–130.

343 I. Eladnani, M. P. Bracciale, M. Damizia, S. Mousavi, P. D. Filippis, R. Lakhmiri and B. Caprariis, Catalytic hydrothermal liquefaction of brachychiton populneus biomass for the production of high-value bio-crude, *Processes*, 2023, **11**, 1–15.

344 T. M. A. Haque, M. Brdecka, V. D. Salas and B. Jang, Effects of temperature, reaction time, atmosphere, and catalyst on hydrothermal liquefaction of Chlorella, *Can. J. Chem. Eng.*, 2023, **1**, 1–15.

345 B. Zhang, Q. Lin, Q. Zhang, K. Wu, W. Pu, M. Yang and Y. Wu, Catalytic hydrothermal liquefaction of Euglena sp. microalgae over zeolite catalysts for the production of bio-oil, *RSC Adv.*, 2017, **7**, 8944–8951.

346 P. Duan and P. E. Savage, Hydrothermal liquefaction of a microalga with heterogeneous catalysts, *Ind. Eng. Chem. Res.*, 2011, **50**, 52–61.

347 S. Cheng, L. Wei, M. Alsowij, F. Corbin, E. Boakye, Z. Gu and D. Raynie, Catalytic hydrothermal liquefaction (HTL) of biomass for bio-crude production using Ni/HZSM-5 catalysts, *AIMS Environ. Sci.*, 2017, **4**, 417–430.

348 C. Ma, J. Geng, D. Zhang and X. Ning, Hydrothermal liquefaction of macroalgae: Influence of zeolites based catalyst on products, *J. Energy Inst.*, 2020, **93**, 581–590.

349 Y. Xu, X. Zheng, H. Yu and X. Hu, Hydrothermal liquefaction of Chlorella pyrenoidosa for bio-oil production over Ce/HZSM-5, *Bioresour. Technol.*, 2014, **156**, 1–5.

350 X. Yan, W. Wang, Y. Zhao and J. Zhou, The effect of different catalysts and process parameters on the chemical content of bio-oils from hydrothermal liquefaction of sugarcane bagasse, *Bioresources*, 2018, **13**, 997–1018.

351 Y. Xue, H. Chen, W. Zhao, C. Yang, P. Ma and S. Han, A review on the operating conditions of producing bio-oil from hydrothermal liquefaction of biomass, *Int. J. Energy Res.*, 2016, **40**, 865–877.

352 C. Zhuo, L. Xueqin, W. Zhiwei, Y. Yantao, S. Tanglei, H. Taoli, L. Peng, L. Yanling, W. Youqing, L. Tingzhou and Q. Jingshen, Techno-economic and whole life cycle assessment of ester fuels production from agricultural waste via hydrothermal liquefaction, *Ind. Crops Prod.*, 2023, **192**, 1–15.

353 E. Tito, G. Zoppi, G. Pipitone, E. Miliotti, A. D. Fraia, A. M. Rizzo, R. Pirone, D. Chiaramonti and S. Bensaid, Conceptual design and techno-economic assessment of coupled hydrothermal liquefaction and aqueous phase reforming of lignocellulosic residues, *J. Environ. Chem. Eng.*, 2023, **11**, 1–15.

354 S. C. Bassoli, Y. A. Fonseca, H. J. L. Wandurraga, B. E. L. Baeta and M. S. Amaral, Research progress, trends, and future prospects on hydrothermal liquefaction of algae for biocrude production: a bibliometric analysis, *Biomass Convers. Biorefin.*, 2023, **1**, 1–16.

355 Y. Zhu, M. J. Biddy, S. B. Jones, D. C. Elliott and A. J. Schmidt, Techno-economic analysis of liquid fuel production from woody biomass via hydrothermal liquefaction (HTL) and upgrading, *Applied Energy*, 2014, **129**, 384–394.

356 P. Ranganathan and S. Savithri, Techno-economic analysis of microalgae-based liquid fuels production from wastewater via hydrothermal liquefaction and hydroprocessing, *Bioresour. Technol.*, 2019, **284**, 256–265.

357 T. H. Pedersen, N. H. Hansen, O. M. Perez, D. E. V. Cabezas and L. A. Rosendahl, Renewable hydrocarbon fuels from hydrothermal liquefaction: a techno-economic analysis, *Biofuels, Bioprod. Biorefin.*, 2018, **12**, 213–223.

358 P. H. Chen and J. C. Quinn, Microalgae to biofuels through hydrothermal liquefaction: open-source techno-economic analysis and life cycle assessment, *Applied Energy*, 2021, **289**, 1–17.

359 M. Kumar, A. O. Oyedun and A. Kumar, Hydrothermal liquefaction of biomass for the production of diluents for bitumen transport, *Biofuels, Bioprod. Biorefin.*, 2017, **11**, 811–829.

360 S. Masoumi and A. K. Dalai, Techno-economic and life cycle analysis of biofuel production via hydrothermal liquefaction of microalgae in a methanol-water system and catalytic hydrotreatment using hydrochar as a catalyst support, *Biomass Bioenergy*, 2021, **151**, 1–15.

361 S. Li, Y. Jiang, L. J. Snowden-Swan, J. A. Askander, A. J. Schmidt and J. M. Billing, Techno-economic uncertainty analysis of wet waste-to-biocrude via hydrothermal liquefaction, *Applied Energy*, 2021, **283**, 1–16.

362 G. Zoppi, E. Tito, I. Bianco, G. Pipitone, R. Pirone and S. Bensaid, Life cycle assessment of the biofuel production from lignocellulosic biomass in a hydrothermal liquefaction – aqueous phase reforming integrated biorefinery, *Renewable Energy*, 2023, **206**, 375–385.

363 B. Hao, D. Xu, Y. Wei, Y. Diao, L. Yang, L. Fan and Y. Guo, Mathematical models application in optimization of hydrothermal liquefaction of biomass, *Fuel Process. Technol.*, 2023, **243**, 1–15.

364 A. Saravanan, S. Karishma, P. S. Kumar and G. Rangasamy, A review on regeneration of biowaste into bio-products and bioenergy: life cycle assessment and circular economy, *Fuel*, 2023, **338**, 1–15.

365 M. L. Calijuri, I. B. Magalhaes, J. Ferreira, J. S. Castro and B. B. Marangon, Chapter 9 - Life cycle assessment of microalgal biomass for valorization, in *Valorization of Microalgal Biomass and Wastewater Treatment*, 2023, vol. 1, pp. 179–196.

366 Y. H. Chan, R. R. Tan, S. Yusup, H. L. Lam and A. T. Quitain, Comparative life cycle assessment (LCA) of bio-oil production from fast pyrolysis and hydrothermal liquefaction of oil palm empty fruit bunch (EFB), *Clean Technol. Environ. Policy*, 2016, **18**, 1759–1768.

367 E. Connelly, L. M. Colosi, A. F. Clarens and J. H. Lambert, Life cycle assessment of biofuels from algae hydrothermal liquefaction: the upstream and downstream factors affecting regulatory compliance, *Energy Fuels*, 2015, **29**, 1653–1661.

368 M.-O. P. Fortier, G. W. Roberts, S. M. Stagg-Williams and B. S. M. Sturm, Life cycle assessment of bio-jet fuel from hydrothermal liquefaction of microalgae, *Applied Energy*, 2014, **122**, 73–82.

369 S. Zhang, S. Zhou, X. Yang, W. Xi, K. Zheng, C. Chu, M. Ju and L. Liu, Effect of operating parameters on hydrothermal liquefaction of corn straw and its life cycle assessment, *Environ. Sci. Pollut. Res.*, 2020, **27**, 6362–6374.

370 S. Valizadeh, S. Pyo, Y.-M. Kim, H. Hakimian and Y.-K. Park, Production of aromatics fuel additives from catalytic pyrolysis of cow manure over HZSM-5, HBeta, and HY zeolites, *Chem. Eng. J.*, 2022, **450**, 1–15.

371 W. A. W. Mahari, S. Awang, N. A. Z. Zahariman, W. Peng, M. Man, Y.-K. Park, J. Lee, C. Sonne and S. S. Lam, Microwave co-pyrolysis for simultaneous disposal of environmentally hazardous hospital plastic waste, lignocellulosic, and triglyceride biowaste, *J. Hazard. Mater.*, 2022, **423**, 1–15.

372 H. Hakimian, S. Pyo, Y.-M. Kim, J. Jae, P. L. Show, G. H. Rhee, W.-H. Chen and Y.-K. Park, Increased aromatics production by co-feeding waste oil sludge to the catalytic pyrolysis of cellulose, *Energy*, 2022, **239**, 1–15.

373 W. A. W. Mahari, E. Azwar, S. Y. Foong, A. Ahmed, W. Peng, M. Tabatabaei, M. Aghbashlo, Y.-K. Park, C. Sonne and S. S. Lam, Valorization of municipal wastes using co-pyrolysis for green energy production, energy security, and environmental sustainability: a review, *Chem. Eng. J.*, 2021, **421**, 1–22.

374 Y.-K. Park, M. Z. Siddiqui, S. Karagoz, T. U. Han, A. Watanabe and Y.-M. Kim, In-situ catalytic co-pyrolysis of kukersite oil shale with black pine wood over acid zeolites, *J. Anal. Appl. Pyrolysis*, 2021, **155**, 1–8.

375 S. Ryu, H. W. Lee, Y.-M. Kim, J. Jae, S.-C. Jung, J.-M. Ha and Y.-K. Park, Catalytic fast co-pyrolysis of organosolv lignin and polypropylene over in-situ red mud and *ex situ* HZSM-5 in two-step catalytic micro reactor, *Appl. Surf. Sci.*, 2020, **511**, 1–10.

376 H. Shafaghat, H. W. Lee, Y. F. Tsang, D. Oh, J. Jae, S.-C. Jung, C. H. Ko, S. S. Lam and Y.-K. Park, In-situ and *ex situ* catalytic pyrolysis/co-pyrolysis of empty fruit bunches using mesostructured aluminosilicate catalysts, *Chem. Eng. J.*, 2019, **366**, 1–9.

